

SANDIA REPORT

2007-7761

Unlimited Release

Printed

Report on the SNL/NSF International Workshop on Joint Mechanics Arlington Virginia, 16-18 October 2006

Daniel J. Segalman, Lawrence A. Bergman, David J. Ewins

Prepared by

Sandia National Laboratories

Albuquerque, New Mexico 87185 and Livermore, California 94550

Sandia is a multiprogram laboratory operated by Sandia Corporation,
a Lockheed Martin Company, for the United States Department of Energy's
National Nuclear Security Administration under Contract DE-AC04-94-AL85000.

Approved for public release; further dissemination unlimited.



Sandia National Laboratories

NOTICE: This report was prepared as an account of work sponsored by an agency of the United States Government. Neither the United States Government, nor any agency thereof, nor any of their employees, nor any of their contractors, subcontractors, or their employees, make any warranty, express or implied, or assume any legal liability or responsibility for the accuracy, completeness, or usefulness of any information, apparatus, product, or process disclosed, or represent that its use would not infringe privately owned rights. Reference herein to any specific commercial product, process, or service by trade name, trademark, manufacturer, or otherwise, does not necessarily constitute or imply its endorsement, recommendation, or favoring by the United States Government, any agency thereof, or any of their contractors or subcontractors. The views and opinions expressed herein do not necessarily state or reflect those of the United States Government, any agency thereof, or any of their contractors.

Printed in the United States of America. This report has been reproduced directly from the best available copy.

Available to DOE and DOE contractors from
U.S. Department of Energy
Office of Scientific and Technical Information
P.O. Box 62
Oak Ridge, TN 37831

Telephone: (865) 576-8401
Facsimile: (865) 576-5728
E-Mail: reports@adonis.osti.gov
Online ordering: <http://www.osti.gov/bridge>

Available to the public from
U.S. Department of Commerce
National Technical Information Service
5285 Port Royal Rd
Springfield, VA 22161

Telephone: (800) 553-6847
Facsimile: (703) 605-6900
E-Mail: orders@ntis.fedworld.gov
Online ordering: <http://www.ntis.gov/help/ordermethods.asp?loc=7-4-0#online>



Report on the SNL/NSF
International Workshop on Joint Mechanics
Arlington Virginia, 16-18 October 2006

Daniel J. Segalman,
Sandia National Laboratories, Organization 01525
PO Box 5800, Albuquerque, NM, 87185-0557

Lawrence A. Bergman, University of Illinois, Urbana, IL
and
David J. Ewins, FRS, Imperial College, London England, UK

Abstract

The NSF/SNL joint mechanics workshop, held in Arlington, Virginia, 16-18 October, 2006, attempted to assess the current state of the art for modeling joint mechanics for the purpose of structural dynamics calculation, to identify the underlying physics issues that must be addressed to advance the field, and to propose a path forward.

Distinguished participants from several countries representing research communities that focus on very different length and time scales identified multiple challenges in bridging those scales. Additionally, two complementary points of view were developed for addressing those challenges. The first approach - the “bottom-up” perspective - attempts to bridge scales by starting from the smallest length scale and working up. The other approach starts at the length scale of application and attempts to deduce mechanics at smaller length scales through reconciliation with laboratory observation.

Because interface physics is a limiting element of predictive simulation in defense and transportation, this issue will be of continuing importance for the foreseeable future.

Acknowledgment

The workshop organizers would like to take this opportunity to thank Drs. Ken Chong and Adnan Akay of NSF and Drs. TY Chu and Arthur Ratzel of Sandia National Laboratories for their financial support and organizational guidance. We also sincerely thank Dr. Kevin Greenaugh of the Department of Energy for his participation in the workshop - particularly for his very helpful motivating remarks at the beginning of the workshop.

Contents

| | | |
|----------|--|-----------|
| 1 | Introduction | 7 |
| 2 | State of Art Review | 9 |
| | Challenges to Joint Modeling in Structural Dynamics | 9 |
| | Issues of Predictive Modeling | 9 |
| | Empirical Properties of Joints | 10 |
| | Sources of Experimental & Analytical Difficulty | 13 |
| | Standard Methods of Non-predictive Modeling | 15 |
| | An Advanced - but Still Inadequate - Approach: the State of the Art . . | 18 |
| | Elements of a Solution | 21 |
| | The Importance of Joints on the Dynamics of Gas Turbine Structures | 23 |
| | Joints in Gas Turbines and Their Effect on Structural Dynamics | 23 |
| | Casing joints | 24 |
| | Blade joints | 24 |
| | Damper devices | 26 |
| | Overview of Current Methods for Including Joint Effects | 26 |
| | Macro models of joints from tests | 27 |
| | Meso models of joint using measured interface properties | 27 |
| | The Way Forward | 32 |
| 3 | Road Map | 33 |
| 4 | Challenges | 37 |

| | |
|--|------------|
| Challenge 1: Experimental Measurements of Joint Properties | 37 |
| Challenge 2: Interface Physics | 38 |
| Challenge 3: Multi-scale Modeling | 39 |
| 5 Summary and Conclusions | 41 |
| Appendix | |
| A Slide Sets Presented at the SNL/NSF Joints Workshop | 43 |
| A.1 Slide Presentation of Dan Segalman, Sandia National Laboratories, Albuquerque, NM: <i>Challenges of Joint Modeling in Structural Dynamics</i> | 44 |
| A.2 Slide Presentation of David Ewins, Imperial College, London, England: <i>The Influence of Joints on the Dynamics of Gas Turbine Structures</i> . . | 67 |
| A.3 Slide Presentation of Evgeny Petrov, Imperial College, London, Eng- land: <i>Analysis of Nonsmooth Nonlinear Dynamics of Structures with</i> <i>Friction and Gaps</i> | 78 |
| A.4 Slide Presentation of David Hills, University of Oxford: <i>Contact Asymp-</i> <i>totics with Particular Application to Quantifying Fretting Damage</i> . . . | 84 |
| A.5 Slide Presentation of David Nowell, University of Oxford: <i>Structural</i> <i>Integrity Issues: Frictional Joints in Gas Turbines</i> | 99 |
| A.6 Slide Presentation of Andreas Polycarpou, University of Illinois, Ur- bana: <i>Significance of Interfacial Micro-Scale Parameters in the Dy-</i> <i>namics of Structures from a Tribologist Perspective</i> | 112 |
| A.7 Slide Presentation of Arif Masud, University of Illinois, Urbana: <i>A</i> <i>Multiscale Framework for Bridging Material Length Scales and Con-</i> <i>sistent Modeling of Strong Discontinuities in Mechanical Joints</i> | 139 |
| A.8 Slide Presentation of Mark Robbins, Johns Hopkins University, Balti- more, MD: <i>Contact and Friction: Connecting Atomic Interactions to</i> <i>Macroscopic Behavior</i> | 160 |
| B Notes From Break-Out Sessions | 181 |
| C Participant List | 195 |

Chapter 1

Introduction

The issue of predictive structural dynamics is of fundamental importance in multiple sectors of our economy, including manufacturing, transportation, and defense. Applications are so broad as to include optimal design of jet engine components and the specification of tolerances for nuclear weapon components. It has been recognized since the 1960's that the fundamental barrier to predictive structural dynamic simulation resides in the nonlinearity and variability of the mechanical interfaces of practical structures. Historically, this limitation has been obviated by approximating the structure as a linear system and tuning the linear model for that system to match its measured properties.

Given the tremendous advances in computer resources - particularly massively parallel computers - and advances in experimental techniques, it is appropriate to reexamine the problem to assess the possibility of actually predicting structural dynamic response even before a prototype is constructed. For this purpose the National Science Foundation and Sandia National Laboratories sponsored a workshop in Arlington, Virginia, 16-18 October, 2006. Participants in that workshop included distinguished investigators from the United States and Europe representing expertise in the various sciences that underlie interface mechanics and structural dynamics. Additionally, representatives from several basic research funding agencies contributed to the broad perspective. (A list of these participants and their home institutions is attached as an appendix.)

The participants were charged with assessing the current state of the art in joint modeling, identifying the core physics pertaining to joint mechanics, and identifying appropriate paths forward. Accordingly, the workshop was organized along the following lines:

- Introductory presentations on the state-of-the-art of mechanical and joint modeling. These talks are summarized in Section II of this report.
- Break out sessions focusing on the mechanics at different length scales inherent to the problem.
- Identification of several grand challenges that should push forward the enabling science relevant to joint mechanics.

Each of the above steps is documented in the following text, along with a set of general conclusions and perspectives on how this difficult but important class of problems can be addressed through near, intermediate, and long term research efforts.

Evolution of perspective on this problem is reflected in a series of roadmaps. The first is a spot chart developed by David Ewins identifying disciplines that focus at different length scales that might be expected to integrate to provide insight and predictive capability to problems of interface mechanics. This roadmap was used heavily in planning the workshop. Focused by the discussions of the workshop, a new multi-length-scale road map was developed that better identified the important underlying physics. A third roadmap was developed that captures probable research paths and suggests the level of effort necessary to address these problems fully. The reader will find these roadmaps, presented with discussion in Chapter 3 of this report, helpful in placing each of the research concepts discussed into context.

A particularly useful outcome of the workshop was the recognition by the participants of the multi-scale nature of predictive joint dynamics, spanning length scales from nano through macro, and the difficulties associated with merging and crossing length and time scales. For example, while the computational integration of nano (atomistic) and micro (continuum) scales has been demonstrated, the small surface areas and time scales currently achievable are inadequate for useful determination of constitutive behavior of mating surfaces at the asperity level. Thus, small-scale tribological experiments must be devised to ascertain this information, consistent with meso-scale analyses of the continuum. This implies the need for a dual, top-down, bottom-up mechanics-based approach, identified by the participants as one of the “grand challenges” to the community. Further insights of this sort can be gleaned from the report.

One of the outstanding values of this workshop was that it exploited the strengths of the different approaches pursued in Europe and the US in addressing this famously difficult problem. The scope of the workshop is illustrated by the slide presentations made there and reproduced in Appendix A. Among those presentations were an overview of atomistic simulation of interface interactions (Prof. Mark Robbins of Johns Hopkins University), a talk on a tribological view of joint mechanics (Professor Andreas Polycarpou, University of Illinois), two discussions on current capabilities with respect to solving elastic-frictional contact problems (Professors David Nowell and David Hills, University of Oxford), a discussion on computational nonlinear dynamics of structures with friction and gaps (Evgeny Petrov, Imperial College), and a talk on computational approaches to multi-scale modeling and their potential role in the simulation of joint mechanics (Professor Arif Masud, University of Illinois).

Chapter 2

State of Art Review

The workshop began with presentations by Dan Segalman, David Ewins, Evgeny Petrov, David Hills and David Nowell. That information is presented at length in the following two sections, and the relevant slide sets can be found in the appendix.

Challenges to Joint Modeling in Structural Dynamics

Issues of Predictive Modeling

Daniel J. Segalman, Sandia National Laboratories, Albuquerque, NM

A number of circumstances make the capability for predictive structural dynamics increasingly important. Among these diverse circumstances are the development of devices for space such as large aperture telescopes that cannot be tested on Earth, the huge cost of building prototypes of modern jet engine assemblies, and the current conventions against underground testing of nuclear weapons. These circumstances are representative of the general motivations for predictive structural dynamics: the impossibility of testing, the expense of testing, or programmatic reasons not to test. Two other developments drive the move to predictive simulation: the emergence of massively parallel computers and the prospect of computational uncertainty quantification.

In general, engineers have used computer simulations very productively for the following purposes:

- To interpolate/extrapolate among experiments (using processes relying on tuned parameters).
- To help explain experiments.
- To help design experiments.
- To provide design guidance.

- To estimate factors of safety.

Simulations have not been used to make precise predictions for systems that have not yet been built. Though the computer resources available to engineers have expanded tremendously in recent years, resolution into some of the core components common to dynamics problems has not grown as rapidly. Among these areas are quantitative understanding of loads and of initial and boundary conditions. Additionally, interface mechanics is poorly understood and inadequately modeled.

In this regard, the modeling of mechanical joints is a major weak point in the predictive process. Depending on circumstances, mechanical joints can be the major source of nonlinearity, uncertainty, and mechanical damping in structures. Predictive structural dynamics is contingent on the development of constitutive models for joints that possess both physical fidelity and sufficient simplicity of form that they can be integrated into structural dynamics models.

Empirical Properties of Joints

The two features of mechanical joints most relevant to their role in structural dynamics are energy dissipation and softening. The energy dissipation is often the primary source of vibration damping and its nonlinear nature is fundamental to predicting resonant vibration response. Softening (apparent reduction in stiffness) with force amplitude is a factor in predicting frequency response at modest forces, but its effect on structural response is profound as joint loads approach macro-slip levels. These features are illustrated in the following figures.

When a lap-type joint is subject to longitudinal harmonic loading, the energy dissipation per cycle appears to conform to a power-law relationship with the amplitude of force over several decades of load. As the load amplitude approaches the macro-slip load, the curve turns sharply upward. In general the slope of the power-law dissipation curve for mechanical joints is a number larger than 2 and less than 3. Note that all linear systems have power-law dissipation slopes of 2. This feature is illustrated in Figure 2.1.

It is this dissipation that is primarily responsible for vibration damping in structures without significant viscoelastic components.

When a lap-type joint is subjected to a monotonic pull, the force-displacement curve first appears almost linear (though there is always some nonlinear dissipation). At larger loads the curve begins to bend over, and at loads sufficient to cause macro-slip the curve levels out. This softening can also be seen in harmonic loading, where the resonant frequencies decrease as load amplitude is increased. At very high loads, the macro-slip response serves as vibration isolation. Though there is not complete consensus in the research community, these three regimes are often referred to as:

micro-slip, partial slip, and macro-slip. See Figure 2.2.

Another aspect of the nonlinearity of jointed structures is path dependence. The force response at any instant depends not only on the current deformation or deformation rate of the joint, but also on the history of the deformation. This feature is often referred to as “nonlocality” since the joint response depends on loads or deformations that are not recent in time.

Though the qualitative properties of nominally identical joints are generally quite similar, there is almost always substantial quantitative variability. This is illustrated in Figure 2.3. Shown here are the shock response spectra of identical shell structures, each connected to a base excitation by nominally identical joints. The huge difference in spectra illustrates the variability in mechanical properties among even nominally identical joints.

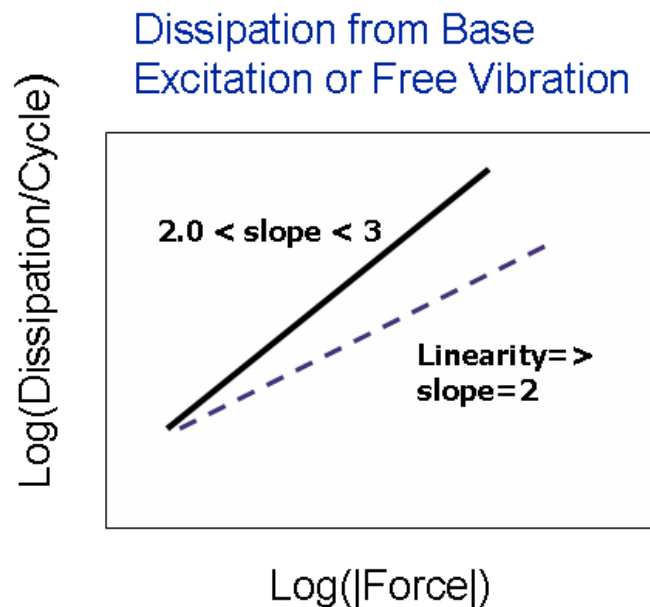


Figure 2.1. When a lap-type joint is subject to oscillatory longitudinal loads, the dissipation per cycle is observed to conform to a power-law relationship with force amplitude over large ranges of load. For linear systems, the dissipation is quadratic in force amplitude so a power-law slope other than 2 is an indication of nonlinearity.

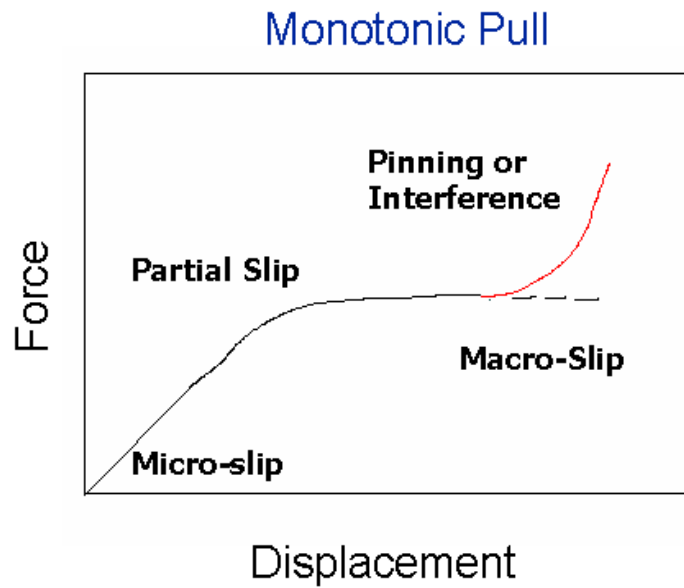


Figure 2.2. When a lap-type joint is subject to monotonic pull, the first portion of the force displacement curve appears linear (though there is always some dissipation on reversal). At larger loads the force-displacement begins to bend over and at very high loads macro-slip ensues.

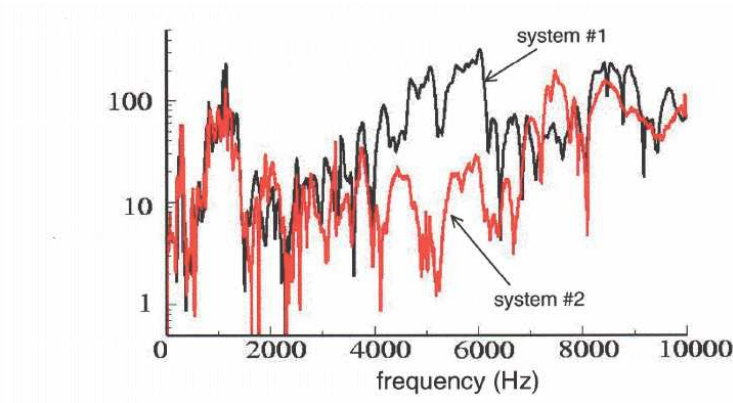


Figure 2.3. The shock response spectra of identical shell structures each connected to a base by nominally identical joints. The vast difference in spectra illustrates the variability in properties among even nominally identical joints.

Sources of Experimental & Analytical Difficulty

The fundamental difficulty with experimental investigations of joint physics is that the relevant phenomena take place exactly where they cannot be observed. Three other features of joints make the measurement of their properties very difficult:

- The kinematics of the slip process is spatially distributed so there is no unambiguous displacement to measure.
- The compliance of a joint is usually small compared to that of the rest of the test specimen of which it is a part, so deduction of joint properties must be done very indirectly. This remains the case up to loads near those necessary to cause macro-slip and explains why quasi-static tests on joints have little value beyond identifying macro-slip forces.
- Attachment of test specimens to the testing apparatus results in new interfaces, new compliances, and new sources of dissipation, further obscuring the properties to be measured.

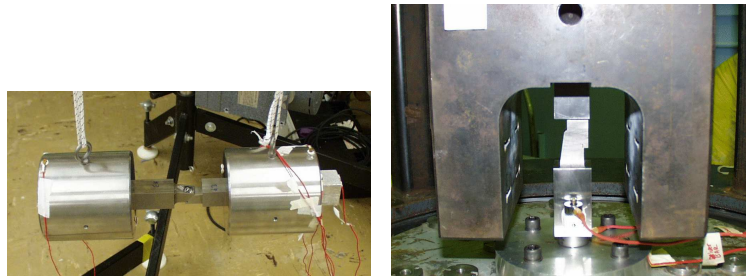


Figure 2.4. *A version of “joint resonator” design of Gaul et al. implemented by Gregory and co-workers is shown on the left. In this configuration, the left hand mass is struck by a calibrated impulse hammer and accelerometers on both masses are used to deduce the relative acceleration. On the right is Gregory’s “Big Mass Device” where the jointed specimen is sandwiched between a large reaction mass and a large electro-mechanical shaker.*

This combination of difficulties is partially overcome through the use of several innovations that were developed over the last five decades. The first is Ungar’s change in focus from immeasurable joint displacements to dissipation per cycle as a function of load amplitude in harmonic experiments. Though Ungar’s observable quantity was integrated over a full cycle and could provide no detail about the kinematics of the interface, it did capture features that distinguish one joint from another and that

are of direct significance to structural dynamics. Gaul and colleagues developed a “joint resonator” design consisting of a jointed sample sandwiched between two large masses that could be individually excited. The Gaul design greatly simplified the characterization of structural joints.

As the Gaul device is used to measure transient harmonic response of a jointed structure, another device by Gregory and co-workers is used to measure the steady-state response. In their design (Figure 2.4), the jointed specimen is placed between a large, suspended mass and a very large electromechanical shaker. The shaker is driven slowly through the first resonant frequency of the combined system. System damping is determined by the Q of the frequency response curve, and system stiffness is deduced from the resonant frequency.

Interpretation of this data is improved tremendously by another innovation of Gregory. For every jointed specimen designed, a superficially identical jointless specimen is machined out of a single piece of metal. Comparison of the energy dissipation and stiffnesses measured from the jointless and jointed structures permits the calculation of energy dissipation and stiffness to be attributed to the jointed interface.

The fundamental barrier to direct numerical simulation (DNS) of the dynamics of jointed structures is the multiple length scales involved. In general, the problems with which structural dynamicists deal are systems such as satellites, aircraft, or machinery having dimensions in meters. The first several vibrational modes of these systems will have inter-nodal distances also on the order of meters. Components of those systems may have dimensions on the order of centimeters, and the contact patches will have dimensions on the order of fractions of a centimeter. At accelerations substantially lower than those necessary to cause macro-slip, the frictional slip will occur only in the outer portions of the contact patch. During each cycle the thickness of the slip annulus will grow from zero to fractions of a millimeter and then shrink back to zero. The physics in each of these length scales are coupled. An effort to perform DNS of the full system requires such small elements to capture the contact mechanics correctly that the calculations become intractable. This situation is illustrated by the problem of the lap joint in Figure 2.5. The laps are each chosen to be one centimeter thick, the normal tractions are distributed so that the contact patch is two centimeters in diameter, and the magnitude of the normal force N is set at 4000 Newtons (about the working load in a quarter inch bolt).

The range of longitudinal load of interest is assumed to be on the order of $L \in (0.05\mu N, 0.8\mu N)$ where μ is the coefficient of friction, and we assume that the dynamic range of interest lies in $f \in (100Hz, 3500Hz)$. For the sake of estimation, we further assume that the contact patch is invariant over that load cycle and that the stick slip boundary abides by the Mindlin solution for the two-sphere problem, so that

$$\frac{c}{a} = \left[1 - \frac{L}{N\mu} \right]^{1/3} \Rightarrow \frac{c}{a} \in (0.58, 0.98) \Rightarrow \frac{a-c}{a} \in (0.02, 0.42)$$

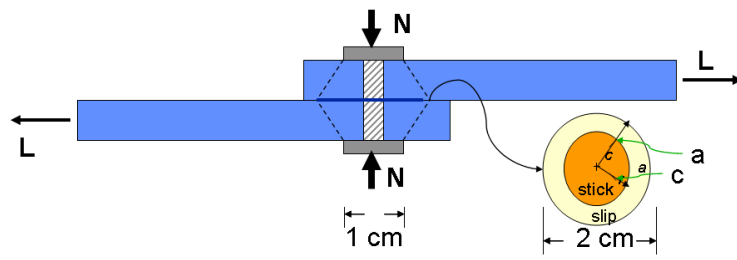


Figure 2.5. *We consider a simple bolted lap joint of convenient dimensions, and we use a Mindlin 2-sphere approximation for the contact mechanics.*

To get any resolution on the dissipation process, one needs approximately ten elements through the thickness of the slip annulus. For the case of the lower loads, this means that elements must be on the order of $20\mu m$. For structural materials, a representative speed of sound would be 6000 meters/second, and the Courant time would be less than 4 ns. To model just one cycle of structural response at 100 Hz, would require 2,500,000 explicit time steps. Simulation of at least ten cycles would be necessary for any kind of frequency resolution and the problem is very quickly seen to be intractable. If one were to slave a quasi-static contact analysis of the same fine mesh for the interface to a dynamic model for the full structure, the problem would again be found to be intractable because of the number of iterations necessary to follow the nonlinear contact process.

Beyond the intractable nature of DNS of the contact domain as part of the dynamic problem, there are other reservations to be seen with a direct finite element treatment of the interface. Those reservations have much to do with the idealizations of Coulomb friction on real surfaces. As one refines the mesh in the contact patch, one also pushes the credible use of the Coulomb friction assumption. Further, it is at the edges of the contact patch where the interesting physics takes place, and it is there that normal loads go to zero.

Standard Methods of Non-predictive Modeling

The usual approach to structural dynamics of jointed systems is to set aside the known nonlinear nature of joints and to tune linear models to approximate the full response of the system. For the purpose of discussion, we consider the structure shown in Figure 2.6.

This structure consists of two monolithic substructures connected by three bolted joints. in conventional structural dynamics, each substructure would be represented

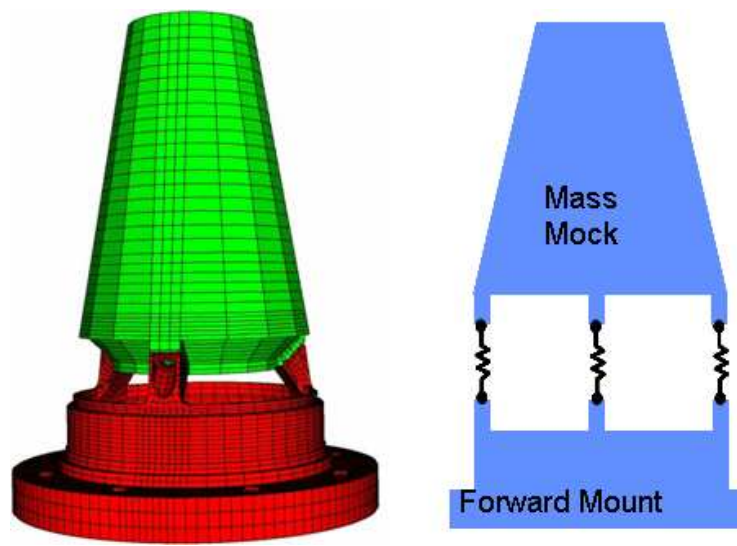


Figure 2.6. *This simple structure consists of two monolithic structures connected by three bolted joints. In conventional finite element analysis, such structures would be represented by a finite element mesh of each substructure and a set of tunable springs connecting them.*

by a finite element mesh and the joints would be represented by springs. The full system would be constructed and tested - usually modally - to identify apparent elastic modes and frequencies and to measure damping of those modes. The springs would be tuned so that the resulting linear structural model reproduces the measured modes and frequencies as closely as possible. Modal or proportional damping values would be selected to reproduce the measured damping. The resulting model would then be used to make predictions of structural response to loads similar to those used to calibrate the model.

Some of the features of the above approach are illustrated in Figure 2.7. There we see that when the spring stiffnesses and modal damping are selected to match the behavior of the structure at low loads, the resulting model can predict that behavior reasonably well. In this case the base of the structure is subjected to the acceleration history of a Morlet wavelet of period 4 and amplitude 10g, and the measured acceleration is that at the top of the upper substructure

When that same linear model is used to predict the response of the structure at much higher loads (108g base excitation), the agreement is much poorer (Figure 2.8). In particular we attribute the disagreement to three factors:

1. The experimental amplitude is much less than that predicted by the linear

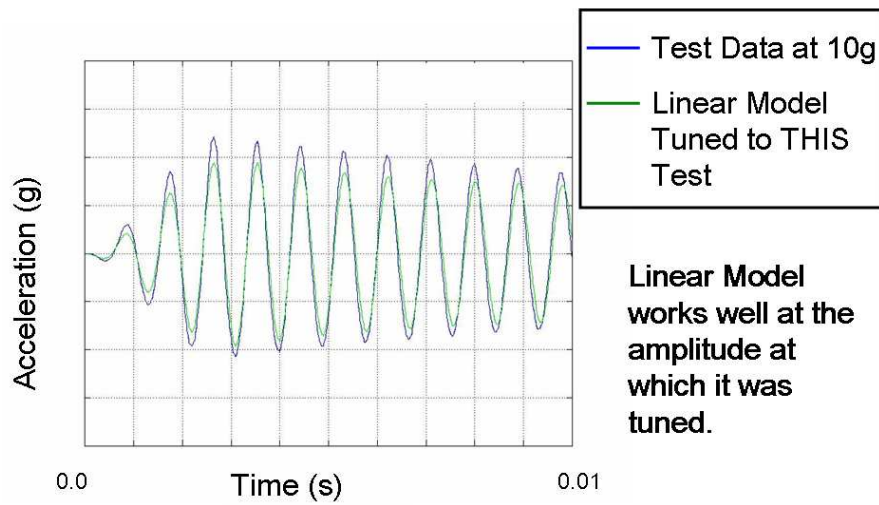


Figure 2.7. *When the spring stiffness and model damping are selected to reproduce the measured features of the prototype at particular loads (low loads in this case) the resulting model predicts that behavior reasonably well. Show here is the acceleration at the top of the structure when the base is accelerated by a Morlet wavelet of period 4 and amplitude 10g.*

model. This is true both because of the greater dissipation of the nonlinear joint than that which a linear model can accommodate and because macro-slip during loading provides vibration isolation of the upper structure from the base.

2. The predicted period is shorter than that found experimentally. This is a manifestation of joint softening under load.
3. There are many high frequency components in the experimental response. (There would be much more high frequency response shown had a low-pass filter not been used to process the experimental signals.) These high frequency components are common in jointed systems undergoing macro-slip and are a result of the sudden changes of system parameters during the slip process.

Such models as described above are not predictive in the sense that one must first build a prototype in order to tune the mode. They have validity only under conditions similar to those to which they have been tuned, and they have proven themselves to be very useful engineering tools. There is a substantial body of literature on how to deduce model parameters for the linearization of structures such as those discussed here.

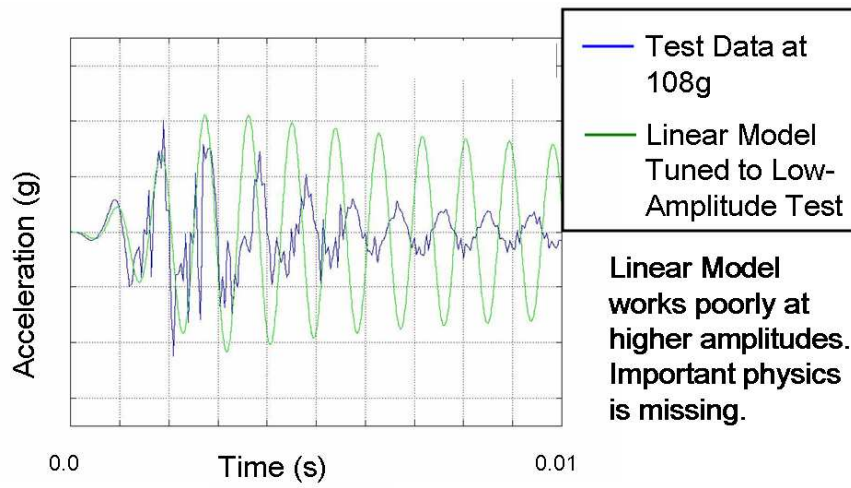


Figure 2.8. *When the model having spring stiffnesses and modal damping tuned to reproduce the structural response at low load is applied to a high load case, the agreement is generally very poor. Show here is the acceleration at the top of the structure when the base is accelerated by a Morlet wavelet of period 4 and amplitude 108g.*

An Advanced - but Still Inadequate - Approach: the State of the Art

Following is outlined an approach to incorporating measured joint properties into structural dynamics calculations. The approach presented is quite inelegant, but it justifiably can be argued to be the most advanced method for performing structural dynamics of jointed systems. Most significantly, this approach illustrates what can be achieved by accounting explicitly for joint mechanics in structural dynamics and how essential better joint models are to make significant progress in predictive structural dynamics.

The key notion introduced here is that of imposing a simplified joint kinematics that lives entirely in the macro-world and absorbing all the nano-, micro-, and meso-mechanics into macro-scale constitutive models constructed to reproduce the measured properties of joints. The first of these elements is called a “whole-joint” approximation.

The “whole-joint” approximation involves imposing simplified kinematics across the joint interface, relating the kinematics of all the nodes on each side of the interface to the kinematics of a representative node. The simplest version of this approximation is indicated in Figure 2.9, where all the nodes on each side of the interface are

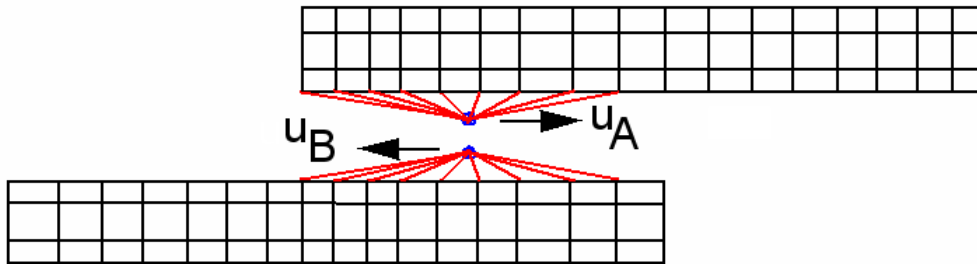


Figure 2.9. The “whole-joint” approximation imposes a simplified kinematics across the interface. All nodes on each side of the interface are slaved to a representative node. The two representative nodes are then related by a constitutive model constructed to reproduce measured joint properties.

slaved to move exactly with their representative node (u_A and u_B). (There are other implementations that do not require rigidization, but the formalism is slightly more complex.)

The joint mechanics are now absorbed into the relative motion of macroscopic displacements u_A and u_B and the force associated with that relative motion. To predict that force, we must employ some constitutive equation for the joints that relates macroscopic motion and macroscopic forces. A good formalism for the purpose is Iwan’s continuum of Jenkins elements, suggested in Figure 2.10.

The Iwan formalism has significant generality among one-dimensional plasticity models. For instance, one can show that all Masing models can be represented by Iwan models. The Iwan model is entirely defined by the population density $\rho(\phi)$ of Jenkins elements of strength ϕ . Segalman has postulated a four-parameter form for $\rho(\phi)$ that is capable of reproducing the power-law behavior of dissipation with force, nearly linear behavior at low amplitude, and macro-slip at high load and that can be fitted neatly to experimental joint data.

When the finite element models for subsystems are coupled by these whole-joint models, important physical behavior that cannot be captured by linear models is manifest. In Figure 2.11 we see that a linear model fitted to the full structural response at low amplitude of the structure grossly over-predicts the acceleration seen at the top of the structure when very large base excitations are imposed. Also shown is the predicted acceleration from a model employing whole-joint models tuned to jointed specimens, but with no tuning to the full structure. Though the nonlinear model does over-predict accelerations, the predictions are close enough to be of used in engineering decision making. Further, though not evident from the figure, the whole-joint model does predict the pumping of energy into higher frequencies.

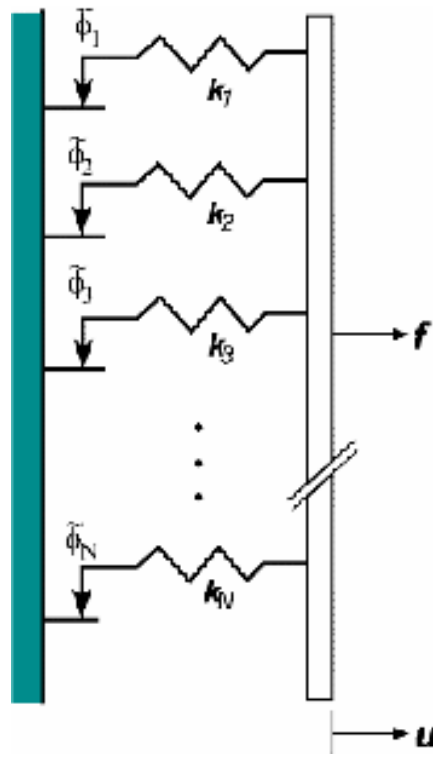


Figure 2.10. *The Iwan formalism consists of a continuum of Jenkins elements.*

There are some serious limitations to the modeling approach presented here:

- It does not account for the multi-dimensional nature of loads.
- The true complexity of contact (i.e. moving contact patch, varying normal loads. etc.) are not represented.
- Fallacious stress fields near contact are introduced.
- All joint parameters are deduced from experiment. This could be mitigated by meso-scale finite element modeling of the joint interfaces, but such an approach would be limited to the few cases where an adequate friction model is available and surface contaminants or oxide layers are not a serious complication.

The limitations of the above approach should serve as a partial guide to appropriate new areas for research.

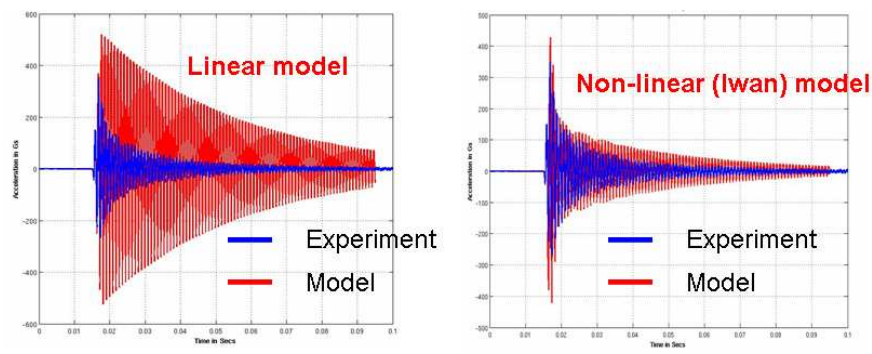


Figure 2.11. When a linear model fitted to the full structural response is used to predict the response of the three-legged structure to loads sufficient to cause macro-slip, the acceleration response is grossly over predicted. When a structural model employing a whole-joint model fitted to measured joint response (but not tuning to the full structure) much better prediction is achieved.

Elements of a Solution

One hopes that growing computational resources will provide additional tools to address the problems outlined above. In these days when massively parallel computing is applied to molecular modeling of various sorts, there is some impulse to attempt to employ “physics-based” modeling to the dynamics of jointed systems. Currently the capability to model all the way from atomistic to structural modes does not exist, but identification of the gaps can provide guidance as to fertile areas. These gaps include those between atomistics and asperity mechanics, between asperity mechanics and continuum mechanics (the current state of the art only goes so far as to provide estimates for Coulomb friction), between the fine-scale continuum mechanics relevant to slip mechanics and the continuum mechanics of structural dynamics.

However the above research issues are addressed, two important notions must be kept in mind:

- Though useful insights might be achieved through massive computing at nano and micro levels, those insights are no more “physics-based” than properties experimentally measured from actual joints. In fact, the micro- and nano-scale material and interface properties that one would use in those simulations would themselves be deduced from experimental observation.
- The most important measure of success is whether resulting mathematical models can be used as effective engineering tools. A useful tool will most likely be

distributed in nature, facilitate the use of tabulated model parameters, and involve time steps natural to the dynamics problems being analyzed.

The Importance of Joints on the Dynamics of Gas Turbine Structures

D. J. Ewins, Imperial College, London UK

with contributions provided by David Nowell (University of Oxford) and Evgeny Petrov (Imperial College London)

Abstract

Many of the issues on joints and interfaces discussed in the previous paper (Segalman) are directly applicable to the structures used in aero-engine gas turbines and other high-performance, high-speed machines. In these applications, the influence of joints and interfaces can be particularly important because (i) uncertainty as to their exact behavior inevitably results in conservative, and thus heavy, designs and (ii) in some special cases, their characteristics are specifically required to be designed in to control severe resonance conditions. For some years, efforts have been made to include these joint effects in the structural dynamic analysis of the more critical components but these have all required extensive experimental data input. Such an approach clearly falls far short of the predictive models that are necessary and, as a result of these considerations, much-improved **predictive** models of joints are urgently sought for a number of key components in gas turbines.

Joints in Gas Turbines and Their Effect on Structural Dynamics

There are hundreds of structural joints in a typical aero engine gas turbine and many of these have little or no influence on the dynamics of the structures concerned. However, there are a significant number of structural components whose dynamics are of critical importance to the engine's performance or integrity and which are influenced by the joints and interfaces that form part the overall assembly. These cases are the focus of the attention now being paid to the modelling of joints because it is increasingly the case that the joint properties are often the limiting factors in the design, and the source of much of the uncertainty and variability in performance that is observed in a fleet of engines in service.

The joints in a gas turbine which are of particular interest fall largely into 2 groups, illustrated in Figure 2.12 - (a) those associated with the whole engine or sub-assemblies and which comprise the non-rotating parts of the machine, and (b) the critical and highly-stressed rotating components, usually related to the blading. The second group are generally the most critical as they represent the most highly-loaded components, both mechanically and thermally, and the most vulnerable to failure.

Casing joints

For the first category, the main influence of the joints is to bring about a reduction in the stiffness of assembled structure(s) which - in turn - has the effect of lowering natural frequencies (by comparison with the values expected from perfect, or rigid, joints - which is the configuration represented by a model which does not specifically include the joints as mechanical components). This is more important from the perspective that the natural frequencies may not be where they were expected to be, than from the fact that they are lower. There is a second feature that is introduced by real joints, and that is that they provide a source of damping which, from a dynamics perspective, is an advantage in that it serves to reduce resonant vibration levels and to reduce the possibility of instability. In many cases, these beneficial effects may be almost negligible in magnitude. Nevertheless, they are positive and, more interestingly, there is a prospect that with much better understanding and modelling of the behavior of these joints, it might well be possible to design in much higher levels of damping (and stiffness) than we obtain today more or less by chance. The overall effect of being able to actively design joints which have specific, desired, dynamic properties would certainly be to achieve more efficient and reliable structural designs.

Blade joints

The more urgent interest today is in the second group of cases, where the significance of the joints is much more of a critical, performance-limiting, nature. Most turbo-machinery blading, at least until very recently, has included a root fixture between each blade and the disc or drum on which it is carried: see Figure 2.13 (b). These roots are the focus of extremely high steady loads (because of centrifugal effects), often at elevated temperatures (in turbines), and any vibration which is added to these conditions can be very damaging. Thus, in these applications, it is vital to be able to predict and control the flexibility that is introduced by the blade-disc interface in order to predict the natural and resonant frequencies with great precision - so that they can be avoided under operating conditions. Secondly, since it is not possible to avoid all such resonances that exist in a multi-bladed disc, there is always a need for damping from all sources to mitigate the resonant vibration levels in those modes which cannot be avoided. Interfaces such as those in a blade-disc root have the possibility of providing a non-negligible amount of mechanical damping from the dry friction effects and micro slip which can occur at these interfaces. It should also be noted here that the benefits that damping can bring come at the cost of possible damage to the surfaces in question -sometimes as wear but sometimes in the initiation of fatigue cracks that can propagate to failure. Thus, the optimal design of blade-disc roots demands a comprehensive treatment of a wide range of phenomena associated with the conditions at the interfaces.

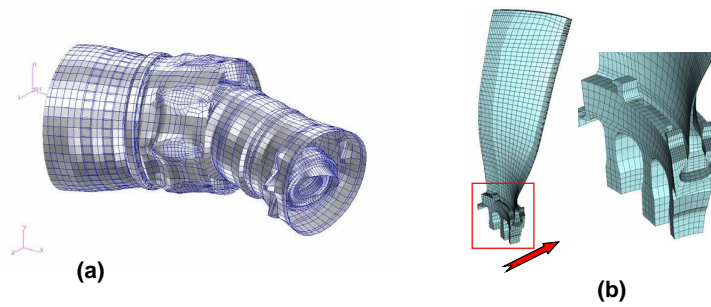
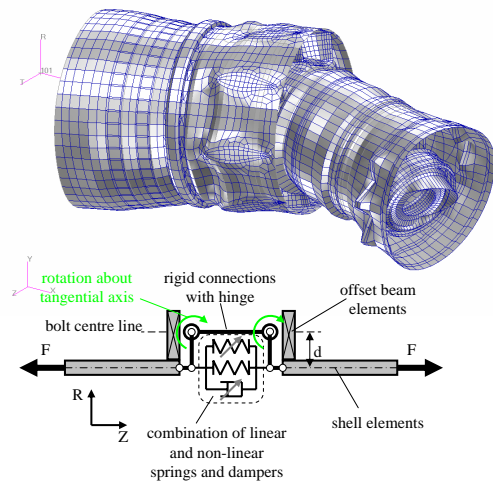


Figure 2.12. Two Areas of Particular Interest & Concern: (a) Whole-engine Casings & (b) Bladed Assemblies



Courtesy: University of Kassel

Figure 2.13. Modelling Approach for Bolted Flange Joints.

In some bladed assemblies, there are similar interfaces between adjacent blades when these are fitted with interconnected shroud elements, and the same comments apply here in those cases. However, probably the most significant of all the interfaces in a gas turbine from the structural dynamics viewpoint are those found in the underplatform dry friction dampers (and, increasingly, other friction devices which are following the underplatform concept). Here, an interface is designed and used expressly to control the dynamics of the host structure - a blade. In the past, underplatform dampers were “designed” largely by experimental trial-and-error development but in recent years they have been the subject of much analytical attention as the benefits to be gained can be very sensitive to basic design parameters. As a result, there are now several tools that allow the numerical analysis of different inter-blade damper configurations, and these are an essential feature in the design of modern blading. As mentioned earlier, there are two characteristics of importance: firstly, (a) the amount of damping that can be usefully delivered to the bladed disc and, also, (b) the flexibility that is introduced, and the effect that has on the precise values of the natural frequencies of the blading. Both features (flexibility and damping) can be used as a design control, both to contain resonance amplitudes in forced vibration and also to raise stability margins in situations where flutter may occur.

The overriding weakness in these attempts to provide a predictive tool for the designer in this important area is the dependence of all the theoretical models on the need to acquire the basic interface properties by direct measurement. The fact that these measurements must be made at all the frequencies, loads, amplitudes, temperatures, that will be encountered in service mean that these are far from predictive models. There is a marked lack of understanding of the underlying physical phenomena at work in these joints and interfaces and that results in an inability to predict these important effects without a heavy reliance on experimental observations and measurements.

Overview of Current Methods for Including Joint Effects

We shall now describe in a little more detail the two approaches currently employed on the two categories of problem, with the objective of illustrating clearly the limitations of these methods and the need for a major breakthrough in joints modelling: identifying the underlying physical phenomena, modelling these efficiently, and using these models to develop predictive tools for the various characteristics of interest to the structural dynamicist.

The example used is that shown in Figure 2.12 (a) and comprises an assembly formed of two major subassemblies connected by a bolted flanged joint. Such joints are designed to meet criteria which are quite unrelated to any dynamics effects and so it is not surprising that their dynamic characteristics are far from ideal for the structural dynamicist. Figure 2.13 shows the system analyzed: two casing structures described in some detail using conventional FE models, plus a third component - the flanged joint - introduced schematically by a “macro” model of springs and dampers, but without any specific values for the constituent parameters. Here, it is assumed that, rather than connecting corresponding nodes on the flanges of the two components directly - or rigidly, a set of nonlinear springs and dampers should be inserted between them. A prototype test structure of this subassembly is then constructed and subjected to a modal test (see Figure 2.14(a)), measuring - specifically - a series of FRFs on the assembled structure, exemplified by the plots shown in Figure 2.14(b). These response functions can be analyzed by conventional modal analysis methods to reveal the stiffness (indirectly, via natural frequencies) and damping properties both of which have a clear non-linear amplitude-dependent characteristic - see Figure 2.15. Once determined in this way, these properties can be introduced to the mathematical model and that used to compute the response functions which have been measured, and then compared with these measurements (see Figure 2.16). It must be remembered that the computed curves shown here are not predicted in the literal sense, because it was first necessary to measure the structure’s behaviour in order to deduce the stiffness and damping values for the model. Nevertheless, this model can then be used with confidence to predict the response to as many other excitations as are required, without the need to repeat the measurements again.

Meso models of joint using measured interface properties

The second category of problem requires a more pro-active approach to the development of joint models than was used above. For the design of underplatform blade dampers (and, now increasingly, for other dry friction devices elsewhere in the engine) it is necessary to be able to design the detailed geometry of these devices and that requires a first-level model of the phenomenon, rather than the device as was used for the flanged joint.

In this case, a finite element representation (a “meso” model) of two mating interfaces forming a joint has been developed over the past 5 years - see various applications in Figure 2.17. Each contact element allows for the two matching structural elements to stick and to move as one, or to slip with relative motion, and to stay on contact or to separate, according to the normal loads that are transmitted across that element. Two connected surfaces may have some elements stuck while others are slipping, representing what is generally referred to as micro-slip: local slipping at an interface but without any global relative motion of the two bodies in contact.

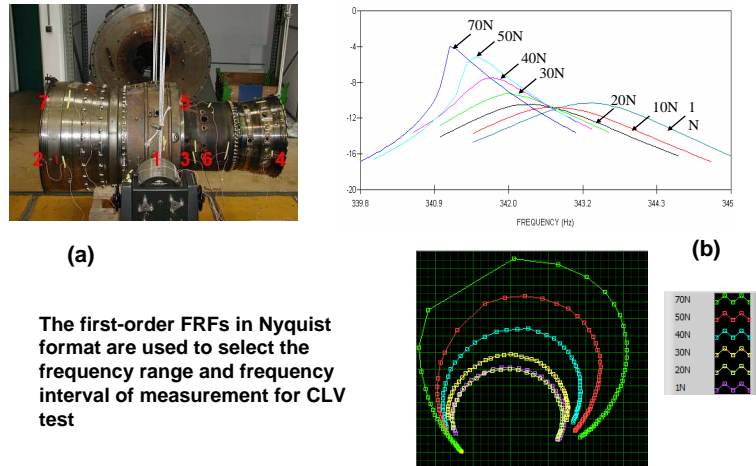


Figure 2.14. Frequency Responses Measured on Engine Casing Structure.

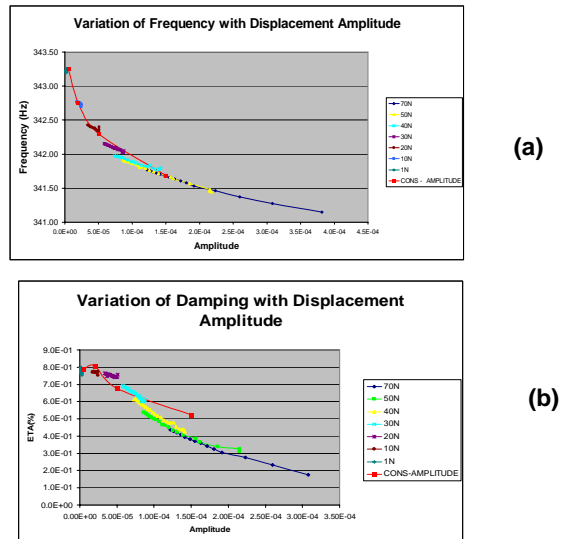
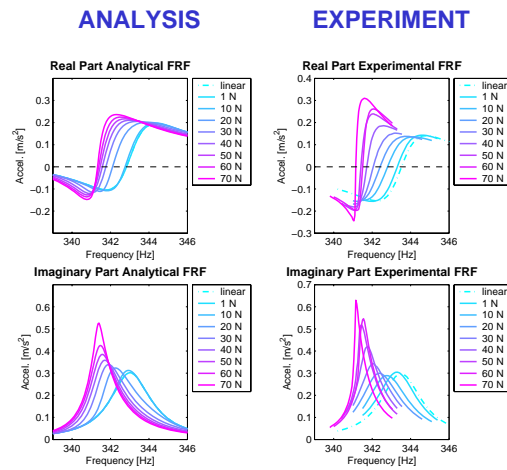


Figure 2.15. Variations of (a) Stiffness and (b) Damping with Vibration Amplitude.



Courtesy: University of Kassel

Figure 2.16. Comparison of Computed and Measured Response Functions.

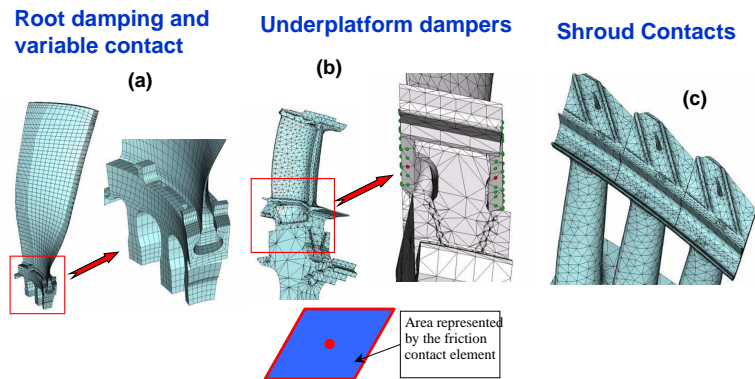


Figure 2.17. Models of Dynamic Contacts in Bladed Assemblies.

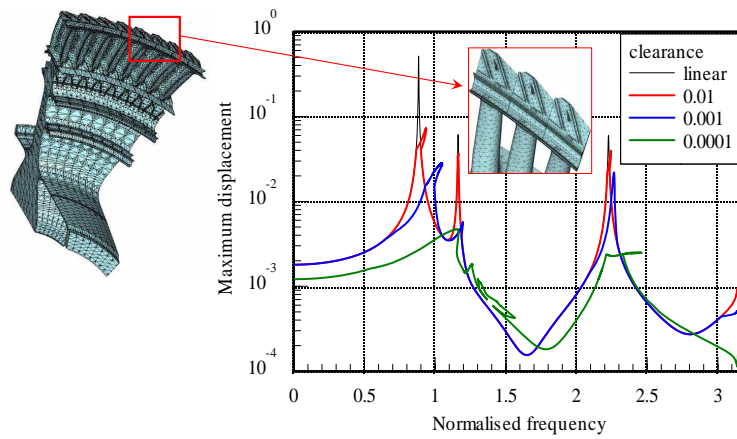


Figure 2.18. Computed Responses for Contacting Shrouds in Bladed Disc.

With these models, and access to a suitable non-linear response analysis code, it is possible to compute the response of a structure containing any number of these interfaces to a wide range of excitation conditions. Because of the complex nature of the actual contacts, these motions are highly complex, and very amplitude-dependent. As a result, standard response functions may not be applicable to such situations and it is then necessary either to use time domain solutions or to use an advanced multi-harmonic balance frequency-domain methods which are more applicable for the steady-state periodic excitations that are common in a running gas turbine: Figure 2.18.

Notwithstanding the availability of these more advanced modelling and analysis processes, it is still necessary to supply the contact elements with data describing the essential dynamics at the interface: essentially, the friction coefficient and the contact stiffness properties, often provided in the form of a set of hysteresis loops, see Figure 2.19. These data must be measured for a wide range of temperatures, frequencies, loads, surface finishes, So, here again, the models are not truly predictive for, although it is possible to use the data at one set of conditions for a wide range of excitations that may be applied, it is not possible to extrapolate from the interface data at one set of conditions to those which will apply at another set of conditions. Figure 2.20 shows a typical rig used to measure the required interface properties.

Here, again, we reach a situation where further development and refinement of our prediction tools - necessary now to ensure the integrity of these critical structures while at the same time optimizing their performance and efficiency, is blocked by the absence of a truly predictive capability for the mechanics of two mating interfaces in

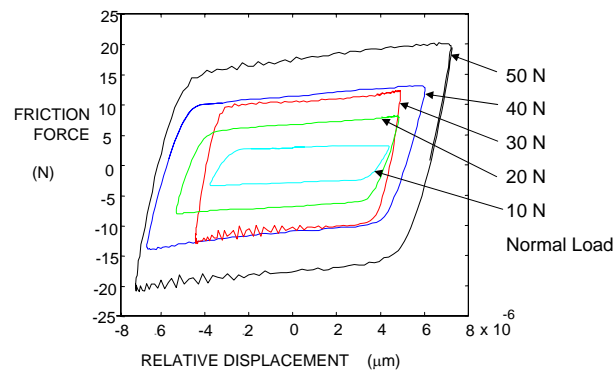


Figure 2.19. Set of Hysteresis Loops, Measured at Different Normal Loads.

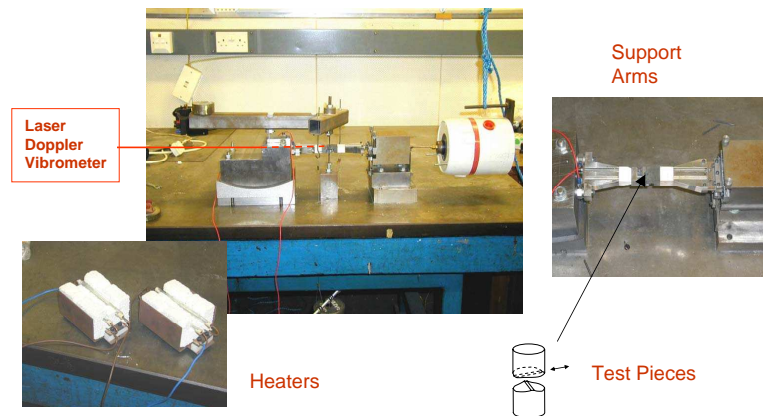


Figure 2.20. Test Rig for Measuring Hysteresis Characteristics.

The Way Forward

In this particular application area of high-speed rotating machinery, there is a view that the modelling of almost all the individual structural components that make up the critical structures is now at an advanced stage. Recent evidence suggests that the reliability or accuracy of typical finite element models of structural components is comparable with the uncertainty or variability in the properties found in a batch of nominally-identical items of the same design. However, when two or more individual components are connected together to form an engineering structure, the accuracy of the predicted dynamic behaviour falls by a significant amount, sometimes by an order of magnitude when there are several joints. It is considered that in many cases the reason for this loss of predictive capability is due in very large measure to the paucity of our models of the joints and interfaces themselves. Quite often, no models are included to represent the joints at all. Those that are included are often considerably less accurate than are those used for the structural components themselves. To a large extent, further improvements in the predictive capability for designing reliable and efficient complex structures such as those used in turbomachinery, cannot be made until there are major advances in joint modelling methods.

Chapter 3

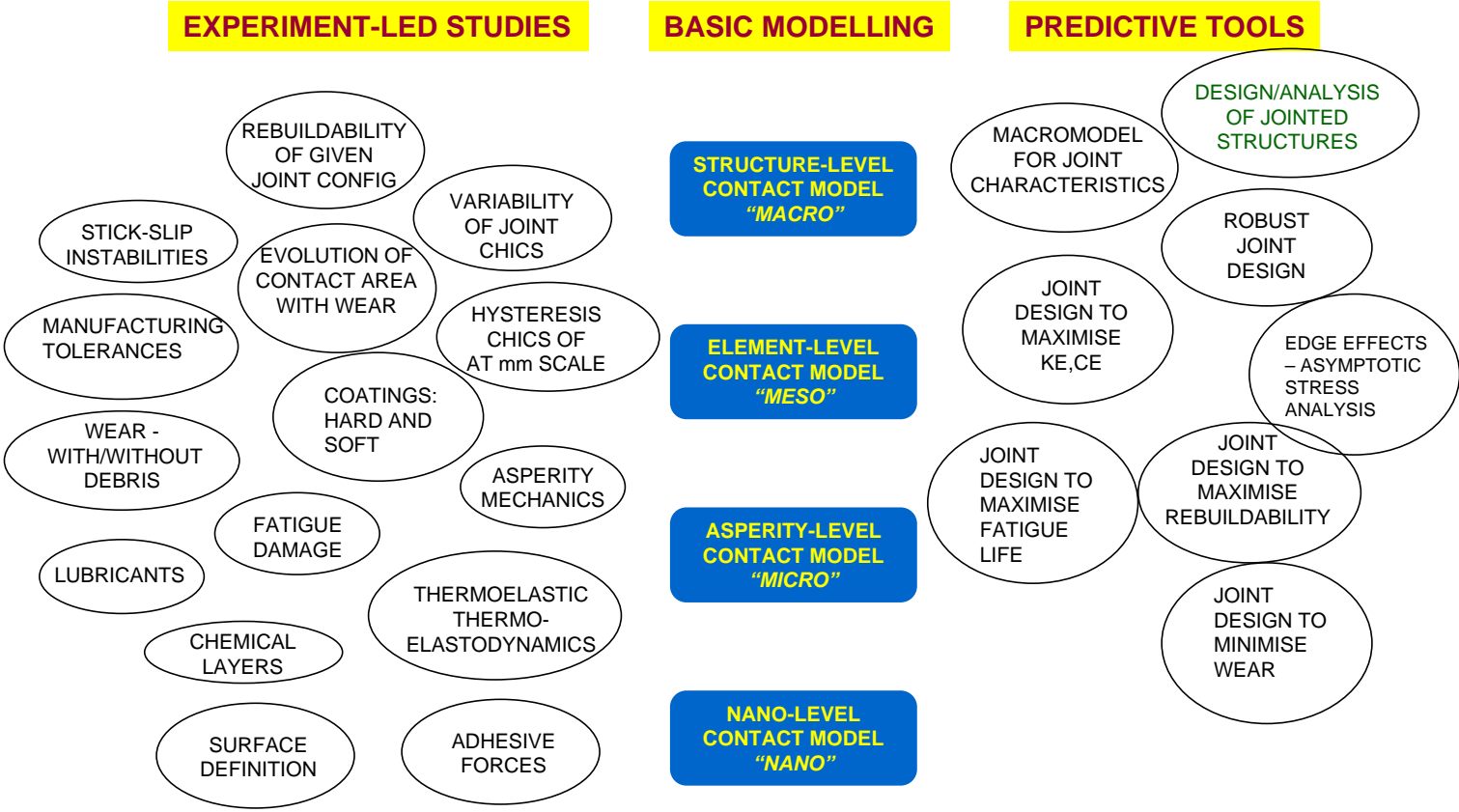
Road Map

During the initial breakout sessions it quickly became apparent that developing a scientific basis for joint modeling must involve understanding the physics at the multiple length scales that underlie interface physics. Further, it became evident that mastering the physics at each length scale must be guided by understanding of physics at the next smaller length scale and that generally verification of physical models at each sub-continuum level can be achieved only indirectly through measurements at a larger length scale.

One of the particularly interesting developments of the breakout sessions was the realization that the mathematical models that might be appropriate at one length scale can be entirely meaningless at another. For instance, Coulomb friction - however inaccurate - has meaning at the continuum level, but has no meaning when simulating individual asperity's. Further, even different continuum scales may call for consideration of different physics. While a local friction model might be appropriate in finite element modeling of aluminum-aluminum sliding on the micrometer level, models that account for surface chemistry would be appropriate for finite element modeling at smaller levels.

The evolution of these concepts is reflected in Figures 3.1, 3.2, and 3.3. The first of these is a list of disciplines associated with different length scales that might be expected to combine in a coherent manner to provide insight and predictive capability to the field of interface mechanics. This figure, Roadmap Version 1, played a major role in development of the workshop and identification of appropriate participants. As the discussions at the workshop commenced, the original draft of a roadmap (Figure 3.1) evolved so that at the end of the sessions, it had become Version 2 (Figure 3.2). Subsequent digestion of the various reports which emerged from the different sessions at the workshop then led to a third generation Road Map, which is shown in Figure 3.3. The group found these figure useful both to make conceptual connections and to identify programmatic opportunities.

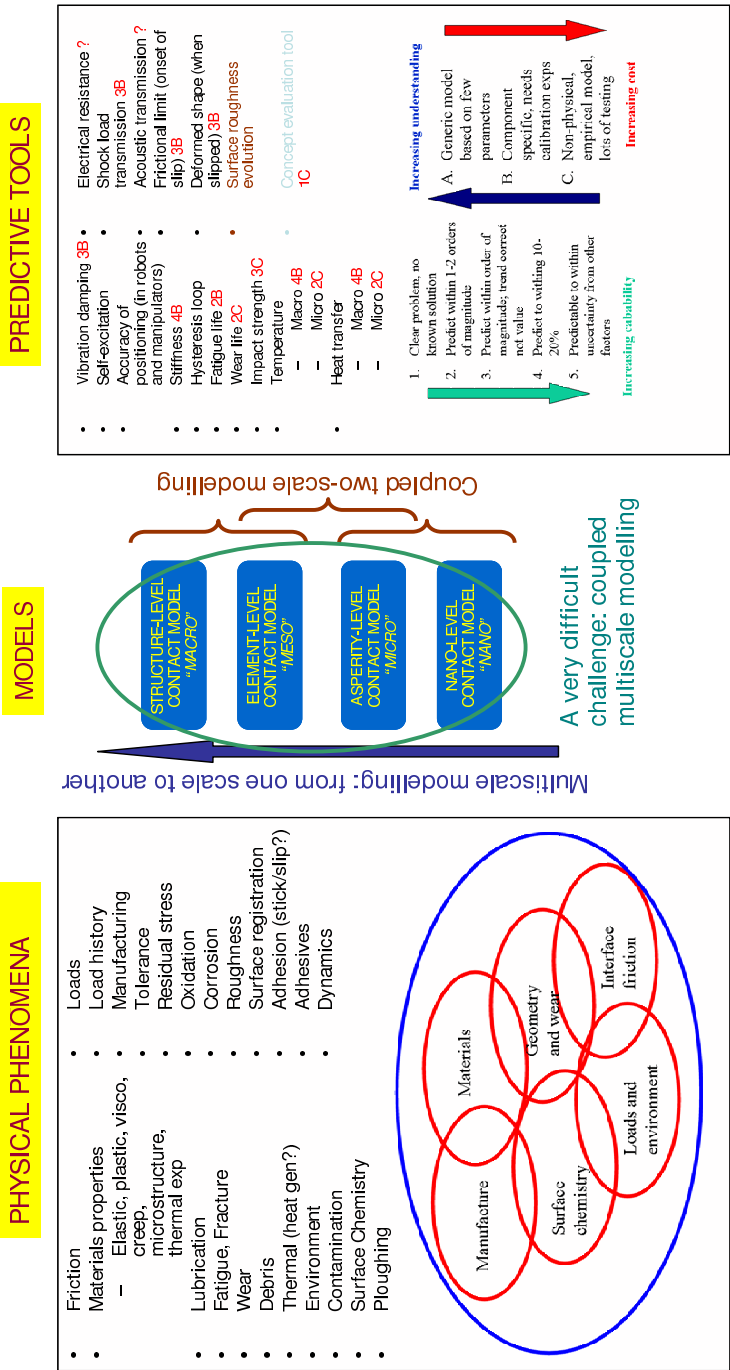
RESEARCH ROADMAP FOR FRICTION CONTACT AND WEAR IN STRUCTURES



Friction CONTACT ROADMAP v.1

Figure 3.1. Initial topic plot employed prior to the workshop to suggest physics disciplines that might be relevant to addressing frictional interface mechanics.

RESEARCH ROADMAP FOR FRICTION CONTACT AND WEAR IN STRUCTURES



Friction CONTACT ROADMAP v 2.

Figure 3.2. Roadmap developed during workshop discussions identifying physical phenomena, modeling tools, and levels of resolution that might be applicable to frictional interface mechanics.

Bottom-Up and Top-Down Vision for Research in Physics of Joint Mechanics

Much of the underlying physics is not understood.

The intrinsic multi-scale nature of the problem makes it resistant to a blind attack by computer simulation.

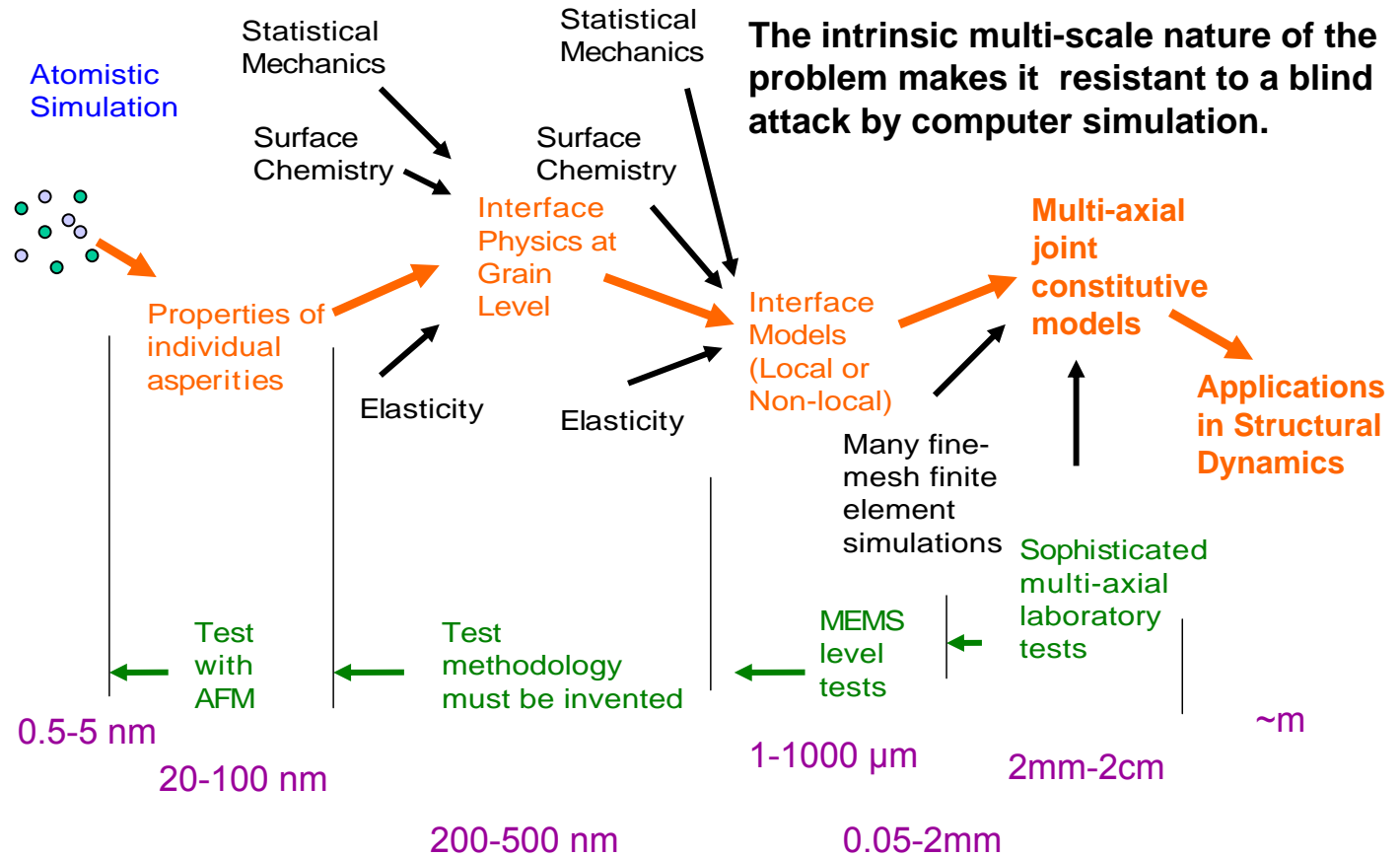


Figure 3.3. A roadmap developed by the conference organizers, having digested and reflected on the workshop discussions and products.

Chapter 4

Challenges

Repeated break-out sessions, involving several remixing of participants, identified three key challenges. Each of these challenges is narrowly enough focused that they might be tractable, yet accomplishment of any one of them would be a major step forward in addressing the problem of modeling joint mechanics from a physics basis.

Challenge 1: Experimental Measurements of Joint Properties

This challenge represents a first step in developing a “top down” joint model along the lines identified at the workshop. An essential prerequisite for this approach is a consensus on how to measure joint behaviour experimentally. The “challenge” therefore has two parts: (i) a standardization of experimental techniques and (ii) “top down” modelling and validation using the results from these experiments.

1. A “round-robin” exercise is envisaged where different laboratories measure the (quasi-static) tangential force/tangential displacement hysteresis loop for a well-characterized contact geometry and a “well-behaved” engineering material pair at a range of normal and tangential loads. A suitable contact might, for example, be a stainless steel sphere on a stainless steel flat. Displacements would be referenced to a particular pair of points within the contacting bodies and the challenge would be to measure the behaviour and subtract the compliance of the apparatus and the ‘non-contact’ part of the bodies to arrive at the hysteresis loop.
2. The second part of the challenge will draw upon the results of (i), together with other experiments, which may be conducted at the discretion of those taking part. The challenge will be to build a physically-based ‘top down’ model which will use experiments to derive an interface ‘constitutive law’ and then to use this model to predict the hysteresis loop in a contact configuration which is outside the range of those used to establish the material parameters in the law (e.g. a different surface roughness and/or a different material).

Challenge 2: Interface Physics

Physics-based understanding (both modeling and experiments) of the joint interface is needed. This interface is under partial slip regime and includes multi-scale surface topography and dynamic effects. Such physics-based research should include basic interfacial properties from nano-scale to micro-scale as well as the coupling between shear and normal degrees-of-freedom. Outcome would be a physics-based cohesive model that would be validated with structural (large scale) experiments and computational simulations.

Further details:

1. What is the friction behavior (physics) under partial slip conditions, including realistic roughness conditions, and vibroimpacts (not necessarily transients such as contact condition evolution with time, but more like steady-steady (or run-in) surfaces).
2. Develop physics-based contact and friction models applicable to joint interfaces.
3. Physics-based models could be based on/validated with careful interfacial experiments. Such experiments could include the measurement of shear contact stiffness and contact damping, and interfacial displacements, including micro-slip and micro-stick regions.
4. Physics-based models could also include elements of “bottom-up” approach, i.e., atomistic information that could somehow be coupled to realistic/observable properties.
5. Basic roughness effects are critical and need to be better understood. Issues involve measurements issues, scale issues, manufacturing processes, operating changes, protective thin film nano-coatings etc.
6. Once a physics-based model for a joint interface is developed, then it could be used to build up a new joint finite element that could be compared directly with the simple Coulomb model that is currently used.
7. A computational exercise described in (f) could also shed light to the extend of validity of a simple Coulomb friction versus a more accurate physics-based model.

Challenge 3: Multi-scale Modeling

This challenge represents a first step toward the development of a multi-scale framework that accommodates the simultaneous top-down and bottom-up coupling approach. In this two-way coupling approach, each interface is treated as an independent entity that can be represented at various scales through different types of “constitutive relations”.

1. With a bottom-up view, the first part of the challenge will be the development of a hierarchical material model that has roots in nano-mechanics (10^{-9}) while providing the mechanical material properties at micro-scales (10^{-6}). This model needs to account for the local state of deformation at the interface, thus transferring information from macro- and micro-scales (or computable scales) to nano-scales (or modeled scales). Micro-scale range may be envisioned as the scales associated with asperities, and therefore appropriate to describe the interfaces which are considered as “entities”. Now, with a top-down view, for large 3-D configurations, computational grids can be discretized down to millimeter scale (10^{-3}). That still leaves a gap of three orders of magnitude that needs to be bridged via, for example, the recently proposed Multi-scale Variational Framework. Here, the sub-scale modeling concept is to employ different PDEs at different levels in a variationally consistent manner.
2. The second part of the challenge will draw upon the results of item 1, together with experimental (sensor) data, to merge the two in a consistent fashion. For example, sensor data may be available at locations other than the joint interface. The challenge will be to build a mathematical framework that can accommodate this data in a physically consistent fashion, thus helping drive the mathematical problem with some discrete information on how the physical/experimental system behaves. This will address issues related to uncertainty in joint and other physical properties as well as boundary conditions in the physical systems under consideration.

Chapter 5

Summary and Conclusions

As illustrated by the Challenge documents developed by the workshop participants, the key barriers to solution of putting the engineering problem on a scientific footing derive from the multiple length scales involved. These length scales span approximately nine orders of magnitude and the mathematical models appropriate for each scale differ from those appropriate for smaller and larger scales. The three challenges have to do with different approaches to accommodating the resulting complexities: 1) making systematic measurements of joint properties and development of “top-down” models, 2) making measurements at intermediate (micro) length scales to develop quantitative but phenomenological friction models that can be used in a “middle-up” modeling effort, 3) development of mathematical tools to assist in mapping the physics calculated at one length scale to models that live at the next larger length scale.

One of the particularly interesting developments of the workshop was the realization that the mathematical models that might be appropriate at one length scale can be entirely meaningless at another. For instance, Coulomb friction - however inaccurate - has meaning at the continuum level, but has no meaning when simulating individual asperities. Further, even different continuum scales may call for consideration of different physics. While a local friction model might be appropriate in finite element modeling of aluminum-aluminum sliding on the micrometer level, models that account for surface chemistry would be appropriate for finite element modeling at smaller levels.

Another realization manifest in the workshop was a greater understanding of the difficulty of obtaining a “first principles” model for joint mechanics. Clear understanding of the physics dominant at each length scale requires some understanding of that occurring at smaller length scales. On the other hand, verification of the models at small length scales can be obtained only indirectly through experiments at larger length scales.

The path forward necessarily involves three components:

- Continued development of “joint models” for structural dynamics applications. This constitutive modeling will be used to add a predictive component to modeling, since the joint models are parameterized by measurement, but the pre-

dictions can be made before a structure is assembled. Further these models can be used with finite element models to validate friction models developed from work at smaller length scales.

- Experimental and computational scientific investigations at each length scale, usually involving phenomenological models suggested by experiment at the current length scale and by simulations at the next smaller scale.
- Development of mathematical tools for bridging length scales. This is of course much more easily said than done. Most applications of multi-scale modeling exploit features that are not readily apparent in joint interface models; homogenization techniques do not appear applicable and techniques that postulate simple physics at the smaller length scale would not appear appropriate. Nonetheless the technological reward for success is so significant, that this area of research must be pursued.

Finally, the workshop demonstrated the value of bringing together people working at the many length scales inherent in joint physics.

Appendix A

Slide Sets Presented at the SNL/NSF Joints Workshop

The scope of the workshop is illustrated by the following slide sets of presentations made there. Leading researchers from the United States and Europe brought their perspectives on the state of physics understanding at each length scale relevant to the problem. Among those presentations were an overview of atomic simulation of interface interactions (Prof. Mark Robbins of Johns Hopkins University), a talk on a tribological view of joint mechanics (Professor Andreas Polycarpou, University of Illinois), two discussions on current capabilities with respect to solving elastic-frictional contact problems (Professors David Nowell and David Hills, University of Oxford), a discussion on computational nonlinear dynamics of structures with friction and gaps (Evgeny Petrov, Imperial College), and a talk on computational approaches to multi-scale modeling and their potential role in the simulation of joint mechanics (Professor Arif Masud, University of Illinois).

One of the outstanding values of this workshop was that it exploited the strengths of the different approaches pursued in Europe and the US in addressing this famously difficult problem.

A.1 Slide Presentation of Dan Segalman, Sandia National Laboratories, Albuquerque, NM: *Challenges of Joint Modeling in Structural Dynamics*



Challenges in Joint Modeling in Structural Dynamics

**Why This Issue is Important and
Why These Problems are Hard**

Daniel J. Segalman

**NSF/SNL Workshop On Joint Modeling of
Structures, Arlington DC 16-18 October 2006**



Sandia is a multiprogram laboratory operated by Sandia Corporation, a Lockheed Martin Company,
for the United States Department of Energy's National Nuclear Security Administration
under contract DE-AC04-94AL85000.




Outline

- **Predictive Modeling**
 - Where it is Important
 - The Tall Pole in the Tent
- **Empirical Properties of Joints: Softening and Dissipation**
- **Why Joint Modeling is Hard**
 - More Elements is not a Solution
 - Local Properties are only Part of the Story
- **Standard Practice**
- **The Beginning of an Approach to Accommodate Joint Nonlinearities**
- **How Life Should Be**
 - Mapping from multiscale physics to FE environment
 - Roark's Handbook for properties and parameters

2








Where We *Must* be Predictive -

Where correct answers are necessary and either experiments are just too expensive or are impossible

- satellites
- next generation space telescopes
- jet engines and jet engine failure
- nuclear weapons systems

3



 



Predictive Modeling – Is that not what we already do?

- In general, engineers use simulation
 - To interpolate/extrapolate among experiments
 - Note the tuned parameters
 - To help explain experiments
 - To help design experiments
 - To provide design guidance
 - To estimate factors of safety
- We generally do not try to predict with precision
 - Finer than the intrinsic variability of the problems
 - That which requires physics for which there are no models

4

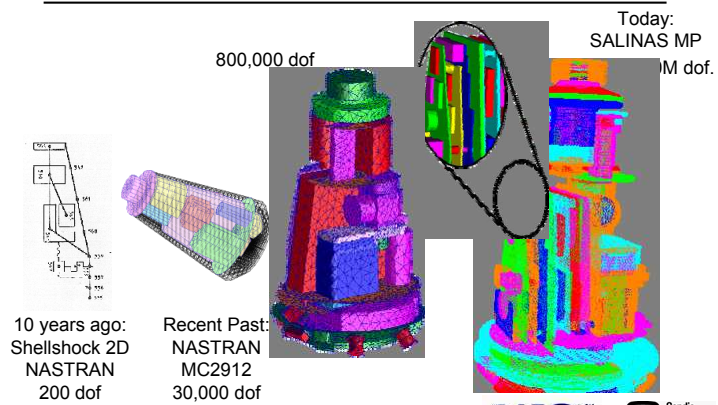
Traditional Barriers to Predictive Modeling

- Discretization error
- Uncertainty in Material Properties
- Uncertainty in loads/boundary conditions
- Missing Physics - Interface Mechanics (Joints)

5




Discretization Error: Less of an Issue Now Than in the Past



6





Traditional Barriers to Predictive Modeling

- Discretization error
 - Mitigated substantially by MP technology
 - Uncertainty in Material Properties
 - Subject of separate research efforts
 - Uncertainty in loads/boundary conditions
 - Better measured, calculated, or bounded
 - Missing Physics
 - Interface Mechanics (Joints)
 - The Tall Pole in the Tent
 - Topic of this workshop
- Topics include misfit, interference, and variability

7



Significance of Joint Mechanics to Structural Dynamics

- A (*the**) major source of vibration damping
- A (*the* *) major source of system non-linearity
- A (*the* *) major source of part-to-part variability
- A (*the* *) principle missing physics element of the simulation effort

*depending on configuration and load

8



Major Experiments on Joints



Base Excitation
at Resonance



Ring-Down of
Free Vibration



Quasi-Static
Pull

Intrinsic difficulty of joint testing – the key physics is in a hidden interface

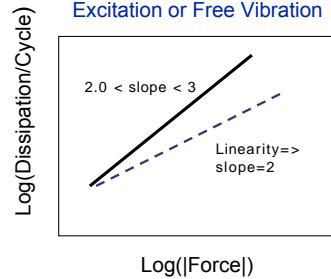
- The necessity of complementary joint-less specimens
- The limitations of quasi-static pull

9



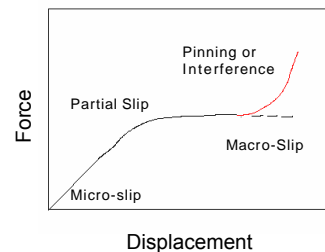
Empirical Nonlinearity of Joints

Dissipation from Base
Excitation or Free Vibration



**Nonlinearities even at
Small Displacement**

Monotonic Pull

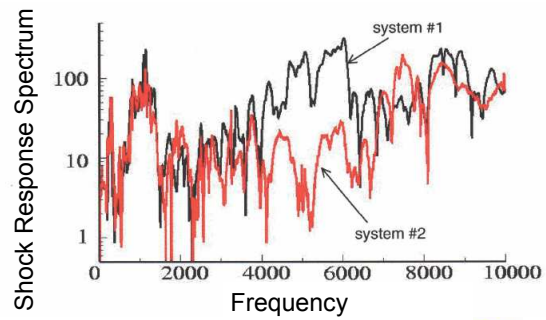


Large Displacement

10



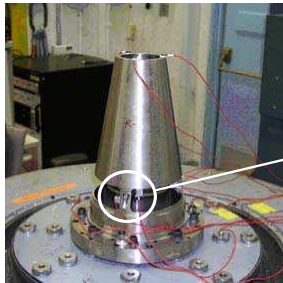
Example of Variability Due to Joints



11



Example of Nonlinearity Due to Joints



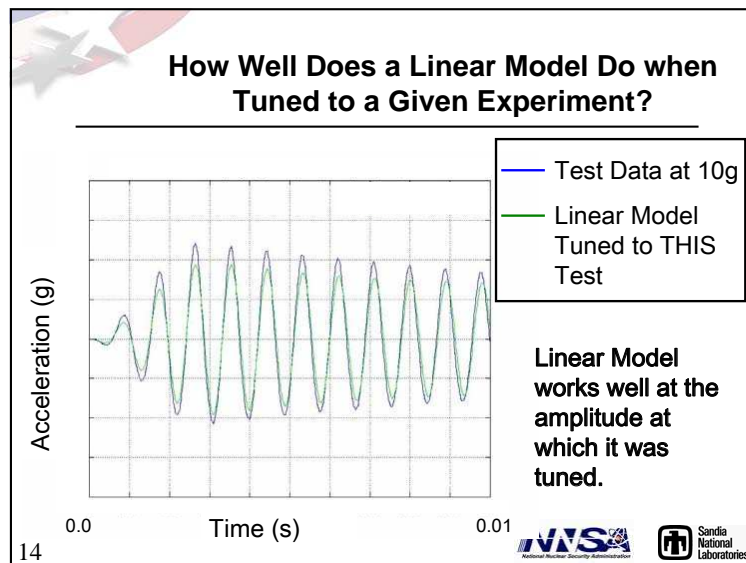
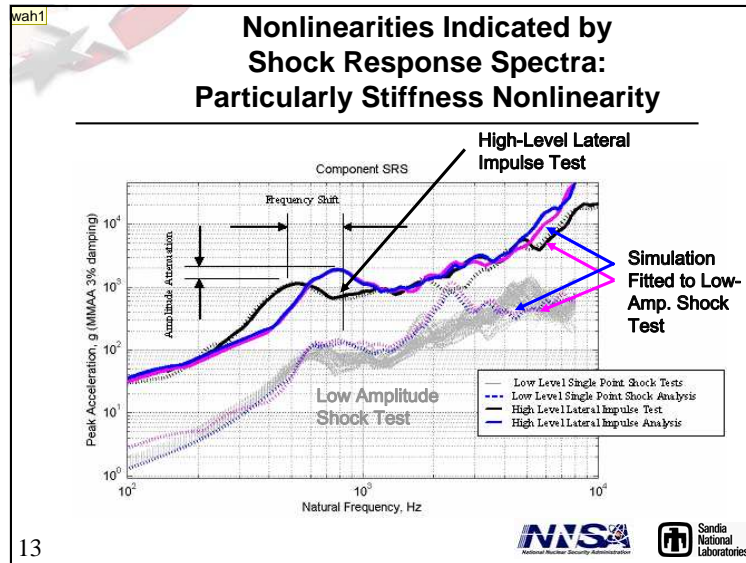
Mock sub-structure of a generic built-up assembly



Subject to various levels of transient lateral base excitation.

12





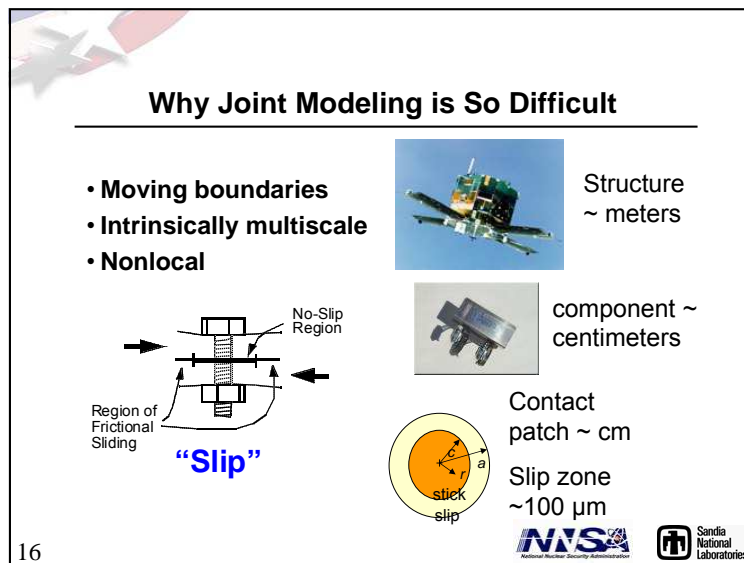
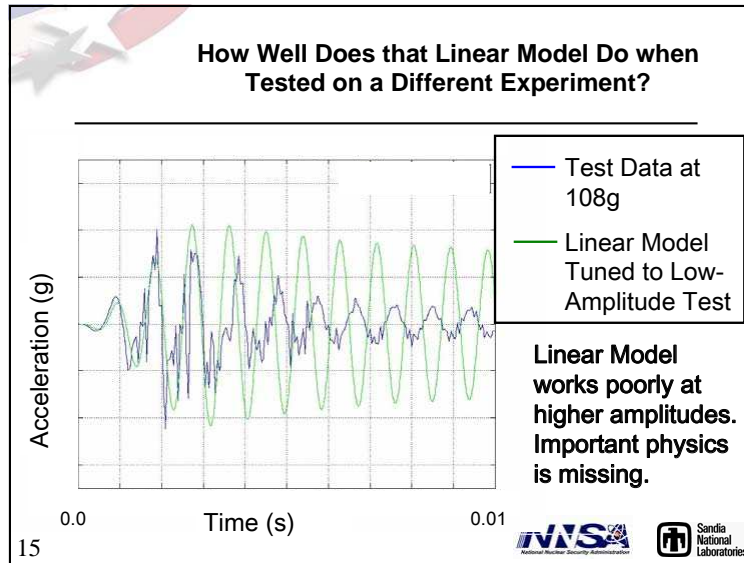
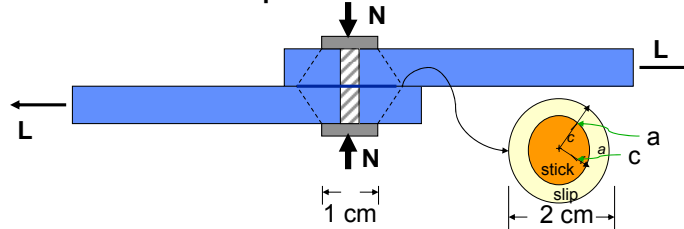


Illustration of Computational Difficulties

- Consider a lap joint with dimensions selected so that the contact patch is circular of radius $a=1\text{ cm}$

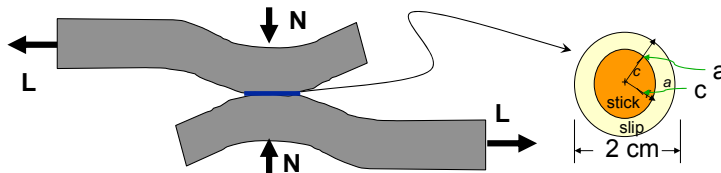


- Approximate the elastic contact problem with the Mindlin solution for two spheres.

17



Estimation of Interface Dimensions



- Normal Load** $N = 4000\text{ Newtons}$
 - Lateral Loads** $L \in (0.05\mu N, 0.8\mu N)$
 - Elasticity that of Steel**
 - Slip Zone:**
- Say our interest in structural response is in 100Hz-3500Hz

$$\frac{c}{a} = \left[1 - \left(\frac{L}{\mu N} \right) \right]^{1/3} \Rightarrow \frac{c}{a} \in (0.58, 0.98) \Rightarrow \frac{a-c}{a} \in (0.02, 0.42)$$

18



Necessary Finite Element Scales Courant Times

- For case of small tangential loads $L = 0.05 \mu N$
element dimension in slip zone necessary to
capture dissipation is $l = \frac{a-c}{10} = 20 \mu m$ and
Courant time is 4 ns
- To simulate 10 ms (one cycle of 100 Hz
vibration) requires 2.5E6 time steps.

Compare this with 3E4 time steps if the
problem were linear and solved implicitly

19



Even if This Problem is Solved Quasi-Statically

- In each load cycle, the width of the slip zone twice spans
from $a - c = 0$ to $a - c = 0.42$
- With characteristic element size in the contact patch

$$l = \frac{a-c}{10} = 20 \mu m$$

- Observing that quasi-static contact has difficulty
changing stick-slip status of more than one node at a
time and each time step required numerous iterations
- Approximately 800 steps per cycle are required, each
representing hundreds of iterations.

Conservation of Cussedness

20



Simply Employing More Elements is not the Solution

- One cannot reasonably directly slave a micro-mechanics contact algorithm to a structural dynamics analysis.
- Tools are needed to cross the dimensions

21



Interface Mechanics Involve More than Local Constitutive Behavior

- The surface degrees of freedom on an elastic body are coupled through the elastic fields within the body.

$$\tau(x) = \int_S G(x, y) u(y) dA$$

- Displacement is solved subject to constraints

$$\dot{u}(x) (|\tau(x)| - \mu \sigma_N) = 0 \quad \text{and} \quad |\tau(x)| \leq \mu \sigma_N$$

- Refinement of the friction constitutive equation still leaves a difficult nonlinear system of equations to solve

Refinement of frictional laws may be necessary to obtain better answers, but it cannot simplify the problem

22



Standard Practice for Ignoring the Nonlinearity of Joints in Structural Dynamics

How Elements of Process



Analyst c
coarse m
model pu
tunable s
interface
postulating
proportional/modal
damping

- Assume system to be linear
- Represent each joint DOF as a linear spring
- Build and test a prototype structure
- Tune the spring stiffnesses to match frequencies
- Tune modal (or more complicated) damping to match damping of structure

stiffness and modal
damping to match
test. He then makes
prediction

sis

t is
n
del



23



Not Predictive for Real Systems

If you have to build the full structure in order to predict structural response, then you are not predictive.

The problem is fundamentally nonlinear and important phenomena cannot be captured by tuned linear models. (Silk purse/Sow's ear issue.)

24



The Beginning of an Approach to Accommodate Joint Nonlinearities

What would be the first step to bring more physics into the analysis?

- Explicitly account for the joint nonlinearity
- Place a joint model at the location of the actual joint.

Strategy

- Represent the whole joint with a small number of scalar constitutive models.
- Determine the parameters of these models either from micro-modeling or from experiments on individual joints.

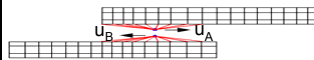
D.J. Segalman *ASME Journal of Applied Mechanics*, V. 72, 752 (2005)

D.J. Segalman, *Structural Control and Health Monitoring* V. 13, Issue 1, (2006)

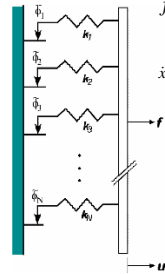
25



The Whole-Joint Approximation and Iwan Models for Shear Joints

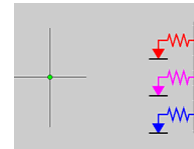


Whole-Joint approximation for interface



$$f(t) = \int_0^\infty \rho(\phi) [u(t) - x(t, \phi)] d\phi$$

$$\dot{x}(t, \phi) = \begin{cases} \dot{u} & \text{if } |u - x(t, \phi)| = \phi \text{ and } \dot{u}(u - x(t, \phi)) > 0 \\ 0 & \text{otherwise} \end{cases}$$



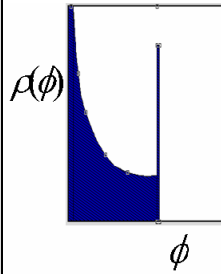
The joint properties are characterized by $\rho(\phi)$

26



A Four-Parameter Iwan Distribution

$$\rho(\phi) = R\phi^\chi (H(\phi) - H(\phi - \phi_{\max})) + S\delta(\phi - \phi_{\max})$$



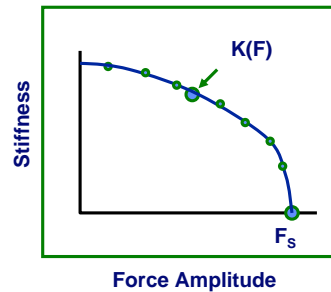
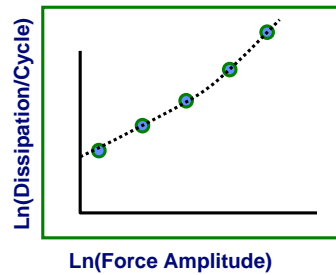
- Nearly linear behavior at low amplitude.
- Power-law energy dissipation
- Manifests micro- & macro-slip
- Physically reasonable
- Tractable

Parameters R, S, χ, ϕ_{\max} map to some or more physical significance
 F_s, K_T, χ, β

27



Determining Joint Parameters: Measured Properties

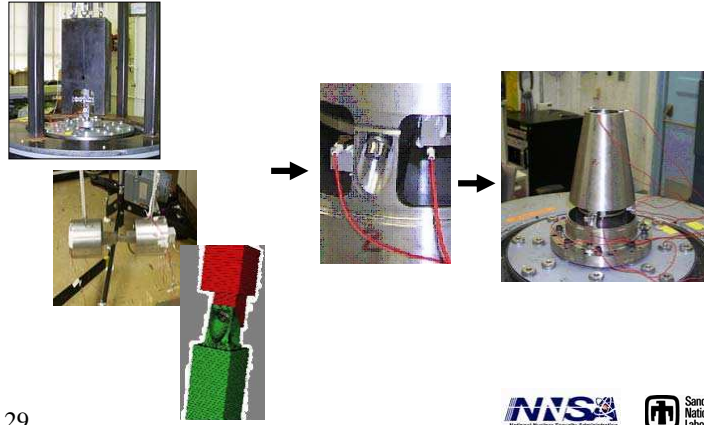


Experiments yield dissipation $D(F)$ as a function of force amplitude, tangent stiffness $K(F)$ at load, and yield force F_s .

28



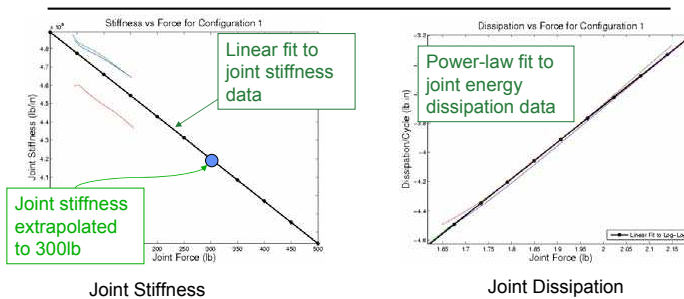
Calibration of Individual Joints to Predict Dynamics of 3-Legged Structure



29



Plot Joint Stiffness and Dissipation as Functions of Joint Force



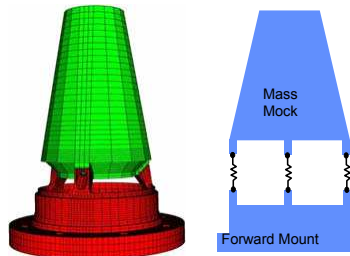
Model Parameters are selected to match the stiffness at 300lb force and to match the apparent power-law dissipation.

30



Predictions with Joint Model

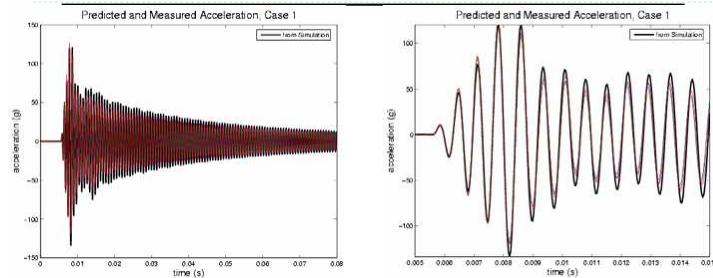
- Employ 4-parameter model at joint
- Represent the rest of the structure with linear finite elements
- Excite base sufficiently to cause macro-slip.



31



Blast Simulation for Configuration 1

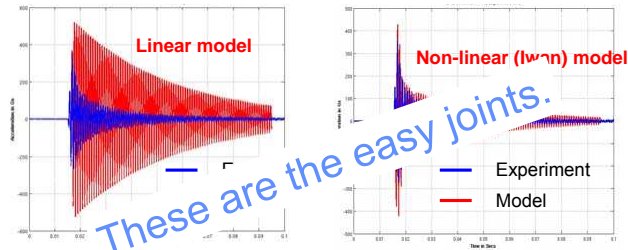


Explicit incorporation of a joint model can significantly improve the quality of predictions.

32



Predictions for Axial Base Excitation that Entails Macro-Slip



Explicit incorporation of a joint model can significantly improve the quality of predictions.

33



Conclusions: I

- Conventional structural dynamics is not predictive in the manner now required
- There are fundamental barriers to incorporating micro-meshes in structural dynamics calculations
- Employing joint models explicitly in structural dynamics can greatly improve the quality of predictions

34





Conclusions: II

- The whole-joint approach, though a significant improvement is no where near adequate
 - Does not account for the multi-dimensional nature of loads.
 - Does not account for the true complexity of contact: moving contact patch, varying normal loads ...
 - Induces fallacious stress fields near contact.
- Fundamental research must be done in understanding joint mechanics and realizing that understanding in terms of predictive and useful structural dynamics tools.

We need not new models, but better models

35



Expectation

- This is a class of problems whose core physics spans many length scales and will require
 - Research at several length scales
 - Development of conceptual tools to span those length scales
 - New methods of incorporating distributed constitutive response into structural dynamics

36





Structural Dynamics of Jointed Structures is Analogous to Hydrodynamics with Turbulence

| Turbulence | Joints |
|---|---|
| • Multiple scales limit DNS | • Multiple scales limit DNS |
| • Closure models are postulated to connect micro-mechanics to continuum | • Closure models are postulated to connect micro-mechanics to continuum |
| • Fundamentally important in Fluid Mechanics | • Fundamentally important in Structural Dynamics |
| • Long-Standing Problem | • Long-Standing Problem |
| • Very significant in drag, less significant in lift | • Very significant in damping, less significant in stiffness |
| • Heuristic, qualitative understanding | • Heuristic, qualitative understanding |

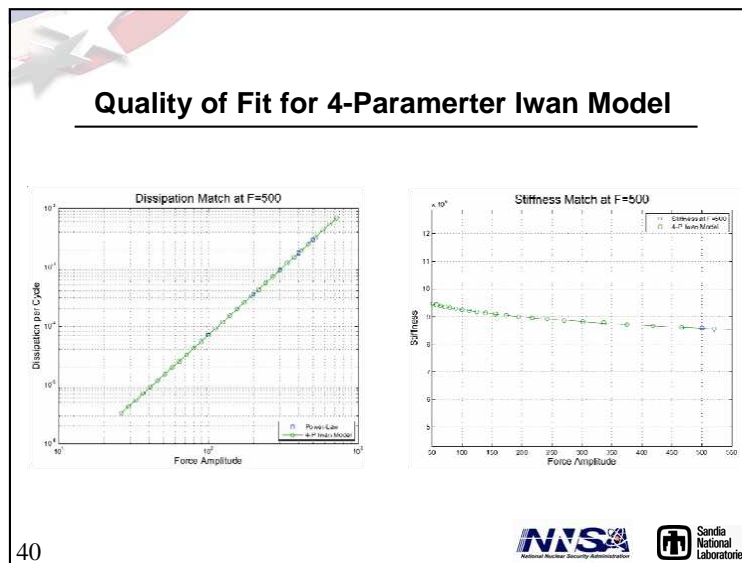
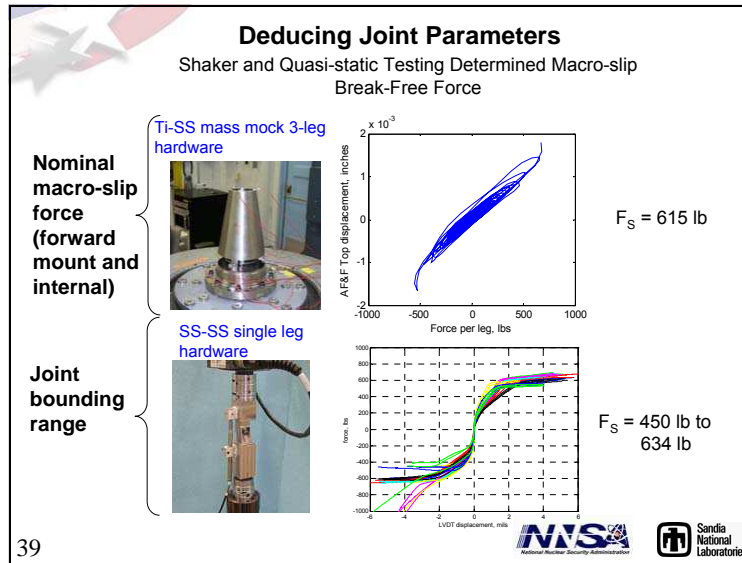
37

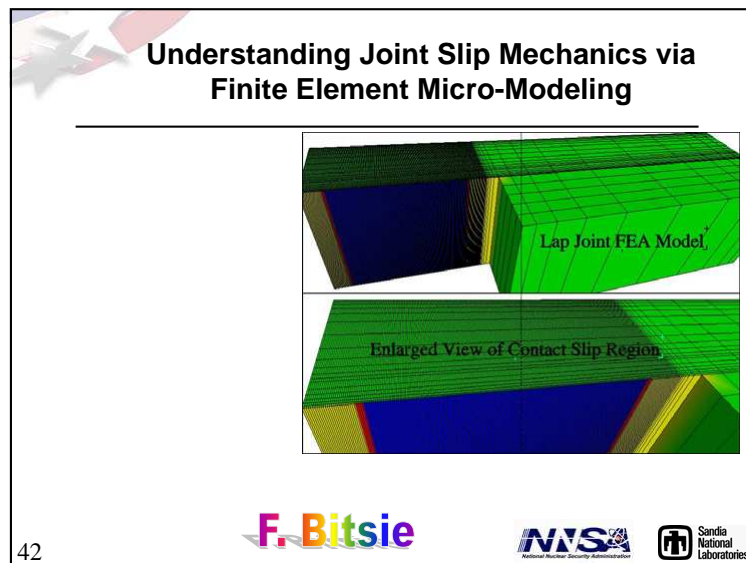
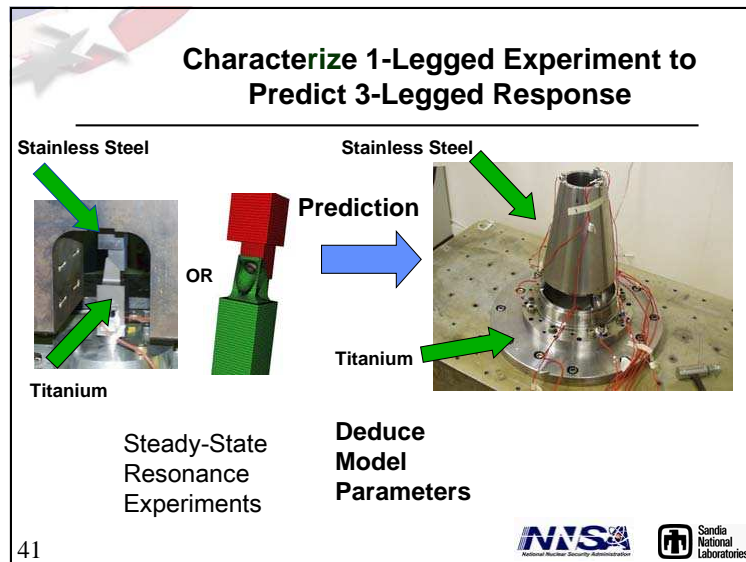



Backup

38











Review and Approval
Unclassified, Unlimited Release

- **SAND Number: 2006-6117C**
- **tracking (document) number is: 5246333.**

43

A.2 Slide Presentation of David Ewins, Imperial College, London, England: *The Influence of Joints on the Dynamics of Gas Turbine Structures*

The Influence of Joints on the Dynamics of Gas Turbine Structures

David Ewins

Imperial College London

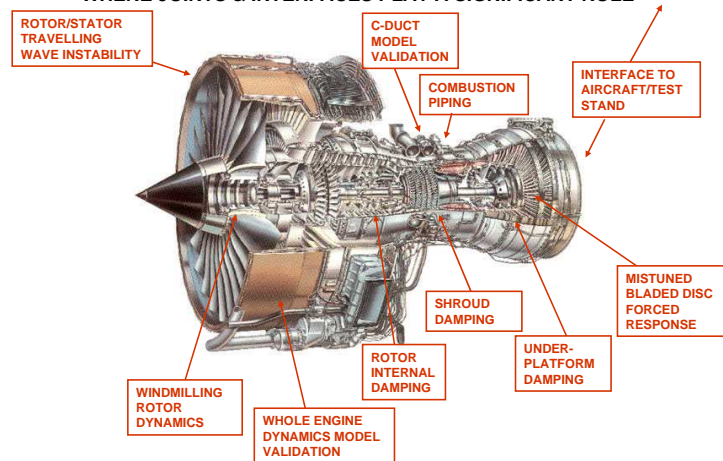
NSF-Sandia Joints Modeling Workshop, Arlington, USA, 16-18 October, 2006

D J Ewins

Centre of Vibration Engineering

Imperial College
London

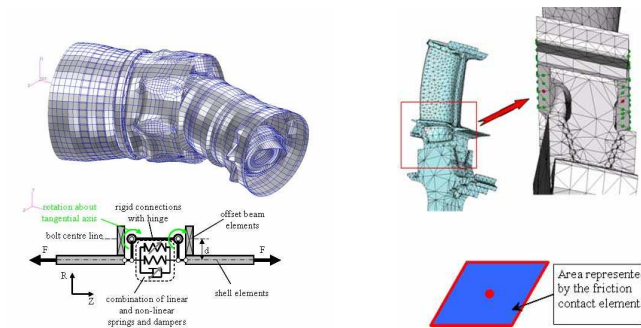
TYPICAL VIBRATION PROBLEM AREAS IN JET ENGINES WHERE JOINTS & INTERFACES PLAY A SIGNIFICANT ROLE



NSF-Sandia Joints Modeling Workshop, Arlington, USA, 16-18 October, 2006

D J Ewins

Two Areas of Particular Interest & Concern: Whole-engine Casings & Bladed Assemblies



shop, Arlington, USA, 16-18 October, 2006

D J Ewins

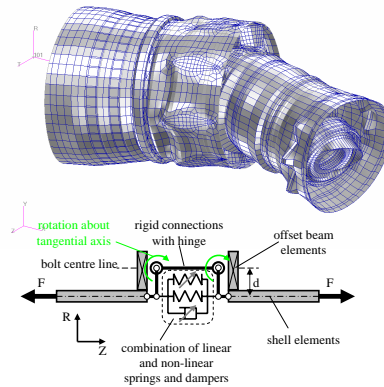
The Critical Influences of Joints on the Dynamics of Gas Turbine Structures

- 'Joints' exert a non-negligible effect on the stiffness (and thus natural frequencies) and damping of all structural assemblies
- Current structural dynamic modelling capabilities are very much less advanced in respect of joints and interfaces than for any of the components that they connect
- Such models as do exist are heavily dependent on the availability of associated experimental measurements, many of which are difficult and expensive to acquire
- Consequently, the optimal design of many critical structures in gas turbines is significantly restricted by the lack of reliable predictive models of joints

NSF-Sandia Joints Modeling Workshop, Arlington, USA, 16-18 October, 2006

D J Ewins

Incorporating Nonlinear Joint Dynamics Behaviour of the Structure into FE Models

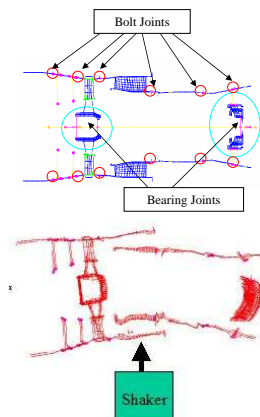
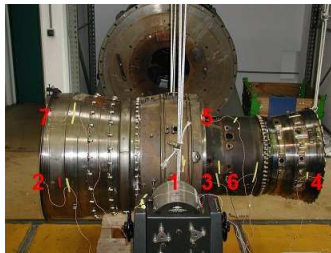


Modelling Approach for Bolted Flange Joints

NSF-Sandia Joints Modeling Workshop, Arlington, USA, 16-18 October, 2006

D J Ewins

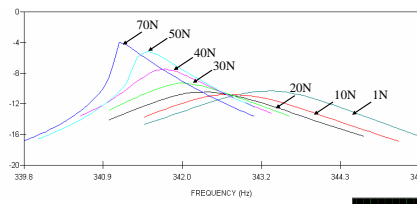
Aero-engine Casing Test Configuration



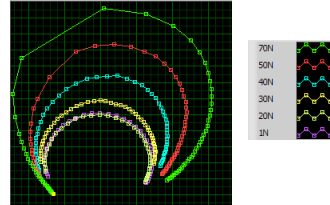
NSF-Sandia Joints Modeling Workshop, Arlington, USA, 16-18 October, 2006

D J Ewins

Test Data Obtained Using Force-Control Test



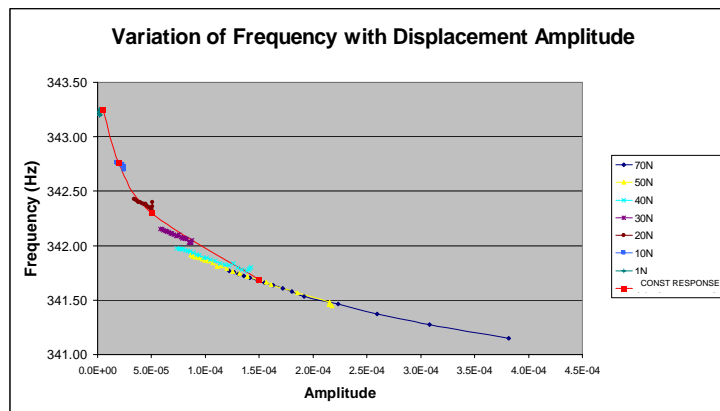
The first-order FRFs in Nyquist format are used to select the frequency range and frequency interval of measurement for CLV test



NSF-Sandia Joints Modeling Workshop, Arlington, USA, 16-18 October, 2006

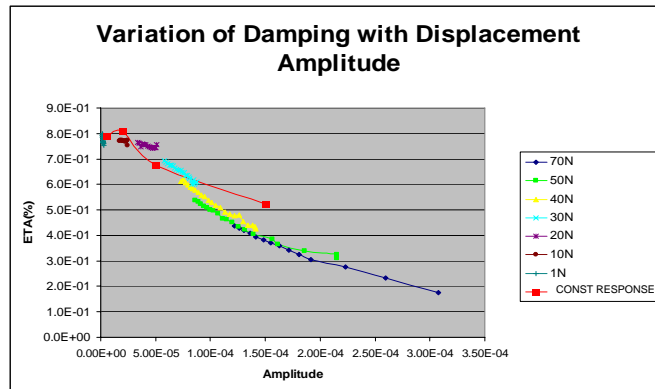
D J Ewins

Variation of Frequency with Displacement Amplitude



NSF-Sandia Joints Modeling Workshop, Arlington, USA, 16-18 October, 2006

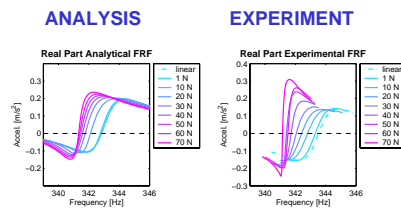
D J Ewins



NSF-Sandia Joints Modeling Workshop, Arlington, USA, 16-18 October, 2006

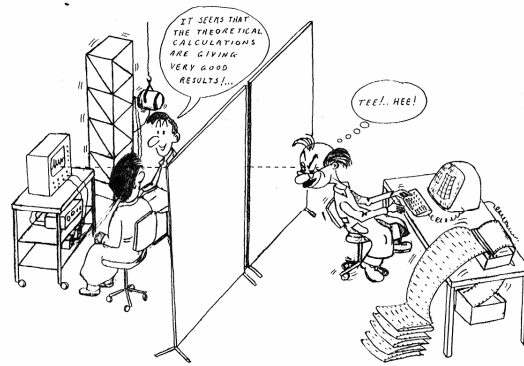
D J Ewins

Comparison of Analytical and Experimental Non-linear FRF



NSF-Sandia Joints Modeling Workshop, Arlington, USA, 16-18 October, 2006

D J Ewins

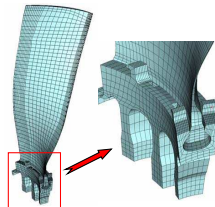
RETRO - PREDICTION

NSF-Sandia Joints Modeling Workshop, Arlington, USA, 16-18 October, 2006

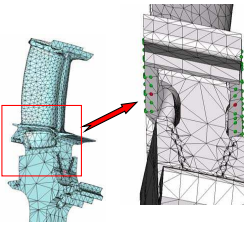
D J Ewins

Examples of dynamic contact phenomena in bladed discs

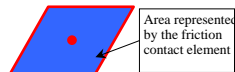
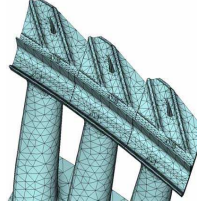
**Root damping and
variable contact**



Underplatform dampers



**Contact of
shrouds**



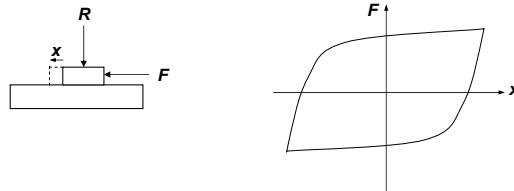
NSF-Sandia Joints Modeling Workshop, Arlington, USA, 16-18 October, 2006

D J Ewins

Characterization of Non-Linear Structural Elements

Non-linear, inertia-free structural components are generally characterized by a restoring force surface $F = f(x, \dot{x})$

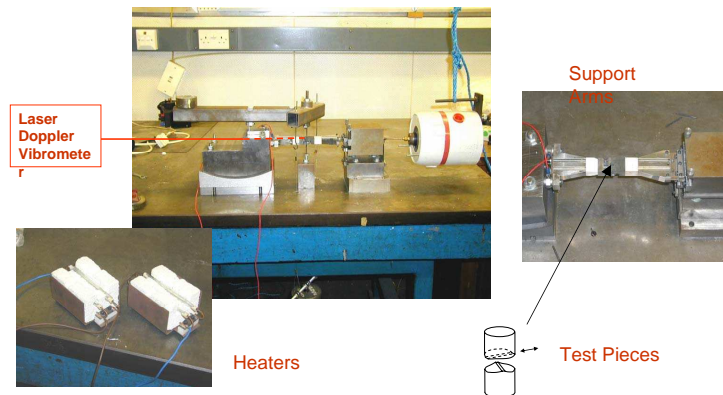
For a friction contact it is reasonable to assume that $F = f(x, \text{sign}(\dot{x}))$ and a Force/Relative Displacement hysteresis loop is used.



NSF-Sandia Joints Modeling Workshop, Arlington, USA, 16-18 October, 2006

D J Ewins

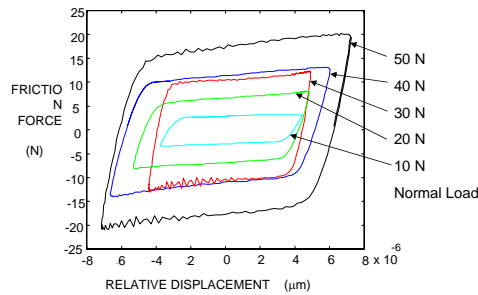
FRICTION HYSTERESIS LOOP TEST RIG.



NSF-Sandia Joints Modeling Workshop, Arlington, USA, 16-18 October, 2006

D J Ewins

A set of hysteresis loops, measured at different applied normal loads.



NSF-Sandia Joints Modeling Workshop, Arlington, USA, 16-18 October, 2006

D J Ewins

The Structural Dynamics & Integrity Needs for Much Better Modelling of the Joints in Gas Turbines – 1/2

- Current methods to account for the effects of joints and interfaces on the dynamics and integrity of gas turbine structures are basic, expensive and 'post'dictive, rather than predictive (sometimes referred to as 'retropredictive')
- They do not provide a full understanding of the controlling physics and, as a result, a model constructed for one particular joint cannot readily be extrapolated to another joint
- Today's joint models are much less advanced than those of the components which they connect
- The essential need for measured data inhibits attempts to use today's models to design joints so that they exhibit specific properties

.....

NSF-Sandia Joints Modeling Workshop, Arlington, USA, 16-18 October, 2006

D J Ewins

The Structural Dynamics & Integrity Needs for Much Better Modelling of the Joints in Gas Turbines – 2/2

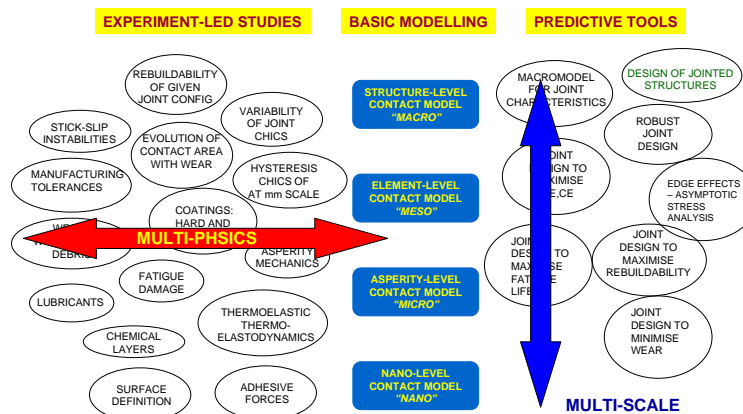
.....

- Truly predictive models for joints and interfaces are now urgently required:
 - (i) to restore a balance between the models of all the individual components in a complex structural assembly, and
 - (ii) to pave the way to proactive design of joints to provide required properties (rather than simply representing characteristics that have been observed by measurement) and thereby to better optimise the design of these complex structures

NSF-Sandia Joints Modeling Workshop, Arlington, USA, 16-18 October, 2006

D J Ewins

RESEARCH ROADMAP FOR FRICTION CONTACT AND WEAR IN STRUCTURES



Friction CONTACT ROADMAP v 6.3

NSF-Sandia Joints Modeling Workshop, Arlington, USA, 16-18 October, 2006

D J Ewins

GOAL, OBJECTIVE, TASK

GOAL

To be able to optimise design of structures with joints and interfaces from structural dynamics and integrity considerations

OBJECTIVE

To be able to construct mathematical models of joints and interfaces from conventional input data

TASK

To formulate the problems involved in the effective modelling the dynamics of structural joints involving friction contacts
- to define the terrain containing all the phenomena that must be included in an effective model

NSF-Sandia Joints Modeling Workshop, Arlington, USA, 16-18 October, 2006

D J Ewins

AN APPROACH TO THE TASK

Using the RoadMap as a guide,

- (i) compile a list of all individual phenomena which need to be taken into account in modelling joint dynamics behaviour
- (ii) Define the status of current modelling capability for each phenomenon
- (iii) Develop the interdependencies between these various phenomena, and assess the status of their development
- (iv) Chart possible scenarios for developing a uniform-level and consistent capability embracing all the critical phenomena, in graded stages – basic, design, advanced,...

NSF-Sandia Joints Modeling Workshop, Arlington, USA, 16-18 October, 2006

D J Ewins

A.3 Slide Presentation of Evgeny Petrov, Imperial College, London, England: *Analysis of Nonsmooth Nonlinear Dynamics of Structures with Friction and Gaps*

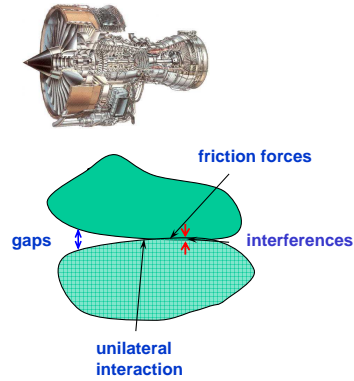
Analysis of nonsmooth nonlinear dynamics of structures with friction and gaps

Evgeny Petrov
Imperial College London

Centre of Vibration Engineering

Imperial College
London

Nonlinear dynamics of structures: sources of nonlinear structural behaviour



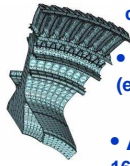
Sources of nonlinearities:

- friction forces;
- unilateral interaction;
- variable contact area;
- variable contact stiffness
(e.g. Hertzian contact or special devices)
- gaps and interferences

NSF-Sandia Joints Modelling Workshop, Arlington, USA, 16-18 October, 2006

E.Petrov

Methodology developed for analysis of nonlinear dynamics of complex structures

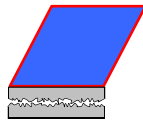
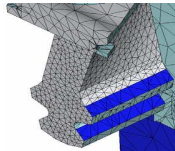


- Realistic large-scale models of $\sim 10^6$ DOFs (which are currently used in linear analysis)
- Appropriate modelling of friction contact interaction (e.g. Coulomb friction model is often not acceptable)
- Accurate calculation of forced response levels (up to 16 meaning figures in numbers computed)
- Fast calculations (typical: ~minutes, for some cases ~hours)
- Generic methods applicable to different machinery structures
- Effective frequency-domain methods (e.g. MHB) for steady-state vibrations

NSF-Sandia Joints Modelling Workshop, Arlington, USA, 16-18 October, 2006

E.Petrov

Modelling of friction contact interfaces: area contact element



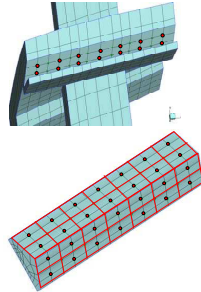
- 1) Size of elements can be (but not necessarily) similar to size of FE mesh at contact interfaces
- 2) New phenomenological friction models (original, not Coulomb) allowing for 3D motion of contacting nodes. Cases of partial or full separation of paring contact surfaces are included.
- 3) Anisotropy, inhomogeneity, and time variation of contact interface parameters can be described
- 4) Expressions for friction and unilateral contact interaction forces are analytically derived: resulting in very fast and accurate calculations
- 5) There is no need to know *a priori* actual contact area: the element determines this area as a result of calculations

NSF-Sandia Joints Modelling Workshop, Arlington, USA, 16-18 October, 2006

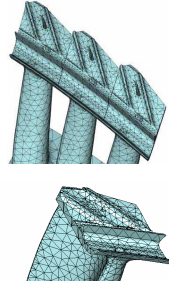
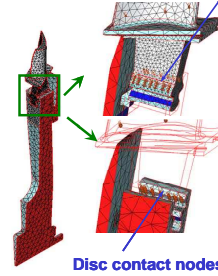
E.Petrov

Modelling of interaction at contact surfaces by area contact elements

Underplatform dampers



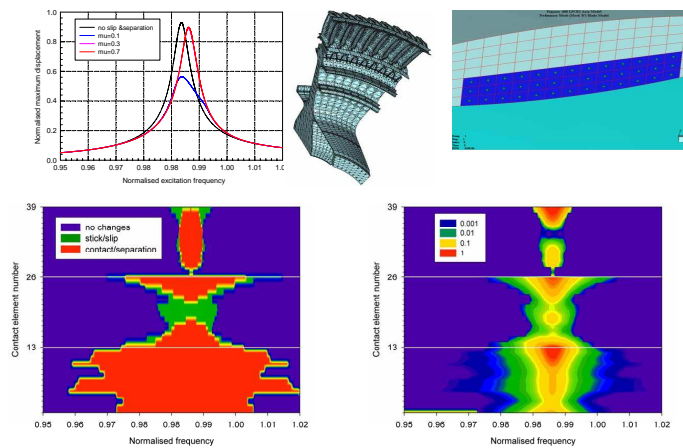
Contact of shrouds

Root damping with variable contact
Blade contact nodes

NSF-Sandia Joints Modelling Workshop, Arlington, USA, 16-18 October, 2006

E.Petrov

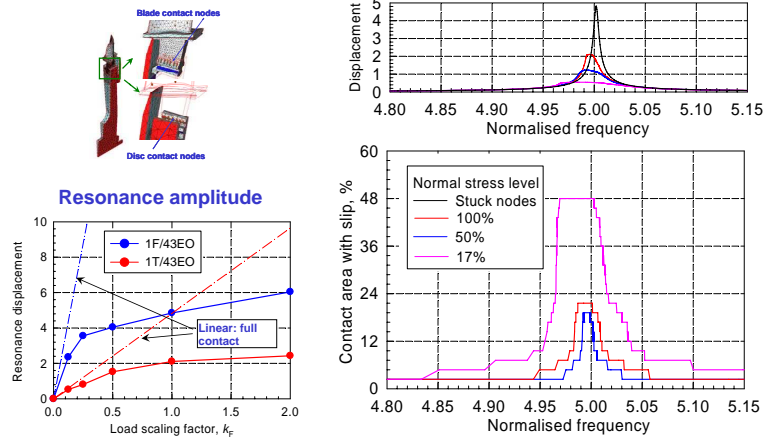
Analysis of forced response of a bladed disc with friction contacts of shrouds



NSF-Sandia Joints Modelling Workshop, Arlington, USA, 16-18 October, 2006

E.Petrov

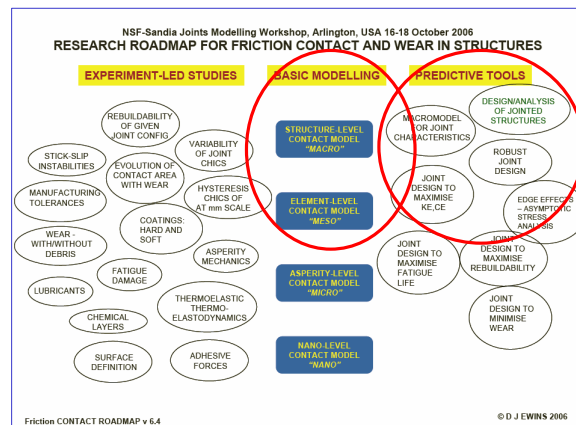
Effects of root damping on forced response



NSF-Sandia Joints Modelling Workshop, Arlington, USA, 16-18 October, 2006

E.Petrov

The Roadmap and our research activities



NSF-Sandia Joints Modelling Workshop, Arlington, USA, 16-18 October, 2006

E.Petrov

Challenges in the predictive analysis of dynamics of structures with friction interfaces

- 1) Difficulty in obtaining parameters of friction contact models: experiments usually require large effort, are not always conclusive and some parameters are currently not determined.
- 2) Inevitable scatter of contact conditions at contact interfaces can produce significantly different dynamic characteristics
- 3) Accurate description of contact interactions requires sometimes to use many contact elements and many harmonics in the response, hence large computational effort.

NSF-Sandia Joints Modelling Workshop, Arlington, USA, 16-18 October, 2006

E.Petrov

References

1. Petrov, E.P. and Ewins, D.J., "State-of-the-art dynamic analysis for nonlinear gas turbine structures" J. of Aerospace Engineering, Proc. of the IMechE, Part G, 2004, vol.218, No G3, pp.199-211
2. Petrov, E.P. and Ewins, D.J., "Generic friction models for time-domain vibration analysis of bladed discs," Trans. ASME: J. of Turbomachinery, 2004, Vol.126, January, pp.184-192
3. Petrov, E.P., "A method for use of cyclic symmetry properties in analysis of nonlinear multiharmonic vibrations of bladed discs," Trans. ASME: J. of Turbomachinery, 2004, Vol.126, January, pp.175-183
4. Petrov, E.P., "Sensitivity Analysis of Nonlinear Forced Response for Bladed Discs with Friction Contact Interfaces", Proceedings of ASME Turbo Expo 2005, June 6-9, 2005, Reno-Tahoe, USA, GT2005-68935, 12pp
5. Petrov, E.P. and Ewins, D.J., "Effects of damping and varying contact area at blade-disc joints in forced response analysis of bladed disc assemblies", Trans. ASME: J. of Turbomachinery, 2006, Vol.128, January, pp.403-410
6. Petrov, E.P., "Direct parametric analysis of resonance regimes for nonlinear vibrations of bladed discs", Proceedings of ASME Turbo Expo 2006, June 8-11, 2006, Barcelona, Spain, GT2006-90147, 10pp

NSF-Sandia Joints Modelling Workshop, Arlington, USA, 16-18 October, 2006

E.Petrov

A.4 Slide Presentation of David Hills, University of Oxford: *Contact Asymptotics with Particular Application to Quantifying Fretting Damage*



Contact asymptotics with particular application to quantifying fretting damage

D.A. Hills
C.M. Churchman
D. Dini

Department of Engineering Science, University of Oxford

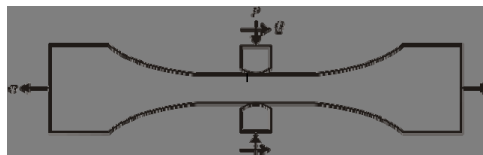


Fretting fatigue tests – incomplete contacts

Dovetail at the root of a turbine blade

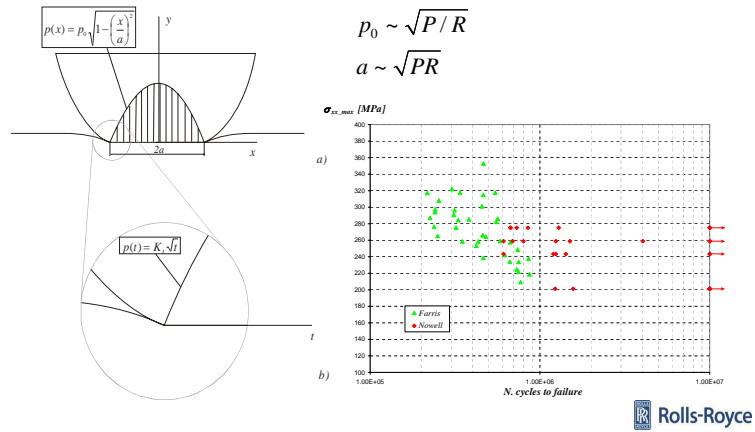


Experiments to determine lifetime of 'incomplete' contacts



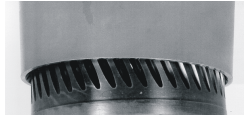


Asymptotics – incomplete contacts

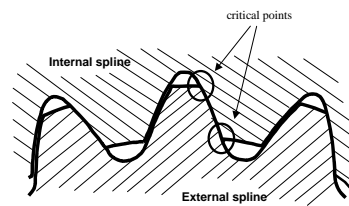


Fretting fatigue tests – complete contacts

Spline coupling in jet engine – connects front and rear shafts

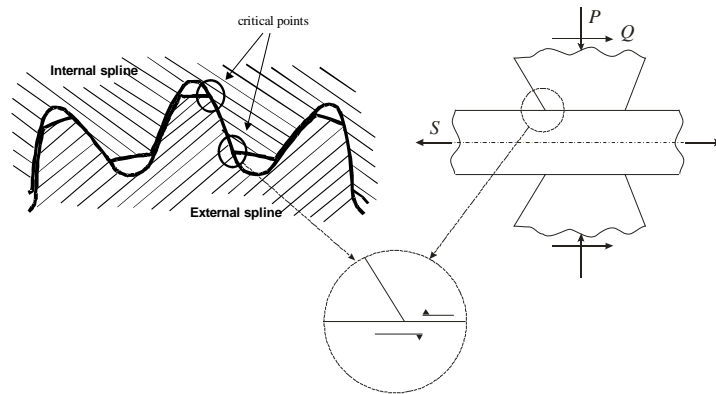


Failure due to fretting fatigue in service – crack nucleates at the contact edge





Fretting fatigue tests – complete contacts



Rolls-Royce

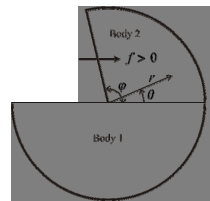


Asymptotics –complete contacts

Wedge sliding on half-plane

$$p(x) = K_s x^{\lambda_s - 1}$$

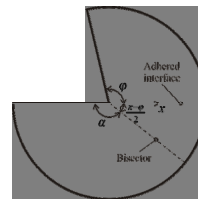
$$q(x) = -f K_s x^{\lambda_s - 1}$$



Wedge adhered to half-plane

$$p(x) = K_I^o x^{\lambda_I - 1} + K_{II}^o x^{\lambda_{II} - 1}$$

$$q(x) = K_I^o g_{r\theta}^I x^{\lambda_I - 1} + K_{II}^o g_{r\theta}^{II} x^{\lambda_{II} - 1}$$



Rolls-Royce



Asymptotics –complete contacts

Example case, $\varphi=90$ degrees

Sliding

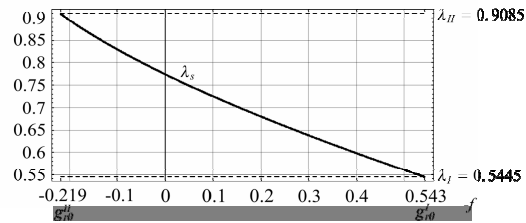
$$p(x) = K_s x^{\lambda_s - 1}$$

$$q(x) = -f K_s x^{\lambda_s - 1}$$

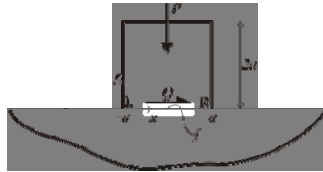
Adhered

$$p(x) = K_I^o x^{\lambda_I - 1} + K_{II}^o x^{\lambda_{II} - 1}$$

$$q(x) = K_I^o g_{r\theta}^I x^{\lambda_I - 1} + K_{II}^o g_{r\theta}^{II} x^{\lambda_{II} - 1}$$



Example problem – Block on half-plane



Example contact geometry

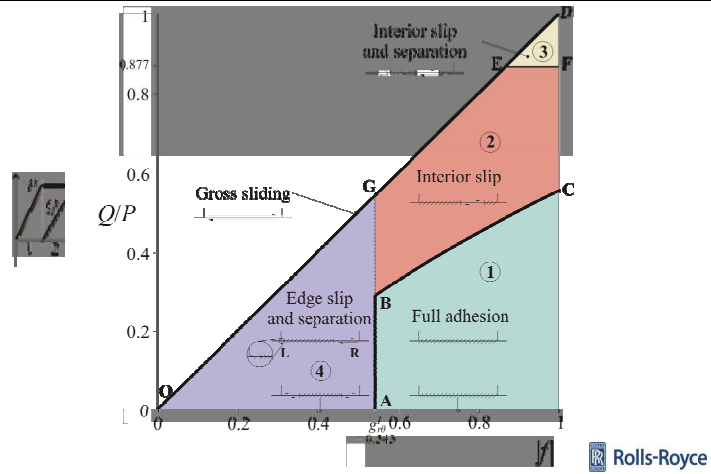


Loading history





Behaviour map for monotonic loading



Full adhesion – asymptotic results

①

Along the x -axis, i.e. the adhered interface, the normal traction, $p(x)$, and the shear traction, $q(x)$, are given by the asymptotic forms:

$$p(x) = K_I^o x^{\lambda_I - 1} + K_{II}^o x^{\lambda_{II} - 1}$$

$$q(x) = K_I^o g_{r\theta}^I x^{\lambda_I - 1} + K_{II}^o g_{r\theta}^{II} x^{\lambda_{II} - 1}$$

Where K_I^o and K_{II}^o are the appropriately scaled mode I and mode II stress intensity factors for the notch (encapsulating information about the remote geometry and loading), while λ_I, λ_{II} and $g_{r\theta}^I, g_{r\theta}^{II}$ are the eigenvalues and eigenvectors respectively of the semi-infinite wedge problem under mode I and mode II loading. For this geometry we have:



$$\lambda_I = 0.5445, \lambda_{II} = 0.9085, g_{r\theta}^I = 0.543, g_{r\theta}^{II} = -0.219$$

Rolls-Royce



Full adhesion – asymptotic results

①

②

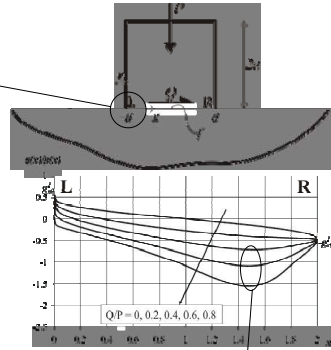
The traction ratio near the contact edge is

$$\frac{q(x)}{p(x)} = \frac{K_I^o g_{r\theta}^I x^{\lambda_I-1} + K_{II}^o g_{r\theta}^{II} x^{\lambda_{II}-1}}{K_I^o x^{\lambda_I-1} + K_{II}^o x^{\lambda_{II}-1}}$$

and because $\lambda_I - 1 < \lambda_{II} - 1 < 0$ the mode I singularity dominates the mode II singularity as $x \rightarrow 0$ to give

$$\frac{q(x)}{p(x)} \Big|_{x \rightarrow 0} = g_{r\theta}^I = 0.543$$

Therefore, *irrespective of the loading applied*, the traction ratio at the corner is **constant**.



$|f| < 0.543$ Slip at the edge of the contact

$|f| > 0.543$ Adhesion at the edge

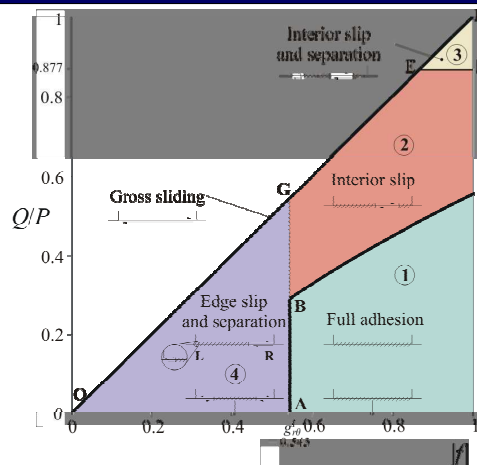
If interior maximum in traction ratio exceeds $|f|$ there is slip at an interior point.



Behaviour Map for Monotonic Loading

①

②





Separation at the trailing edge

3

If the contact edges remain adhered, the tractions are still governed by

$$p(x) = K_I^o x^{\lambda_I-1} + K_{II}^o x^{\lambda_{II}-1}$$

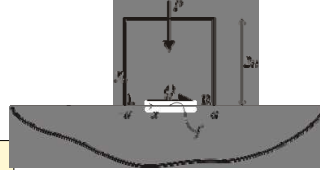
$$q(x) = K_I^o g_{I\theta}^I x^{\lambda_I-1} + K_{II}^o g_{I\theta}^{II} x^{\lambda_{II}-1}$$

If $K_I^o > 0$ we will have separation at contact edge because the normal tractions at the extreme edge become tensile.

It is easy to calibrate the loads in the finite problem with the stress intensity factors as

$$\begin{bmatrix} K_I^o a^{\lambda_I-1} \\ K_{II}^o a^{\lambda_{II}-1} \end{bmatrix} = \begin{bmatrix} -0.157 & 0.179 \\ -0.130 & -0.274 \end{bmatrix} \begin{bmatrix} P/2a \\ Q/2a \end{bmatrix}$$

Therefore, $K_I^o > 0$ when $Q/P > 0.877$



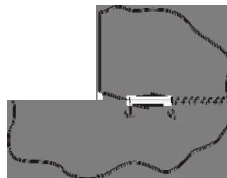
$Q/P > 0.877$ Separation at trailing edge

Rolls-Royce



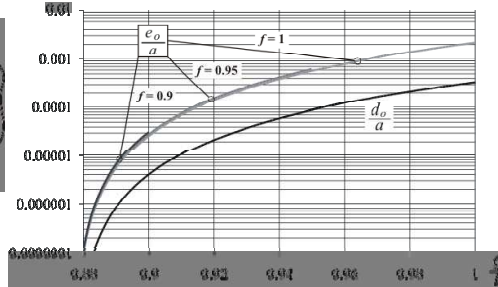
Approximation to the separation length

3



$$d_0 = \left(-\frac{K_I^o}{K_{II}^o} \right)^{\frac{1}{\lambda_{II}-\lambda_I}}$$

$$e_0 = \left(\frac{|f| + g_{I\theta}^I}{|f| + g_{I\theta}^{II}} \left(-\frac{K_I^o}{K_{II}^o} \right) \right)^{\frac{1}{\lambda_{II}-\lambda_I}}$$

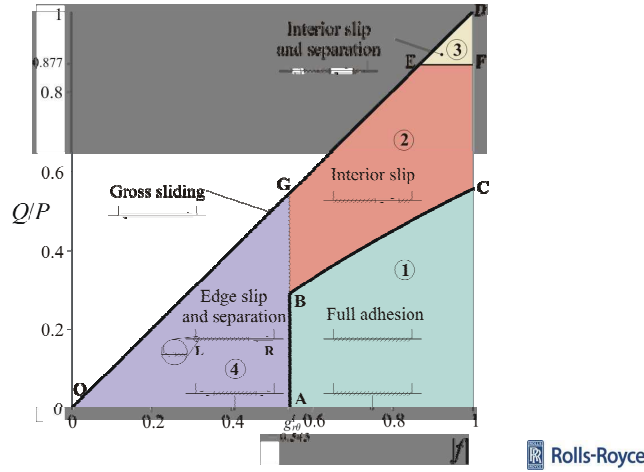


Rolls-Royce



Behaviour Map for Monotonic Loading

3



Separation at the trailing edge

4

If $|f| < 0.543$, the application of a normal load alone will cause slip zones to appear at both contact edges:



The tractions at the edge are then described well by the slipping asymptotic form:

$$p(x) = \frac{q(x)}{-f} = K_s x^{\lambda_s - 1}$$

The application of a shear force, Q , causes the leading edge slip zone to increase in length but the trailing edge slip zone to instantaneously stick. This means that the slipping tractions are locked in and we must add an adhered component to the tractions corresponding to the change in remote load:

$$p(x) = K_s x^{\lambda_s - 1} + \Delta K_I^o x^{\lambda_I - 1} + \Delta K_{II}^o x^{\lambda_{II} - 1}$$

$$q(x) = -f K_s x^{\lambda_s - 1} + \Delta K_I^o g_{I\theta}^I x^{\lambda_I - 1} + \Delta K_{II}^o g_{II\theta}^o x^{\lambda_{II} - 1}$$

We note that $\lambda_I - 1 < \lambda_s - 1 < \lambda_{II} - 1 < 0$ and therefore the mode I component to the tractions dominates the residual slipping tractions.





Separation at the trailing edge

4

From the calibration for the stress intensity factors we note that:

$$\Delta K_I^o a^{\lambda_I-1} = 0.179 \left(\frac{Q}{2a} \right)$$

and therefore that ΔK_I^o is positive for an increase in Q .

This means that the contact edge will separate over a tiny region that corresponds to the dominance of the mode I singularity over the slipping singularity.

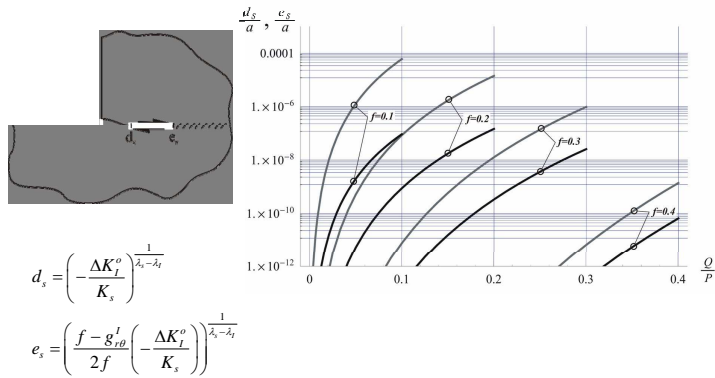


Rolls-Royce



Approximation to the separation length

4

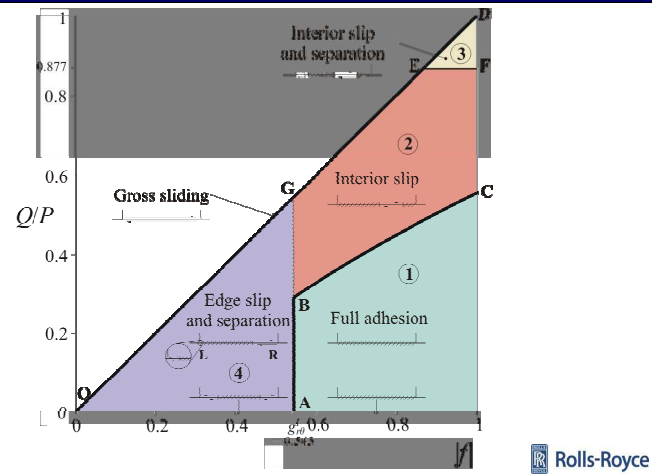


Rolls-Royce

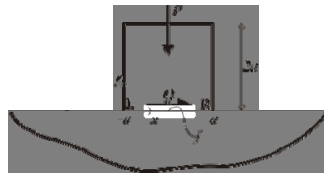


Behaviour Map for Monotonic Loading

4



Cyclic loading



Example contact geometry

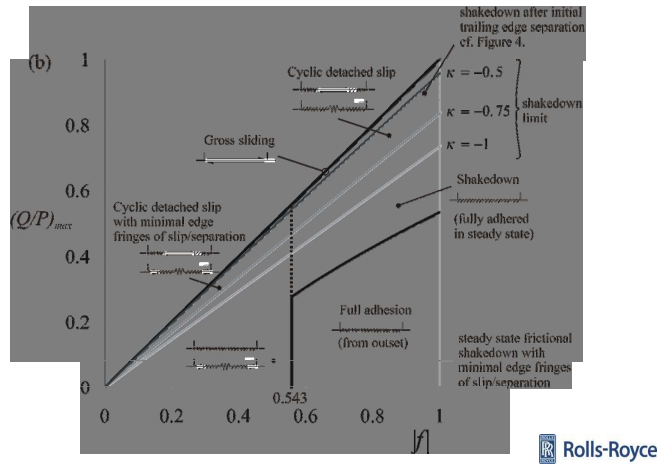


Loading history

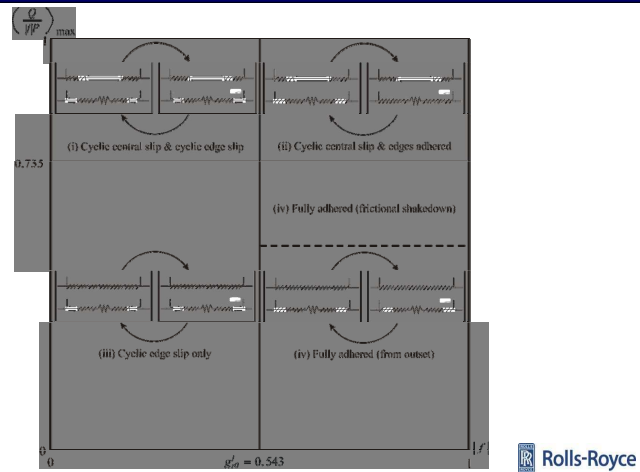




Behaviour map for cyclic loading

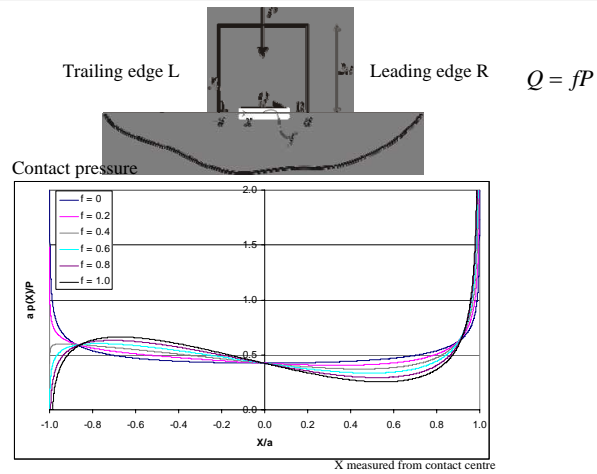


Behaviour map for fully reversing shear ($\kappa = -1$)

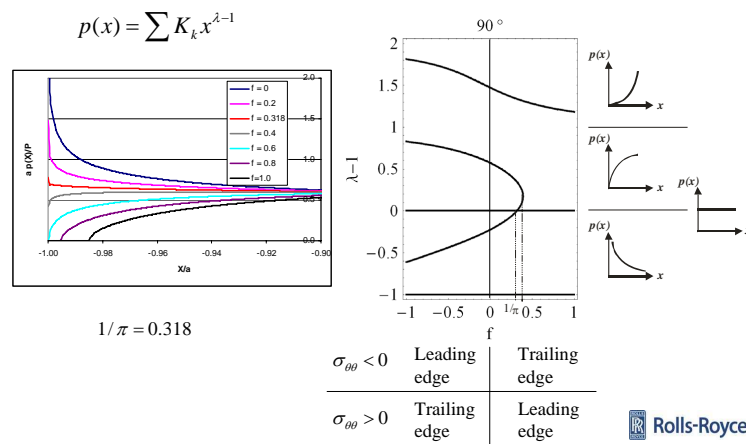




Finite elements - sliding complete contact



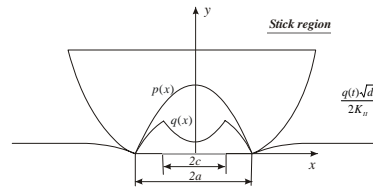
Asymptotics – sliding complete contact





Asymptotics – incomplete contact

Partial slip: shear asymptote



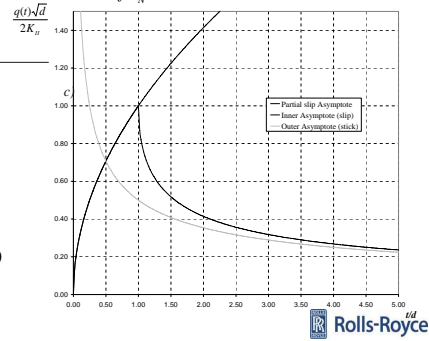
$$q(t) = \frac{2K_T}{d} \sqrt{t} \quad 0 < t < d$$

$$= \frac{2K_T}{d} (\sqrt{t} - \sqrt{t-d}) \quad t > d$$

$$= 0 \quad t < 0$$

$$q(t) = \frac{K_T}{\sqrt{t}} \quad t \gg d$$

$$\frac{K_T}{fK_N} = \frac{d}{2}$$

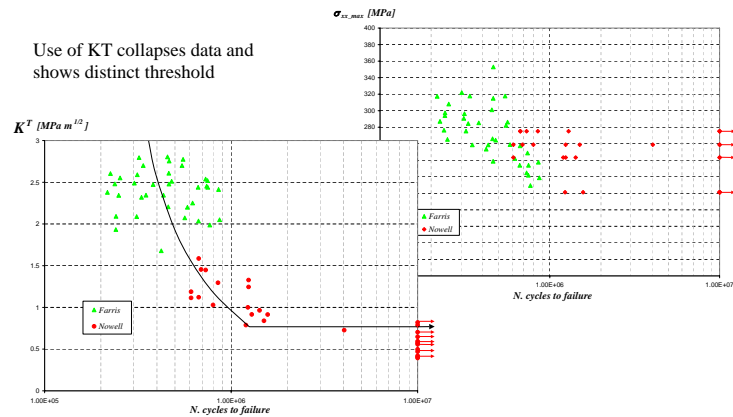


Rolls-Royce



Application of asymptotics to fretting nucleation conditions

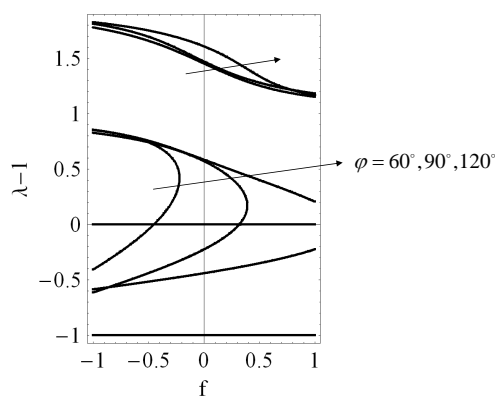
Use of KT collapses data and shows distinct threshold



Rolls-Royce



Slipping asymptote – variation with wedge angle



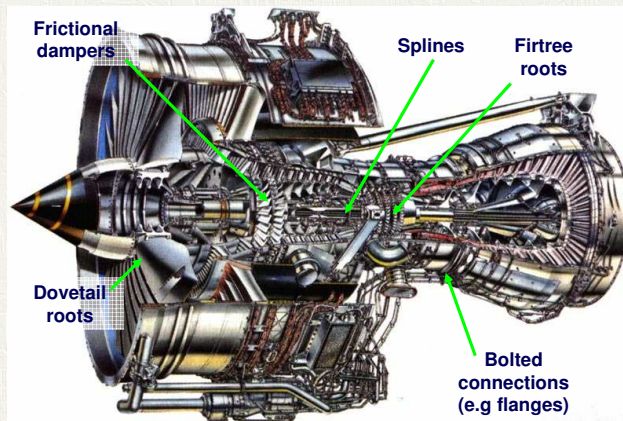
A.5 Slide Presentation of David Nowell, University of Oxford: *Structural Integrity Issues: Frictional Joints in Gas Turbines*



Structural Integrity Issues: Frictional Joints in Gas Turbines

Prof. David Nowell
Director, University Technology Centre for Solid Mechanics
University of Oxford, UK.

Gas Turbine Engine



Joints in gas turbines

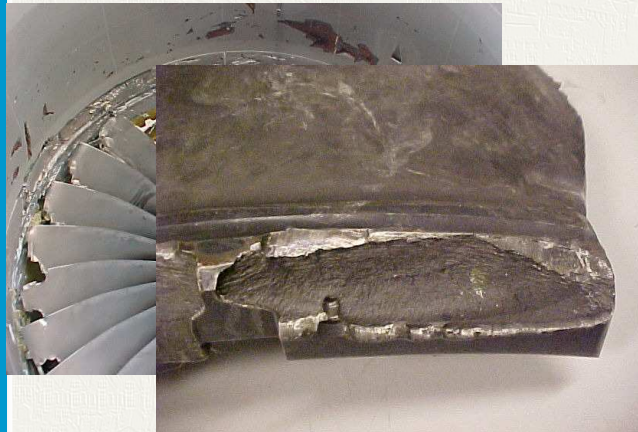
- Joints allow
 - Assembly of components
 - Disassembly for maintenance and repair
 - Joining of dissimilar materials
 - Frictional damping
- Joints compromise structural integrity
 - High frictional stresses (continuum level)
 - High local stresses (asperity level)
 - Wear
 - Crack initiation and propagation (fretting fatigue)



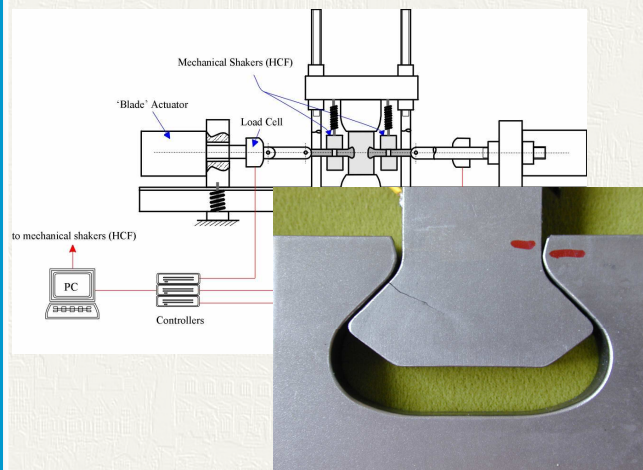
Blade root failure – January 2001



A service failure



Dovetail test



Difficulties in design

- From a structural integrity perspective, there are two significant difficulties:
 1. Understanding the stress state in the neighbourhood of the contact
 2. Using this understanding to predict fatigue life at the contact
- We will look at these two issues in turn

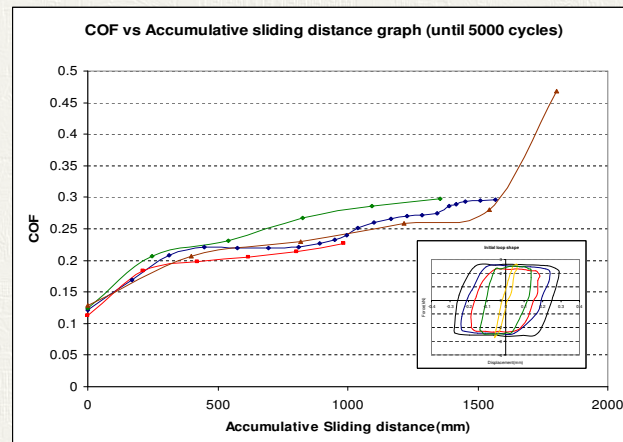


Difficulties in analysing joints

- Frictional behaviour is complex and non-linear
- Friction parameters (e.g. coefficient of friction) difficult to predict and vary with time
- Contact may wear, so geometry is unknown
- Very fine F.E. models are needed to resolve contact stress adequately
 - (Sinclair: 1% of contact radius for 5% accuracy)
- Friction models in FE programs do not always give good convergence



Friction variation – coated surfaces



Measurement and modelling of wear McColl et al, 2004

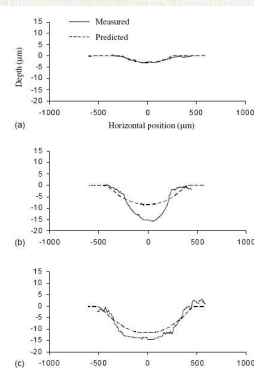


Fig. 11. Comparison of FE prediction and experimental results for worn surface profiles of the first specimen, after 18,000 wear cycle at (a) 185 N normal load, (b) 500 N normal load, and (c) 1670 N normal load. Stroke is 50 μm .

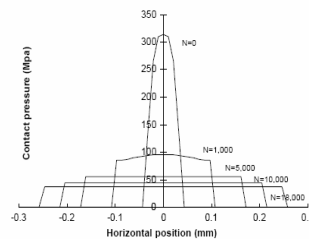


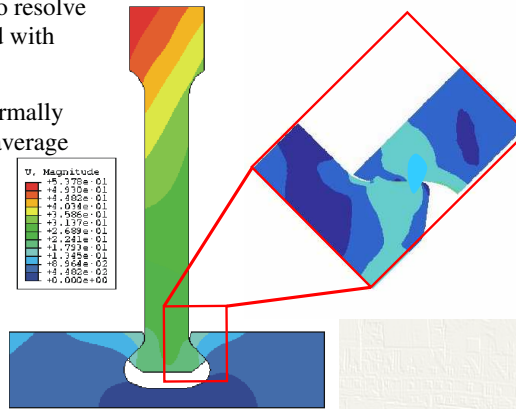
Fig. 14. Predicted evolution of contact pressure with increasing number of wear cycles, N , under 185 N normal load case.

Surface modification at micro (friction) and macro (wear) scales can be important (particularly in full sliding)

Finite element analysis

Difficult to resolve
stress field with
FEA

Design normally
based on average
pressure



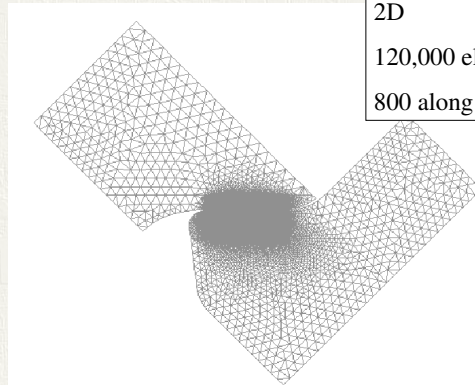
Dovetail rig – ‘Fine’ FE model

Local FE Model

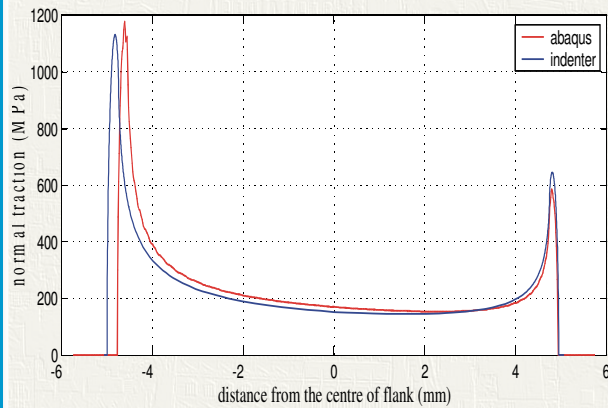
2D

120,000 elements

800 along contact flank



Example – Pressure distribution in dovetail



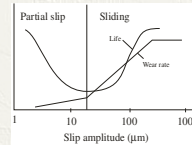
Note that this displays sharp pressure peaks, but is actually 'incomplete'

Analysis of contacts

- Resolution of stress field in neighbourhood of contact requires:
 - Significant computational resource
 - Experimental data on
 - Wear
 - Variation of friction with time
- Accurate analysis of contacts is seldom feasible, even at detailed design stage
- Simplified design criteria are used (e.g. mean contact pressure in frictionless contact) leading to over-conservative design

Fretting Fatigue

- Fatigue failures can result from 'fretting fatigue'
- Fatigue at contacts
 - Usually in the 'partial slip regime'
 - Typical slip amplitudes about $50\mu\text{m}$
 - Larger slip amplitudes may cause fretting wear



- High stress concentration
 - Severe stress gradient
 - Plasticity rather limited



Understanding fretting fatigue

- Even when we have the (cyclic, spatial, time-varying) distribution of contact tractions, prediction of fatigue life is still challenging
- In principle propagation problem is no different from plain fatigue, although
 - Non-proportional loading
 - Multiaxial stress state
 - Variable R-ratio
 - High stress gradients
- Much interest in recent years has therefore been in predicting crack initiation

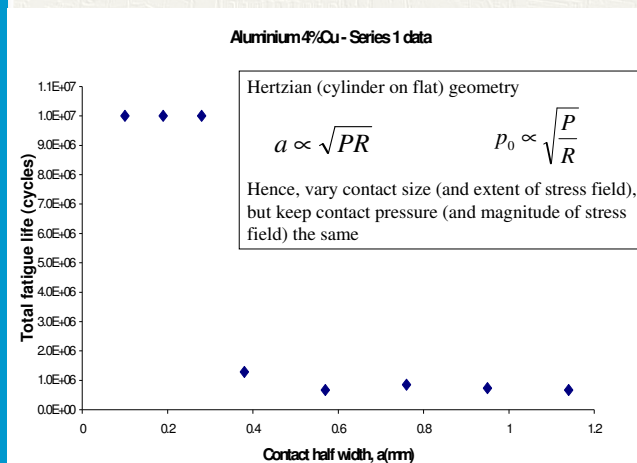


The initiation problem

- Cracks initiate under the influence of contact loading
- Key length scales:
 - Contact size
 - Asperity size distribution
 - Initiated flaw size
 - Long crack threshold size
 - Material microstructure
 - Stress gradients
 - Contact stress field
 - Residual stress field
- These considerations can produce significant 'size effects' in the results



The size effect



The size effect

■ Two main explanations

1. Stressed volume:

- Usual statistical argument that life decreases with stressed volume due to increase probability of flaws (or favourable microstructure)

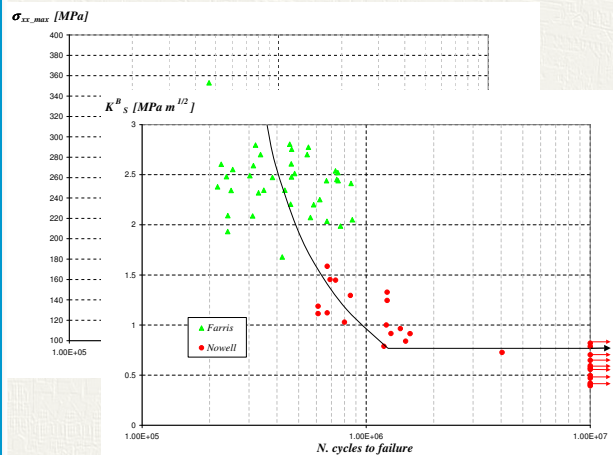
2. Stress gradient

- Stresses may fall off so quickly that crack arrests before (LEFM) propagation can occur. I.e. crack cannot 'escape' from the stress concentration

■ In most cases, 2 is more significant

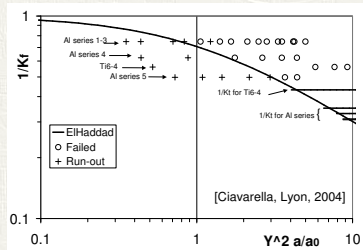


The size effect - illustration



Approaches to predict the size effect

- Volume averaged initiation parameters
- Notch fatigue analogies (e.g. Ciavarella CLNA model)
- Short crack arrest approaches (Hudak et al, Nowell, Dini et al)
- Generalised stress intensity factors (contact asymptotics – Hills et al)



Conclusions

- Frictional contacts are common in complex machines such as gas turbines
- Vibration loading can produce failures by fretting fatigue (or wear)
- Contacts are challenging to analyse and experimental data is required for friction and wear properties
- Even when contact stress field is determined, prediction of fatigue life is difficult
- Experimental data is usually required
- Current design methods are (generally) over-conservative

Challenges for the future

- Importance of microstructure is often overlooked
 - Microstructural dimensions are often similar to characteristic contact length scales
- Residual stress effects are usually ignored
 - All surfaces will have residual stress (either intentional or not)
- Recent developments in predictive methods need to be applied in practical design applications
- Effect of surface damage due to microslip on initiation 'life' remains to be quantified. (i.e. do we need special fretting experiments?)
- Friction parameters need to be measured – can we predict them?



A.6 Slide Presentation of Andreas Polycarpou, University of Illinois, Urbana: *Significance of Interfacial Micro-Scale Parameters in the Dynamics of Structures from a Tribologist Perspective*

Significance of Interfacial Micro-Scale Parameters on the Dynamics of Structures from a Tribologist Perspective

Andreas A. Polycarpou
Microtribodynamics Laboratory
Mechanical Science & Engineering
University of Illinois at Urbana-Champaign

Presented at the NSF-Sandia Workshop
October 16, 2006



Acknowledgements
National Science Foundation-CMS
Center for Microanalysis of Materials, DOE-DEFG02-96-ER45439
Information Storage Industry Consortium
Delphi Saginaw Systems



Outline

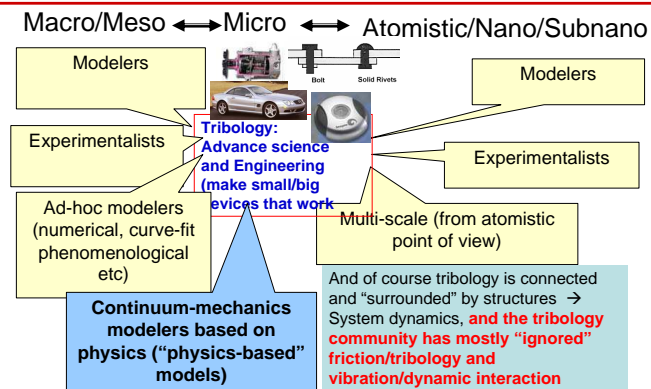
- Modeling approaches to interfacial problems and their coupling to system dynamics
 - Empirical or phenomenological approach
 - Physics-based continuum-mechanics approach
- Application to magnetic storage
 - Significance of micro contact parameters (roughness)
 - Relating micro contact parameters to interfacial (contact, friction, adhesion) and dynamic phenomena
- Normal contact stiffness and contact damping
- Shear lap joint stiffness and damping
- Microslip/partial slip experimental studies
- Summary



The Microtribodynamics research group

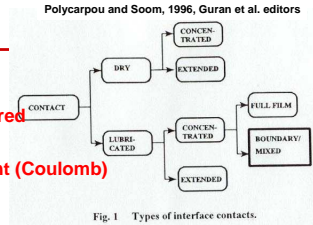


Approaches to Interface (tribology) problems



What's in a contact?

- Contacts can be flat/curved/mixed, Dry/lubricated/Mixed
- **Historically contacts are considered rigid and all contact behavior is characterized by a friction coefficient (Coulomb)**
- However, such simple models do not usually capture realistic contact behavior (especially under dynamic conditions)



- **Approaches in tackling friction/vibration interaction:**
- **A.** Treat the whole system (dynamics/contact) as a whole: Empirical, or semi-empirical at best, and can not be generalized (phenomenological models). **Advantage:** Can readily treat complex systems
- **B.** Develop physics-based contact and friction (interfacial) models (valid for both static and sliding conditions) and then couple them with dynamics of the system



Approach A: Phenomenological models — have been extensively used in joints —

Y. Song et al. / J. Sound and Vibration 273 (2004)

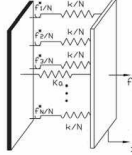
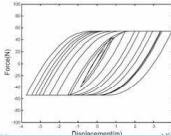


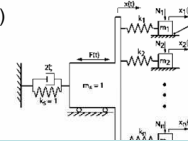
Fig. 4. Adjusted Iwan model.



Using experiments, and parameter identification to fit the data: Phenomenological models: Good agreement with specific data but can not generalize. Small system and or interface changes (loose bolts, humidity) and models may be "invalid"

Interfacial physics of the problem do not typically enter

Coulomb-type (constant) friction is assumed: linearity between the normal and friction forces via a constant



In these works "dynamics" dominate



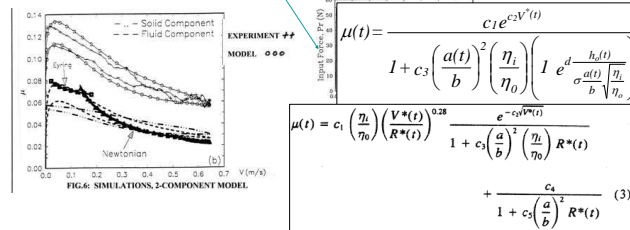
Semi-empirical dynamic friction models (macro)

- Need for friction models and couple them with the system dynamics operating in boundary and mixed lubrication regimes (both asperity and fluid contacts occur)
 - Control Systems (e.g., Robotics)
 - Transient Operation of Machines and Devices (E.g., Bearings)
- Perform steady and unsteady sliding experiments (pure sliding, boundary and mixed regimes)
- Based on these experiments, developed semi-empirical friction models that incorporated the dynamics of the tribosystem
- Independently, obtain the dynamics of the tribosystem via experiments and modeling
- Combine the friction and the dynamic model, to predict low and high friction transients under steady and unsteady conditions.



Semi-empirical models, Polycarpou & Soom 92-95

Both system dynamic and friction models perform very well even under very high frequency transients



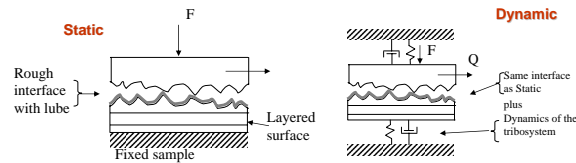
Semi-empirical models: Good models that can also be applied to stick-slip and can be used in other dynamical systems BUT will need new coefficients!

FIG. 9: IMPACT EXCITATION: $V_{max}=0.7 \text{ m/s}$, $W_n=160 \text{ N}$, FORCES



Nature of Friction (Approach B)

- Friction depends on the nature of the contacting surfaces (surface properties, surface roughness etc)
- Under sliding conditions, the dynamics of the overall tribosystem are important, and will affect the contact behavior (friction) and vice versa
- The main conjecture here is that the fundamental nature of friction is the same for both static and dynamic conditions



Microtribodynamics: Coupling of interface and dynamics

- Develop separate “fundamental” or physics-based interfacial models and then couple them with system dynamic models

Basic Interfacial Models:

- Contact
- Friction
- Adhesion
- Roughness

+

System Dynamic Models:

- Simple Linear or nonlinear lumped
- FEM or other models

→

Physics-based Dynamic Models with Contact and Friction

Advantages of this approach is that it (a) specifically includes interface parameters such as roughness (b) can “readily” be generalized as there are no empirical/fitting coefficients (c) clear physical understanding due to decoupling between dynamics and interface

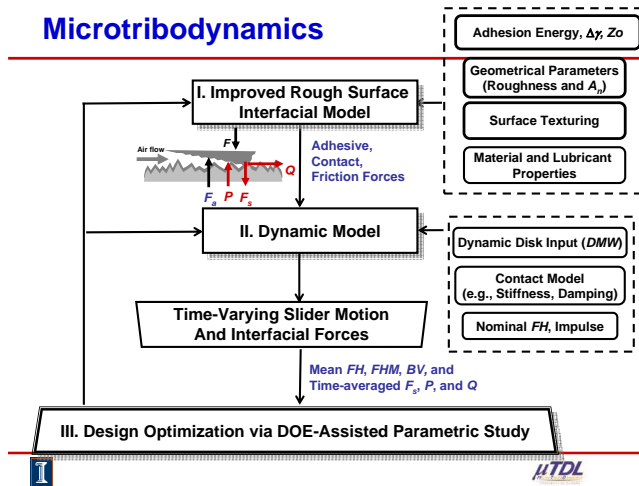


Successful application to Magnetic Storage:

Sub-5 nanometer head-disk interface (at 100 miles per hour) in hard disk drives towards 1 terabit per square inch areal densities

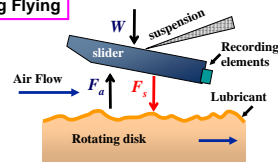


Microtribodynamics



Interfacial forces in ultra-low flying/contacting HDIs

During Flying

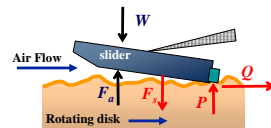


W = Suspension Preload (1-3 g)
 F_a = Air-Bearing Force
 F_s = Adhesive Force

Air-Bearing Surface (ABS)



During Contact



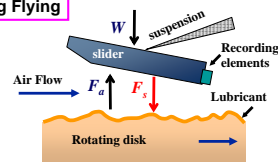
W = Suspension Preload
 F_a = Air-Bearing Force
 F_s = Adhesive Force
 P = Contact Force
 Q = Friction Force



ITDL

Interfacial forces in ultra-low flying/contacting HDIs

During Flying

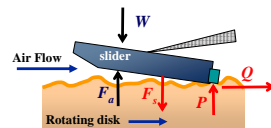


W = Suspension Preload (1-3 g)
 F_a = Air-Bearing Force
 F_s = Adhesive Force

Air-Bearing Surface (ABS)



During Contact



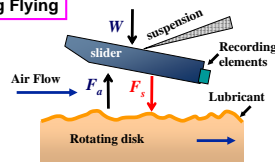
W = Suspension Preload
 F_a = Air-Bearing Force
 F_s = Adhesive Force
 P = Contact Force
 Q = Friction Force



ITDL

Interfacial forces in ultra-low flying/contacting HDIs

During Flying

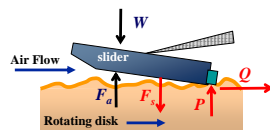


W = Suspension Preload (1-3 g)
 F_a = Air-Bearing Force
 F_s = Adhesive Force

Air-Bearing Surface (ABS)



During Contact



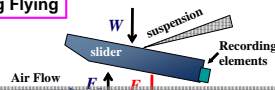
W = Suspension Preload
 F_a = Air-Bearing Force
 F_s = Adhesive Force
 P = Contact Force
 Q = Friction Force



UTDL

Interfacial forces in ultra-low flying/contacting HDIs

During Flying



W = Suspension Preload (1-3 g)
 F_a = Air-Bearing Force
 F_s = Adhesive Force

Air-Bearing Surface (ABS)

How should one **model adhesion/friction** behavior in sub-5 nm ultra-low flying HDIs accounting for realistic interfacial conditions?

Note that atomistic models are unable to treat the whole system (which is needed for design)

In this approach continuum-based models are employed



UTDL

How are the surfaces of slider/disks



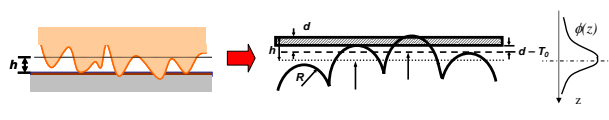
- Surfaces in such devices are not “single asperities” or infinitely smooth, but possess roughness
- Magnetic Media, $R_q = 0.2 - 0.6 \text{ nm}$
- Magnetic Heads, $R_q = 0.4 - 0.6 \text{ nm}$

Any interfacial and dynamic models should include realistic rough surfaces:

It has been shown by (my group and others-Bogy) that failure to include roughness leads to incorrect predictions



Rough surface statistical model



$$F_s = f(h, \sigma, R, \eta, \phi, A_n, T_0, E, H, \nu, \Delta\gamma) \quad P, Q = f(h, \sigma, R, \eta, \phi, A_n, E, H, \nu)$$

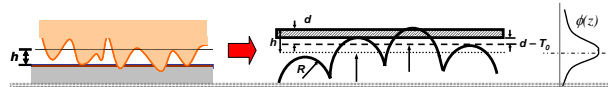
Micro contact Roughness/Geometrical
Material
Micro contact Roughness/Geometrical
Material

Need sphere-on-flat contact, adhesion and friction models

[account for contact as well as the generated adhesive stress → continuum mechanics adhesive models]



Rough surface statistical model



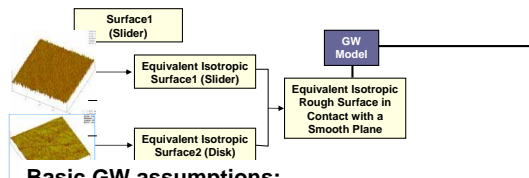
Despite the known limitations of the GW model (e.g., scale dependence of some of its parameters, asperities act independently, constant R etc,

It has been shown that despite its simplicity it gives good results in many engineering situations

Note that in this work, a GW-type model is used as the current models include elastic/plastic contact, may have asymmetric asperity distribution and contain a molecularly thin lubricant on the surface



GW-type roughness model

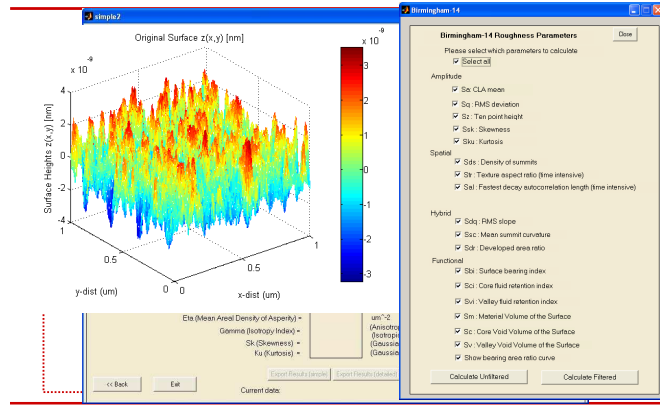


Basic GW assumptions:

- Replace two rough surfaces by a smooth surface and an equivalent rough surface
- Replace asperities with simple geometric shapes
- Use the correct Probabilistic Distribution for Asperity Heights
- GW assumptions can be relaxed without significant loss of accuracy!



Roughness Parameter Extraction

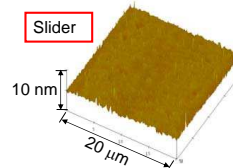
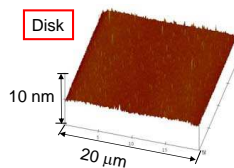
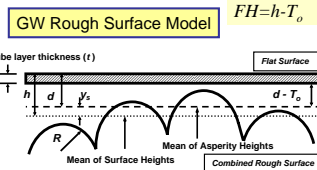


1

μTDL

Rough Surface Model: EHDR Disk/Slider

| Individual measured roughness parameters | | | |
|--|---------------|----------|---------------------------|
| | σ (nm) | R (μm) | η (μm ²) |
| Disk | 0.38 | 7.63 | 9.94 |
| Slider | 0.64 | 7.15 | 8.85 |
| Combined roughness parameters | | | |
| Disk/Slider | 0.74 | 5.22 | 9.33 |



1

μTDL

Rough Surface Model: Material Properties

| Parameter | | Unit | Value |
|-----------------------------------|----------------------------|-----------------|------------|
| Individual elastic moduli | E_{disk}, E_{slider} | GPa | 140, 450 |
| Poisson's ratios | ν_{disk}, ν_{slider} | - | 0.20, 0.21 |
| Combined elastic modulus | E | GPa | 111.59 |
| Hardness of disk-layered material | H_{disk} | GPa | 12 |
| Mobile lubricant thickness | T_o | nm | 0.5 |
| Total lubricant thickness | t | nm | 1.0 |
| Energy of adhesion | $\Delta\gamma$ | N/m | 0.151 |
| Equilibrium spacing | $\varepsilon = z_o$ | nm | 0.098 |
| Nominal area of Contact | A_n | μm^2 | 300 |
| Contact Potential | U | volts | 0.5 |



Surface interactions (adhesion, friction, contact)

start

Intermolecular Adhesion / Contact / Friction Models

Brief Instructions

1. SBL / ISBL Simulation 2. 2-DOF Dynamic Simulation

STEP 1-1: Load Parameters STEP 2-1: Match Dimensions

STEP 1-2: Run SBL/ISBL Model STEP 2-2: Run 2-DOF Model

STEP 1-3: Plot SBL/ISBL Results

University of Illinois at Urbana-Champaign
Copyright Modified Dynamics Lab. All Rights Reserved

Input Parameters

Combine Model

Select • Unlub • Molec • Impr

Force (Q_{max})



Contact, adhesion, and tangential (friction) forces

$$\mu = \frac{Q}{F} = \frac{Q}{P - F_s} \quad \text{Asperity height distribution} \quad \phi(u) = \frac{1}{\sqrt{2\pi}} \left(\frac{\sigma}{\sigma_s} \right) \exp \left[-\frac{1}{2} \left(\frac{\sigma}{\sigma_s} \right)^2 u^2 \right]$$

Contact force

$$P^*(h^*) = \beta \left[\frac{4}{3} \left(\frac{\sigma}{R} \right)^{\frac{1}{2}} \int_{h^*-y_s^*}^{h^*-y_s^*+\omega_c^*} \omega^{3/2} \phi(u^*) du^* + \frac{\pi KH}{E} \int_{h^*-y_s^*+\omega_c^*}^{\infty} (2\omega^* - \omega_c^*) \phi(u^*) du^* \right]$$

Friction force

$$Q^*(h^*) = \frac{4}{3} \beta \left(\frac{\sigma}{R} \right)^{\frac{1}{2}} \int_{h^*-y_s^*}^{h^*-y_s^*+\omega_c^*} \omega^{3/2} f \left(\frac{\omega^*}{\omega_c^*}, \nu \right) \phi(u^*) du^*$$

Adhesion force

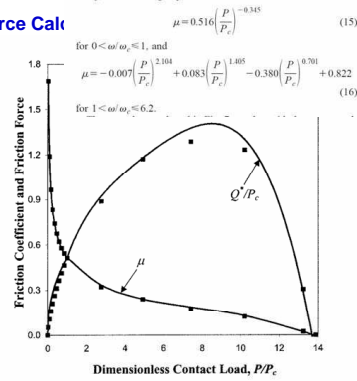
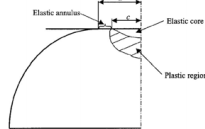
$$F_s^*(h^*) = \frac{8\pi\eta R \Delta \gamma \varepsilon^{*2}}{3E} \left\{ \int_{-\infty}^{h^*-y_s^*-t_o^*} \left[\frac{1}{(\varepsilon^* - \omega^* - t_o^*)^2} - \frac{0.25\varepsilon^{*6}}{(\varepsilon^* - \omega^* - t_o^*)^8} \right] \phi^*(u^*) du^* + \right. \\ \left. + \frac{3}{4\varepsilon^{*2}} \int_{h^*-y_s^*-t_o^*}^{h^*-y_s^*} \phi^*(u^*) du^* + 2 \int_{h^*-y_s^*}^{\infty} \left[\frac{1}{(Z^* - t_o^*)^3} - \frac{\varepsilon^{*6}}{(Z^* - t_o^*)^8} \right] s^* \phi^*(u^*) ds^* du^* \right\}$$

1

μTDL

Rough Surface Friction Force Calc

Friction Force (for a spherical contact stress field under sliding contact)
Kogut and Etsion, 2003



Includes up to elastic-plastic asperity contribution

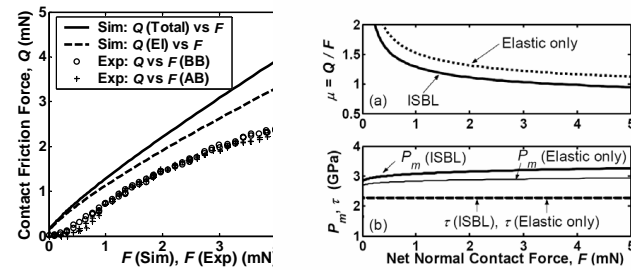
1

Fig. 7 Static friction coefficient, μ , and dimensionless force Q^*/P_c versus the dimensionless contact load, P/P_c , in the elastic and elastic-plastic regimes

μTDL

Rough Surface Friction Force Calculation and model validation

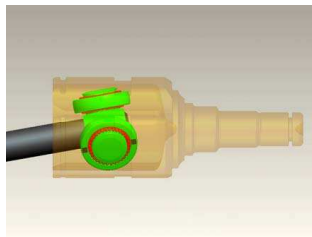
Suh, Mate and Polycarpou, Trib letters, 2006



No empirical coefficients used in these models
No constant (Coulomb) friction coefficient for either spherical
or rough surfaces –Primarily due to adhesion

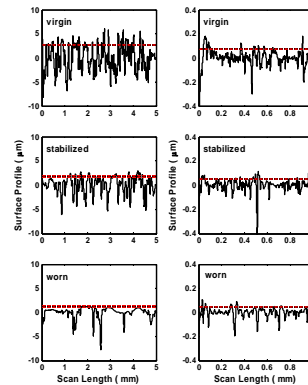


Model validation in Constant Velocity Joint application



Lee CH and Polycarpou, SAE-2005, JoT, in review
Sponsored by Delphi

Carefully measure surface roughness and material properties



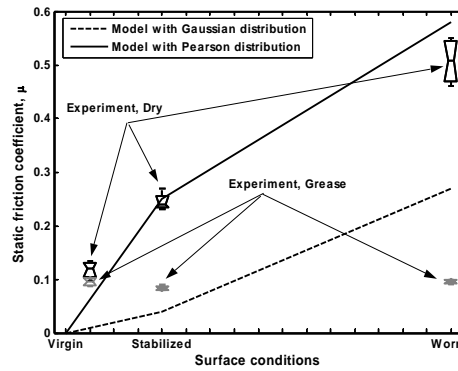
Material, roughness parameters and model validation

| Parts | Type | Young's modulus E (GPa) | Hardness H (HRC / GPa) | Poisson ratio ν | Combined E^* (GPa) |
|---------|--------------|------------------------------|-----------------------------|------------------------|-------------------------|
| Housing | 4121-H Steel | 206.85 | 61 / 7.06 | 0.29 | 105.3 |
| Roller | 52100 Steel | 206.85 | 59 / 6.61 | 0.29 | |

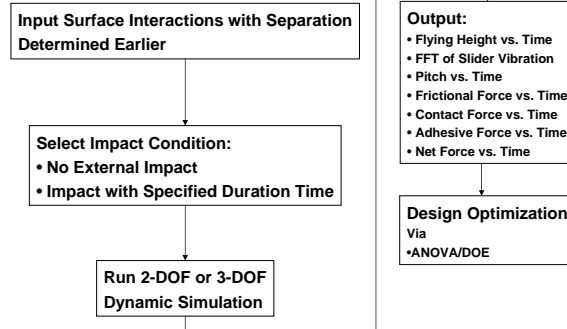
| State | Individual surface parameters | | | | | Combined interface parameters | | | |
|------------|-------------------------------|-------------------------|-------------------------|-------------------------|-----------------------------|-------------------------------|-----------------------------|-------------------------|--------|
| | Part | R_a (μm) | R_g (μm) | R_s (μm) | η ($/\mu\text{m}^2$) | R (μm) | η ($/\mu\text{m}^2$) | R_g (μm) | Ψ |
| Virgin | Housing | 2.223 | 2.660 | 43.65 | 0.373 | 37.49 | 0.500 | 2.661 | 4.55 |
| | Roller | 0.047 | 0.075 | 73.23 | 12.213 | | | | |
| Stabilized | Housing | 1.398 | 1.770 | 141.12 | 0.143 | 97.54 | 0.290 | 1.771 | 2.30 |
| | Roller | 0.033 | 0.053 | 134.98 | 4.794 | | | | |
| Worn | Housing | 0.783 | 1.240 | 237.41 | 0.151 | 156.11 | 0.335 | 1.241 | 1.52 |
| | Roller | 0.029 | 0.042 | 207.22 | 4.645 | | | | |



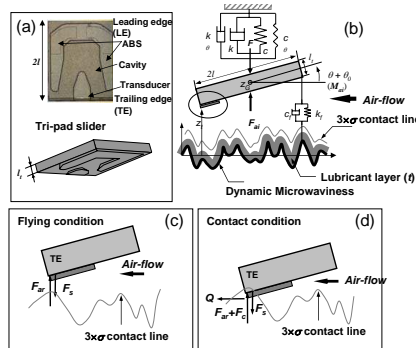
Material, roughness parameters and model validation



Coupling with 2-DOF Dynamic Model



2-DOF NonLinear Tri-State Dynamic HDI Model



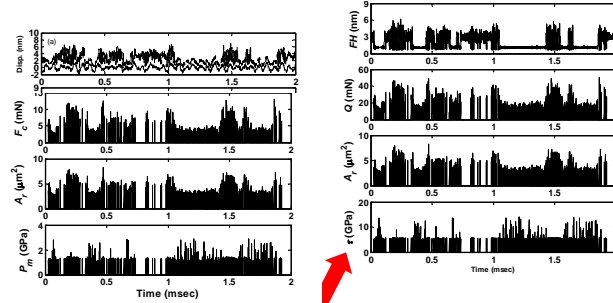
- Model includes 3 switching states:
 - (1) Flying with air-bearing
 - (2) Contacting
 - (3) Flying without air-bearing ($FH > 15 \text{ nm}$)

- Input Parameters
 - Interfacial geometry
 - Interfacial forces
 - DMW measurements

Lee SC and Polycarpou, IEEE, 2004, 2005



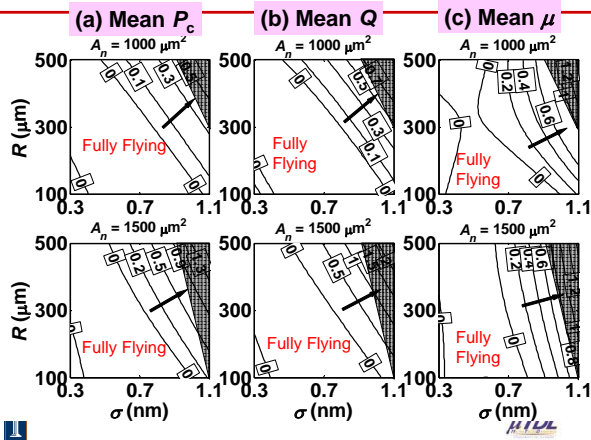
Simulation Results: Nominal FH of 3 nm
Average Shear Stress $\tau (= Q/A_f)$



Mean Shear stress, $\tau = 1.16$ GPa
 Max shear stress $\tau = 14.08$ GPa
 Larger than mean pressure because of the large friction values



ANOVA Parametric studies/Trends



Re-cap

Shown the significance and usefulness of micro contact parameters for predicting performance in systems that include contact, friction (adhesion) and dynamics

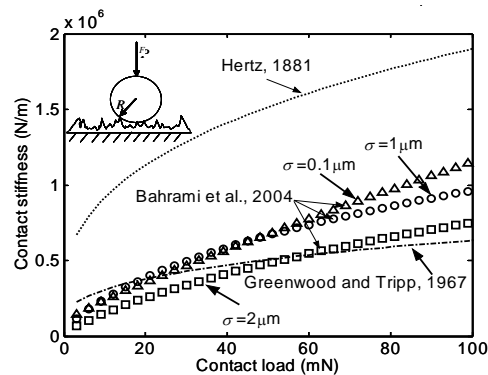
Next,

Lets look at experiments in measuring normal contact stiffness and damping, partial slip

As well as some initial work with mechanical joints (shear contact stiffness and damping)



Theoretical Predication of Contact Stiffness —Spherical Contact

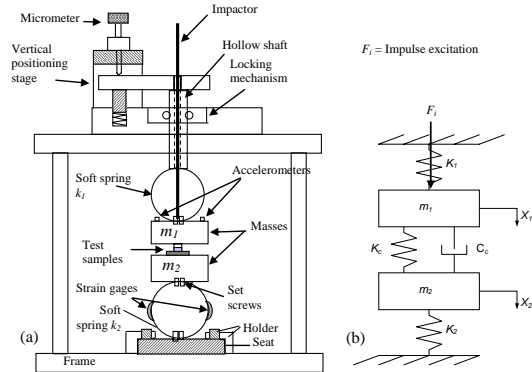


rough Hertz
d Tripp 1967)

rough Hertz
JoT 2005)
ion only



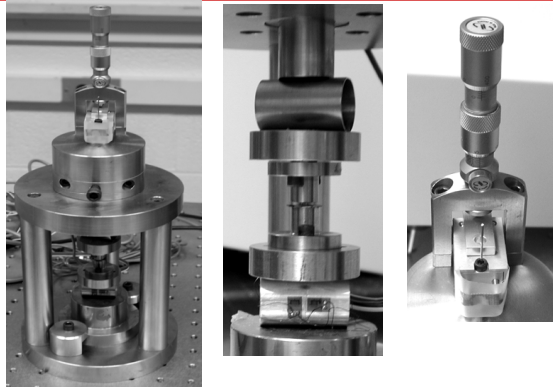
Experimental based on contact resonance method



I

μTDL

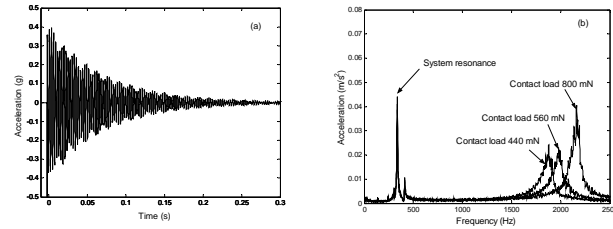
Photographs of tester



I

μTDL

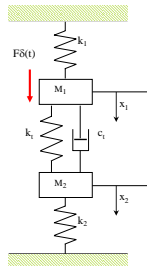
Typical experimental results



(a) Typical acceleration signal (b) Average spectra with three different contact (normal) loads



Extracting contact stiffness from experiments



Equations of motion

$$M_1 \ddot{x}_1 + c_1 (\dot{x}_1 - \dot{x}_2) + (k_1 + k_i) x_1 - k_i x_2 = F \delta(t) \quad (1)$$

$$M_2 \ddot{x}_2 + c_1 (\dot{x}_2 - \dot{x}_1) - k_i x_1 + (k_2 + k_i) x_2 = 0 \quad (2)$$

Contact stiffness through eigenvalue analysis

$$k_i = \frac{M_1 M_2 \omega_i^4 - (M_1 k_2 + M_2 k_1) \omega_i^2 + k_1 k_2}{(M_1 + M_2) \omega_i^2 - (k_1 + k_2)} - j c_1 \omega_i \quad (3)$$

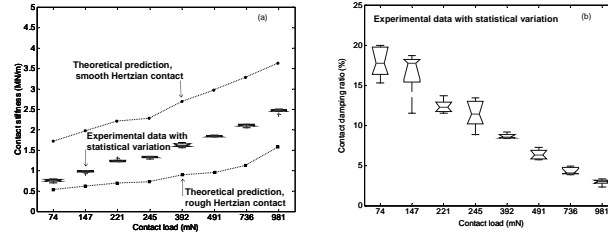
Contact damping extracted directly time responses using Eigen-system Realization Algorithm (ERA)



Spherical contact stiffness and damping

1.59 mm (1/16 inch) diameter stainless steel ($E=192.92\text{GPa}$, $H=2.96\text{GPa}$) sphere contacting a nominally flat stainless steel surface ($\sigma = 0.47\mu\text{m}$)

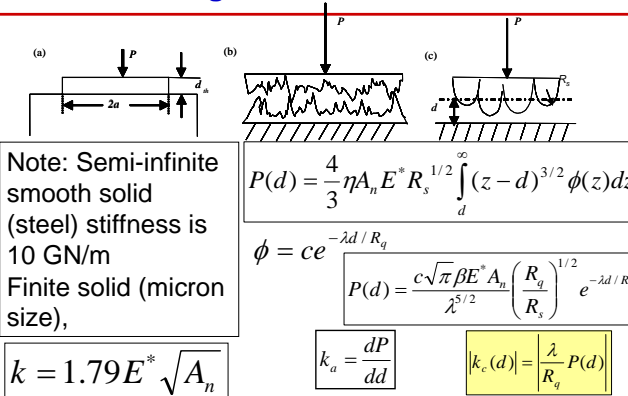
Shi and Polycarpou, JVA, Vol. 127, Feb. 2005



- Contact stiffness nonlinearly increases with increasing contact load
- Contact damping decreases with increasing contact load



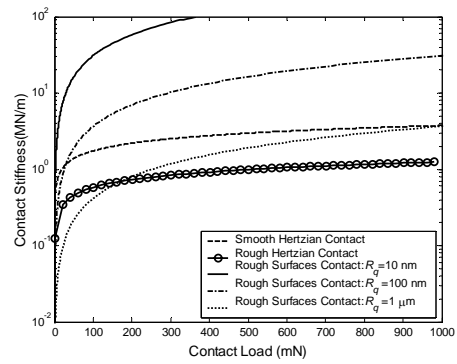
Rough Surfaces Contact



Polycarpou and Etsion, JoT, 1999



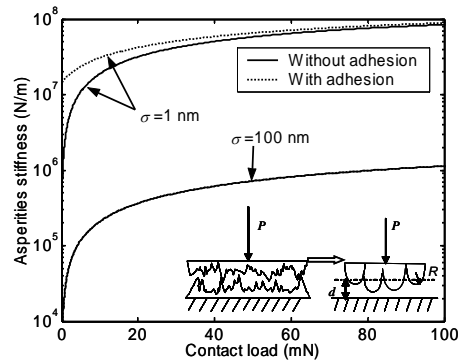
Rough Surfaces Contact



I

μ TDL

Rough Surfaces Contact

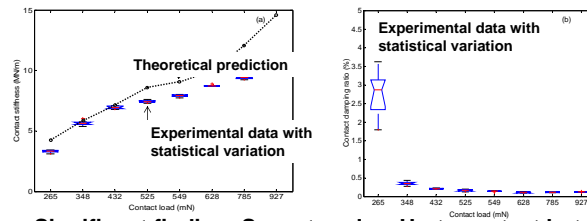


I

μ TDL

Comparison with experiments

| | Individual surface parameters | | | | | Combined interface parameters | | | |
|----------|-------------------------------|-----------|-------------------------|-------------------------|----------------------------|-------------------------------|-------------------------|----------------------------|-------------------------|
| | E (GPa) | H (GPa) | R_q (μm) | R_s (μm) | η (μm^2) | E^* (GPa) | R_q (μm) | η (μm^2) | R_s (μm) |
| Sample 1 | 192.92 | 2.96 | 0.167 | 3.555 | 0.122 | 105.3 | 2.402 | 0.1256 | 0.189 |
| Sample 2 | 192.92 | 2.96 | 0.088 | 7.409 | 0.144 | | | | |



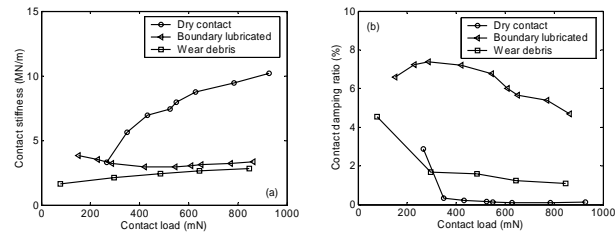
Significant finding: Same trend as Hertz contact but higher contact stiffness, and lower contact damping!



Shi and AAP, JSV, 2004



Effect of lubricant (5 mg) and wear debris



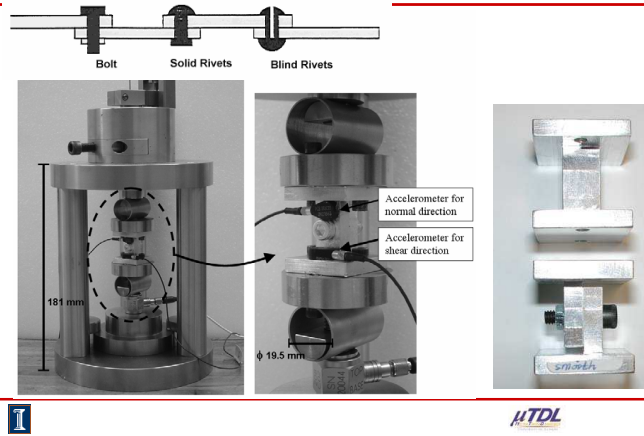
Both lubricant and wear debris decrease contact stiffness significantly!
Only lubricant (1 drop) increases contact damping significantly!!



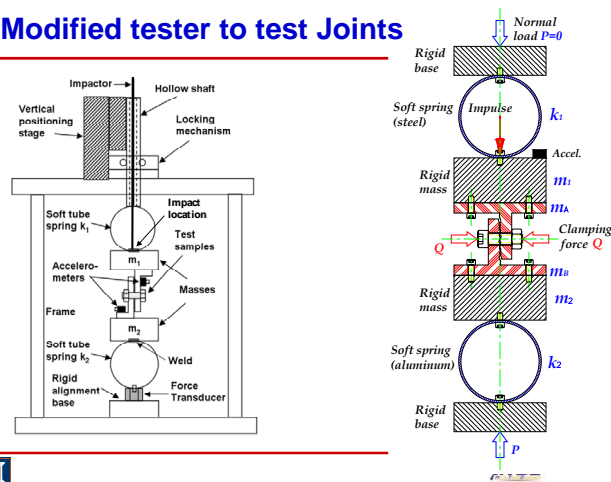
Shi and AAP, JSV, 2004



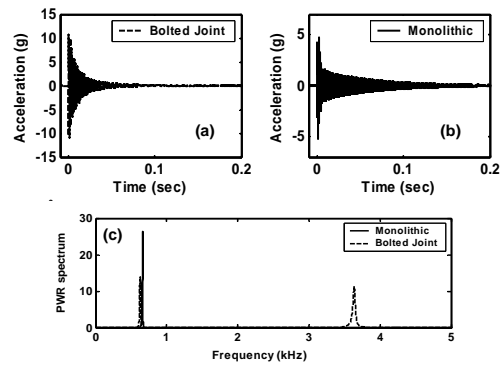
Modified tester to test Joints



Modified tester to test Joints



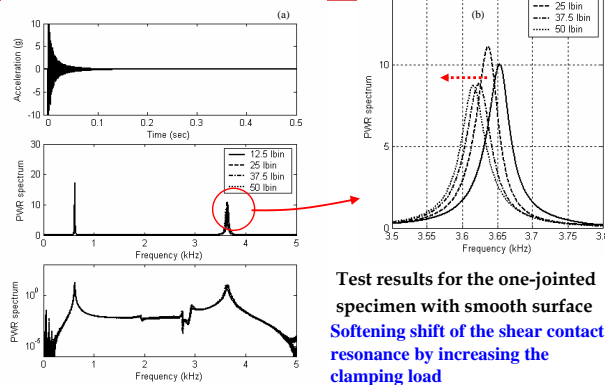
Typical experiments (Joint)



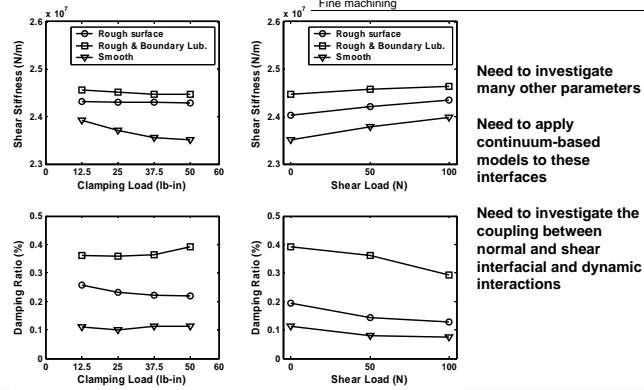
Lee CH and Polycarpou, JVA, in revision, 2006



Clamping effect



Experimental Results



Summary

Micro scale parameters can readily be measured and used in continuum-based interfacial models to predict contact and friction

These models can be coupled with dynamic models to predict coupled dynamic problems with contact

Such modeling approach can also be used in mechanical joints, where currently the interfacial “laws” are oversimplified



A.7 Slide Presentation of Arif Masud, University of Illinois, Urbana: *A Multiscale Framework for Bridging Material Length Scales and Consistent Modeling of Strong Discontinuities in Mechanical Joints*

A Multiscale Framework for Bridging Material Length Scales and Consistent Modeling of Strong Discontinuities in Mechanical Joints

Arif Masud

Associate Professor

**Department of Civil and Environmental Engineering
University of Illinois at Urbana-Champaign**

CEE - UIUC

1

Technical Issues involved in the Modeling of Joints

1. Response functions with embedded scale effects
2. Material models with inherent scale effects
3. Geometric modeling of joint interfaces and scale effects induced by interfaces
4. Sensitivity with respect to the variation in the values of the parameters
5. Predictive capability for the modeling of multiscale effects requires multiscale error estimators
6. Heterogeneous multiscale phenomena with different PDE's appearing at different scales

CEE - UIUC

2

Outline of the Talk

1. One-level scale separation \Rightarrow Sub-scale modeling
 - A linear elastic system
 - A nonlinear material system
2. Incorporation of experimental data via subscale modeling
3. Representation of mechanical joints via discontinuous functions
4. Two-level scale separation and application to nanomechanics
5. A general framework for hierarchical modeling of scales
6. Concluding remarks

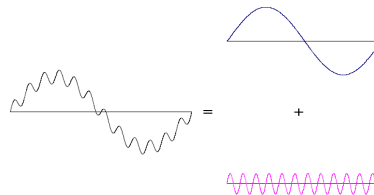
CEE - UIUC

3

Motivation and Objectives

Multiscale Problems

- Multiscale response functions
- Multiscale material models



Key Idea:
$$\underbrace{v(x, t)}_{\text{total sol.}} = \underbrace{\bar{v}(x, t)}_{\text{coarse scale}} + \underbrace{v'(x, t)}_{\text{fine scale}}$$

Develop stable solution algorithms that accommodate large variation in spatial and temporal scales

Develop mathematical framework for error analysis of systems that are multiphysics and multiscale

CEE - UIUC

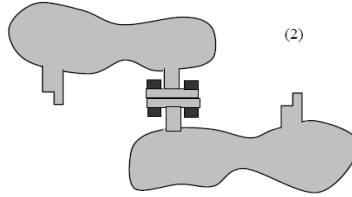
4

A Model Problem

A Mixed Form for Elasticity

$$\begin{aligned} 2\mu\Delta\mathbf{u} + \nabla p + \mathbf{f} &= 0 & \text{in } \Omega \\ \operatorname{div}\mathbf{u} - \frac{p}{\lambda} &= 0 & \text{in } \Omega \end{aligned}$$

- \mathbf{u} := the displacement vector
- p := the pressure field
- \mathbf{f} := the body force vector



Standard Galerkin Form

$$\begin{aligned} (\nabla\mathbf{w}, 2\mu\nabla\mathbf{u}) + (\operatorname{div}\mathbf{w}, p) &= (\mathbf{w}, \mathbf{f}) \\ (q, \operatorname{div}\mathbf{u}) - (q, \frac{1}{\lambda}p) &= 0 \end{aligned}$$

CEE - UIUC

5

One Level Scale Separation

The displacement field

$$\begin{aligned} \mathbf{u}(\mathbf{x}) &= \underbrace{\bar{\mathbf{u}}(\mathbf{x})}_{\text{coarse scale}} + \underbrace{\mathbf{u}'(\mathbf{x})}_{\text{fine scale}} \\ \mathbf{w}(\mathbf{x}) &= \underbrace{\bar{\mathbf{w}}(\mathbf{x})}_{\text{coarse scale}} + \underbrace{\mathbf{w}'(\mathbf{x})}_{\text{fine scale}} \end{aligned}$$

- \mathbf{u}' : envisioned as scale associated with regions of high gradients

The pressure field

$$\begin{aligned} p(\mathbf{x}) &= \bar{p}(\mathbf{x}) + p'(\mathbf{x}) \\ q(\mathbf{x}) &= \bar{q}(\mathbf{x}) + q'(\mathbf{x}) \end{aligned}$$

- Assume (for now) $p' = q' = 0$

Spaces of functions $\mathcal{V} = \bar{\mathcal{V}} \oplus \mathcal{V}'$ (for displacement field)

CEE - UIUC

6

Coarse and Fine Scale Problems

$$\begin{aligned} (\nabla(\bar{\mathbf{w}} + \mathbf{w}'), 2\mu\nabla(\bar{\mathbf{u}} + \mathbf{u}')) + (\operatorname{div}(\bar{\mathbf{w}} + \mathbf{w}'), p) &= (\bar{\mathbf{w}} + \mathbf{w}', \mathbf{f}) \\ (q, \operatorname{div}(\bar{\mathbf{u}} + \mathbf{u}')) - (q, \frac{1}{\lambda}p) &= 0 \end{aligned}$$

Coarse scale sub-problem $\bar{\mathcal{W}}$

$$\begin{aligned} (\nabla\bar{\mathbf{w}}, 2\mu\nabla(\bar{\mathbf{u}} + \mathbf{u}')) + (\operatorname{div}\bar{\mathbf{w}}, p) &= (\bar{\mathbf{w}}, \mathbf{f}) \\ (q, \operatorname{div}(\bar{\mathbf{u}} + \mathbf{u}')) - (q, \frac{1}{\lambda}p) &= 0 \end{aligned}$$

Fine scale sub-problem \mathcal{W}'

$$(\nabla\mathbf{w}', 2\mu\nabla(\bar{\mathbf{u}} + \mathbf{u}')) + (\operatorname{div}\mathbf{w}', p) = (\mathbf{w}', \mathbf{f})$$

CEE - UIUC

7

The fine scale sub-problem (\mathcal{W}')

$$(\nabla\mathbf{w}', 2\mu\nabla\bar{\mathbf{u}}) + (\nabla\mathbf{w}', 2\mu\nabla\mathbf{u}') + (\operatorname{div}\mathbf{w}', p) = (\mathbf{w}', \mathbf{f})$$

$$\begin{aligned} (\nabla\mathbf{w}', 2\mu\nabla\mathbf{u}') &= (\mathbf{w}', \mathbf{f}) + (\mathbf{w}', \nabla p) - (\nabla\mathbf{w}', 2\mu\nabla\bar{\mathbf{u}}) \\ &= (\mathbf{w}', (\mathbf{f} + \nabla p + 2\mu\Delta\bar{\mathbf{u}})) \\ &= (\mathbf{w}', \bar{\mathbf{r}}) \end{aligned}$$

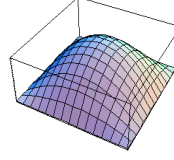
- Note: $\bar{\mathbf{r}}$ is the **residual of coarse scales** over element interiors.

CEE - UIUC

8

Example: Fine scales represented via bubble functions over Ω'_t

$$\mathbf{u}'|_{\Omega^e} = b^e(\boldsymbol{\xi})\boldsymbol{\beta}; \quad \mathbf{w}'|_{\Omega^e} = b^e(\boldsymbol{\xi})\boldsymbol{\gamma} \quad \text{on } \Omega^e$$



1. Substitute \mathbf{u}' and \mathbf{w}' in (\mathcal{W}')

$$\begin{aligned} \boldsymbol{\gamma}^T \left(\int_{\Omega^e} \mu |\nabla b^e|^2 d\Omega \mathbf{I} + \int_{\Omega^e} \mu \nabla b^e \nabla b^{eT} d\Omega \right) \boldsymbol{\beta} &= \boldsymbol{\gamma}^T (b^e, \bar{\mathbf{r}}) \\ \Rightarrow \boldsymbol{\gamma}^T \mathbf{K} \boldsymbol{\beta} &= \boldsymbol{\gamma}^T \mathbf{R} \end{aligned}$$

2. Since $\boldsymbol{\gamma}$ is arbitrary

$$\begin{aligned} \mathbf{K} \boldsymbol{\beta} &= \mathbf{R} \\ \boldsymbol{\beta} &= \mathbf{K}^{-1} \mathbf{R} \end{aligned}$$

3. Reconstruct the fine scale field over the element domain

$$\mathbf{u}'(\mathbf{x}) = b^e(\boldsymbol{\xi}) \mathbf{K}^{-1} \mathbf{R}$$

CEE - UIUC

9

Coarse scale sub-problem $\overline{\mathcal{W}}$

Consider the first equation

$$(\nabla \overline{\mathbf{w}}, 2\mu \nabla \overline{\mathbf{u}}) + (\nabla \overline{\mathbf{w}}, 2\mu \nabla \mathbf{u}') + (\text{div } \overline{\mathbf{w}}, p) = (\overline{\mathbf{w}}, \mathbf{f})$$

$$(\nabla \overline{\mathbf{w}}, 2\mu \nabla \mathbf{u}')_{\Omega} = (\nabla \overline{\mathbf{w}}, 2\mu \mathbf{u}')|_{\Gamma} - (\Delta \overline{\mathbf{w}}, 2\mu \mathbf{u}')_{\Omega}$$

$$\begin{aligned} -(\Delta \overline{\mathbf{w}}, 2\mu \mathbf{u}') &= -(\Delta \overline{\mathbf{w}}, 2\mu b^e \mathbf{K}^{-1} \mathbf{R}) \\ &= -(\Delta \overline{\mathbf{w}}, 2\mu \boldsymbol{\tau} \bar{\mathbf{r}}) \\ &= -(\Delta \overline{\mathbf{w}}, 2\mu \boldsymbol{\tau} (\mathbf{f} + \nabla p + 2\mu \Delta \overline{\mathbf{u}})) \end{aligned}$$

$$(\nabla \overline{\mathbf{w}}, 2\mu \nabla \overline{\mathbf{u}}) + (\text{div } \overline{\mathbf{w}}, p) - (\Delta \overline{\mathbf{w}}, 2\mu \boldsymbol{\tau} (2\mu \Delta \overline{\mathbf{u}} + \nabla p)) = (\overline{\mathbf{w}}, \mathbf{f}) + (\Delta \overline{\mathbf{w}}, 2\mu \boldsymbol{\tau} \mathbf{f})$$

CEE - UIUC

10

Consider the second equation

$$(q, \operatorname{div} \bar{\mathbf{u}}) + (q, \operatorname{div} \mathbf{u}') - (q, \frac{1}{\lambda} p) = 0$$

$$\begin{aligned} (q, \operatorname{div} \mathbf{u}') &= -(\nabla q, \mathbf{u}') \\ &= -(\nabla q, b^e \mathbf{K}^{-1} \mathbf{R}) \\ &= -(\nabla q, (b^e \int_{\Omega^e} b^e d\Omega) [\mu \int_{\Omega^e} |\nabla b^e|^2 d\Omega \mathbf{I} + \mu \int_{\Omega^e} \nabla b^e \otimes \nabla b^e d\Omega]^{-1} \bar{\mathbf{r}}) \\ &= -(\nabla q, \boldsymbol{\tau} \bar{\mathbf{r}}) \end{aligned}$$

Substituting back and rearranging terms

$$(q, \operatorname{div} \bar{\mathbf{u}}) - (q, \frac{1}{\lambda} p) - (\nabla q, \boldsymbol{\tau} (2\mu \Delta \bar{\mathbf{u}} + \nabla p)) = (\nabla q, \boldsymbol{\tau} \mathbf{f})$$

CEE - UIUC

11

The Multiscale Form

To keep notation simple, drop the superposed bars.

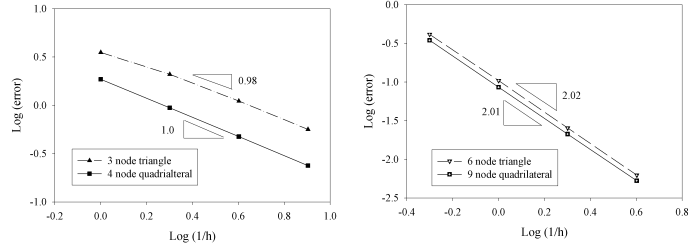
$$\begin{aligned} (\nabla \mathbf{w}, 2\mu \nabla \mathbf{v}) &+ (\operatorname{div} \mathbf{w}, p) + (q, \operatorname{div} \mathbf{v}) - (q, \frac{1}{\lambda} p) \\ &+ ((-2\mu \Delta \mathbf{w} - \nabla q), \boldsymbol{\tau} (2\mu \Delta \mathbf{v} + \nabla p + \mathbf{f})) = (\mathbf{w}, \mathbf{f}) \end{aligned}$$

Remarks:

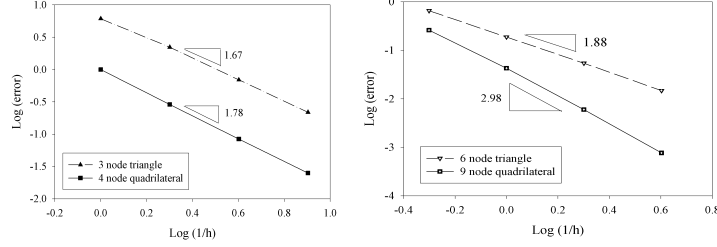
- Additional terms have appeared because of the assumption of existence of fine scales in the problem.
- Additional terms are residual based \Rightarrow The resulting formulation is **consistent** and accommodates the exact solution.
- These terms are performing a **mathematical projection of information from fine scales to coarse scales**.
- Additional terms also improve upon the stability of Galerkin's method.

CEE - UIUC

12



Convergence in the energy norm for linear and quadratic elements



Convergence in the L_2 norm of pressure field for linear and quadratic elements

Incorporation of Experimental Data via Sub-scale Modeling

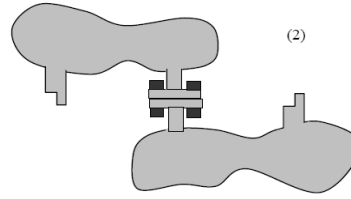
Reconsider the fine scale sub-problem (\mathcal{W}')

$$(\nabla \mathbf{w}', 2\mu \nabla \mathbf{u}') = (\mathbf{w}', \bar{\mathbf{r}})$$

- $\bar{\mathbf{r}}$ is the residual of coarse scales over element interiors.
- For available experimental data, set $\bar{\mathbf{r}} = \bar{\mathbf{u}} - \mathbf{u}^{\text{measured}}$
- Fine scales will now represent corrections to the model predictions
- Variational reduction of error w.r.t. the experimentally measured data

Geometric Modeling of the Joint Interface

Consider the body as one domain



- Employ discontinuous functions only at the joint interface \Rightarrow DG ideas
- Physical fields may or may not be continuous across the strong discontinuity \Rightarrow relative slip is permitted
- Flux terms will weakly enforce the continuity of the fields
- Flux terms will provide a mechanism to embed friction models

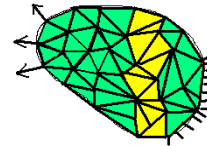
CEE - UIUC

15

One-Level Scale Separation for Material Nonlinearity

Small Deformation Inelasticity

$$\begin{aligned}\nabla \cdot \boldsymbol{\sigma} + \mathbf{b} &= \mathbf{0} \\ (\boldsymbol{\varepsilon} - \boldsymbol{\varepsilon}^p) \cdot \boldsymbol{\delta} - \frac{p}{k} &= 0\end{aligned}$$



The Standard Galerkin Form

$$\begin{aligned}\int_{\Omega} \text{sym} \nabla \mathbf{w} : \boldsymbol{\sigma} \, d\Omega &= \int_{\Omega} \mathbf{w} \cdot \mathbf{b} \, d\Omega + \int_{\Gamma} \mathbf{w} \cdot \mathbf{t} \, d\Gamma \\ \int_{\Omega} q(\boldsymbol{\varepsilon} - \boldsymbol{\varepsilon}^p) \cdot \boldsymbol{\delta} \, d\Omega - \int_{\Omega} q \frac{p}{k} \, d\Omega &= 0\end{aligned}$$

Scale Separation $\mathbf{u}(\mathbf{x}) = \underbrace{\bar{\mathbf{u}}(\mathbf{x})}_{\text{coarse scale}} + \underbrace{\mathbf{u}'(\mathbf{x})}_{\text{fine scale}}$

- \mathbf{u}' can be envisioned as scale associated with regions of high gradients

CEE - UIUC

16

Multiscale Framework

$$\begin{aligned} \int_{\Omega} \text{sym} \nabla (\bar{\mathbf{w}} + \mathbf{w}') : \boldsymbol{\sigma} \, d\Omega &= \int_{\Omega} (\bar{\mathbf{w}} + \mathbf{w}') \cdot \mathbf{b} \, d\Omega + \int_{\Gamma} (\bar{\mathbf{w}} + \mathbf{w}') \cdot \mathbf{t} \, d\Gamma \\ \int_{\Omega} q(\boldsymbol{\varepsilon} - \boldsymbol{\varepsilon}^p) \cdot \boldsymbol{\delta} \, d\Omega - \int_{\Omega} q \frac{p}{k} \, d\Omega &= 0 \end{aligned}$$

The Coarse Scale Problem ($\bar{\mathcal{W}}$)

$$\begin{aligned} \int_{\Omega} \text{sym} \nabla \bar{\mathbf{w}} : \boldsymbol{\sigma} \, d\Omega &= \int_{\Omega} \bar{\mathbf{w}} \cdot \mathbf{b} \, d\Omega + \int_{\Gamma} \bar{\mathbf{w}} \cdot \mathbf{t} \, d\Gamma \\ \int_{\Omega} q(\boldsymbol{\varepsilon} - \boldsymbol{\varepsilon}^p) \cdot \boldsymbol{\delta} \, d\Omega - \int_{\Omega} q \frac{p}{k} \, d\Omega &= 0 \end{aligned}$$

The Fine Scale Problem (\mathcal{W}')

$$\int_{\Omega} \text{sym} \nabla \mathbf{w}' : \boldsymbol{\sigma} \, d\Omega = \int_{\Omega} \mathbf{w}' \cdot \mathbf{b} \, d\Omega + \int_{\Gamma} \mathbf{w}' \cdot \mathbf{t} \, d\Gamma$$

CEE - UIUC

17

Solution of the Fine Scale Problem (\mathcal{W}')

1. Incremental quantities

$$\begin{aligned} \mathbf{u}_{n+1}^{i+1} &= \mathbf{u}_{n+1}^i + \Delta \mathbf{u} \\ &= \bar{\mathbf{u}}_{n+1}^i + \mathbf{u}_{n+1}'^i + \Delta \bar{\mathbf{u}} + \Delta \mathbf{u}' \\ p_{n+1}^{i+1} &= p_{n+1}^i + \Delta p \\ \boldsymbol{\sigma}_{n+1}^{i+1} &= \boldsymbol{\sigma}_{n+1}^i + \Delta \boldsymbol{\sigma} \end{aligned}$$

- Δ := increment in the quantities between two successive iterates

2. Substitute the current state of stress $\boldsymbol{\sigma}_{n+1}^{i+1}$ in $\bar{\mathcal{W}}$

$$\int_{\Omega'} \text{sym} \nabla \mathbf{w}' : \Delta \boldsymbol{\sigma} \, d\Omega = \int_{\Omega'} \mathbf{w}' \cdot \mathbf{b} \, d\Omega - \int_{\Omega'} \text{sym} \nabla \mathbf{w}' : \boldsymbol{\sigma}_{n+1}^i \, d\Omega$$

- $\Delta \boldsymbol{\sigma} = \bar{\mathbf{D}}^{\text{uu}} \Delta \boldsymbol{\varepsilon} + \bar{\mathbf{D}}^{\text{up}} \Delta p$
- $\Delta \boldsymbol{\varepsilon} = \Delta \bar{\boldsymbol{\varepsilon}} + \Delta \boldsymbol{\varepsilon}'$

CEE - UIUC

18

3. Substitute $\Delta\sigma$ and then $\Delta\varepsilon$

$$\begin{aligned} \int_{\Omega'} \text{sym} \nabla \mathbf{w}' : [\overline{\mathbf{D}}^{\text{uu}}(\Delta\overline{\varepsilon} + \Delta\overline{\varepsilon}') + \overline{\mathbf{D}}^{\text{up}} \Delta p] d\Omega &= \int_{\Omega'} \mathbf{w}' \cdot \mathbf{b} d\Omega \\ &- \int_{\Omega'} \text{sym} \nabla \mathbf{w}' : \sigma_{n+1}^i d\Omega \end{aligned}$$

4. Rearranging the terms

$$\begin{aligned} \int_{\Omega'} \text{sym} \nabla \mathbf{w}' : \overline{\mathbf{D}}^{\text{uu}} \Delta\overline{\varepsilon}' d\Omega &= \int_{\Omega'} \mathbf{w}' \cdot \mathbf{b} d\Omega \\ &- \int_{\Omega'} \text{sym} \nabla \mathbf{w}' : [\sigma_{n+1}^i + \overline{\mathbf{D}}^{\text{uu}} \Delta\overline{\varepsilon} + \overline{\mathbf{D}}^{\text{up}} \Delta p] d\Omega \end{aligned}$$

5. Expand fine-scales via higher-order functions: i.e., $\Delta \mathbf{u}' = \mathbf{b}^e(\xi) \Delta \mathbf{u}'_e$

$$\begin{aligned} \mathbf{w}'_e{}^T \int_{\Omega'} [(\nabla \mathbf{b}^e)^T \overline{\mathbf{D}}^{\text{uu}} \nabla \mathbf{b}^e d\Omega] \Delta \mathbf{u}'_e &= \mathbf{w}'_e{}^T [\mathbf{R}_{n+1}^i] \\ \Rightarrow \Delta \mathbf{u}'_e &= \mathbf{K}^{-1} \mathbf{R}_{n+1}^i \end{aligned}$$

6. Construct the fine-scale field: $\Delta \mathbf{u}' = \mathbf{b}^e \mathbf{K}^{-1} \mathbf{R}_{n+1}^i$

CEE - UIUC

19

The Modified Coarse-Scale Problem ($\overline{\mathcal{W}}$): Substitute current σ_{n+1}^{i+1}

$$\int_{\Omega} \text{sym} \nabla \overline{\mathbf{w}} : \Delta \sigma d\Omega = \int_{\Omega} \overline{\mathbf{w}} \cdot \mathbf{b} d\Omega + \int_{\Gamma} \overline{\mathbf{w}} \cdot \mathbf{t} d\Gamma - \int_{\Omega} \text{sym} \nabla \overline{\mathbf{w}} : \sigma_{n+1}^i d\Omega$$

• Split incremental strain into coarse and fine parts

$$\begin{aligned} \int_{\Omega} \text{sym} \nabla \overline{\mathbf{w}} : \overline{\mathbf{D}}^{\text{uu}} \Delta\overline{\varepsilon} d\Omega &+ \int_{\Omega} \text{sym} \nabla \overline{\mathbf{w}} : \overline{\mathbf{D}}^{\text{uu}} \Delta\overline{\varepsilon}' d\Omega + \int_{\Omega} \text{sym} \nabla \overline{\mathbf{w}} : \overline{\mathbf{D}}^{\text{up}} \Delta p d\Omega \\ &= \int_{\Omega} \overline{\mathbf{w}} \cdot \mathbf{b} d\Omega + \int_{\Gamma} \overline{\mathbf{w}} \cdot \mathbf{t} d\Gamma - \int_{\Omega} \text{sym} \nabla \overline{\mathbf{w}} : \sigma_{n+1}^i d\Omega \end{aligned}$$

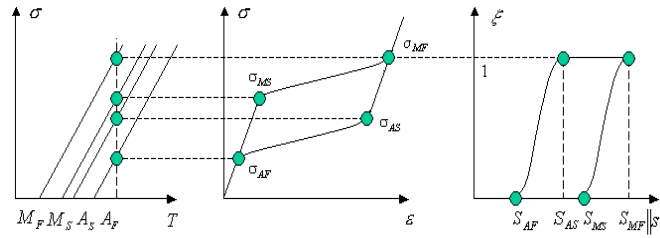
The Modified Equation Containing Coarse and Fine Scales

$$\begin{aligned} &\int_{\Omega} \text{sym} \nabla \overline{\mathbf{w}} : \overline{\mathbf{D}}^{\text{uu}} : \Delta\overline{\varepsilon} d\Omega + \int_{\Omega} \text{sym} \nabla \overline{\mathbf{w}} : \overline{\mathbf{D}}^{\text{up}} \Delta p d\Omega \\ &+ \int_{\Omega} \text{sym} \nabla \overline{\mathbf{w}} : \overline{\mathbf{D}}^{\text{uu}} \tau_1 [(\overline{\mathbf{D}}^{\text{uu}} \Delta\overline{\varepsilon} + \overline{\mathbf{D}}^{\text{up}} \Delta p)] d\Omega \\ &= \int_{\Omega} \overline{\mathbf{w}} \cdot \mathbf{b} d\Omega + \int_{\Gamma} \overline{\mathbf{w}} \cdot \mathbf{t} d\Gamma - \int_{\Omega} \text{sym} \nabla \overline{\mathbf{w}} (1 + \overline{\mathbf{D}}^{\text{uu}} \tau_1) : \sigma_{n+1}^i d\Omega \end{aligned}$$

CEE - UIUC

20

Shape Memory Alloy Model

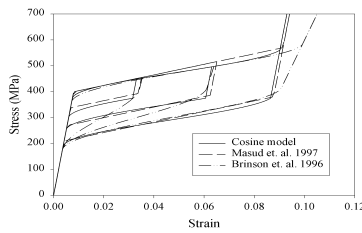


Assumptions in the model:

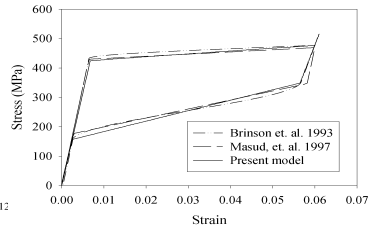
- Process is isothermal
- Phase-transformations depend only on the deviatoric part of stress
- Absence of phase transformation \Rightarrow material is elastic

CEE - UIUC

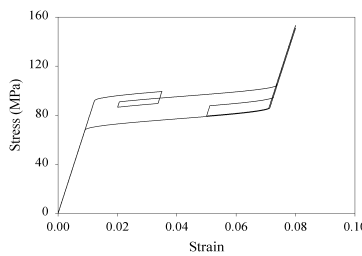
21



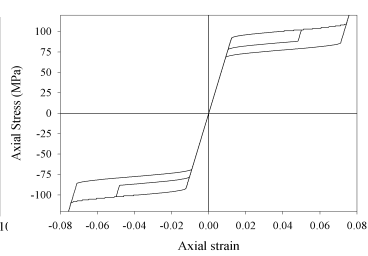
Unloading from $\xi = 1/3, 2/3$ and 1.



Unloading from $\xi = 1$.



Incomplete $A \rightarrow M$ and $M \rightarrow A$

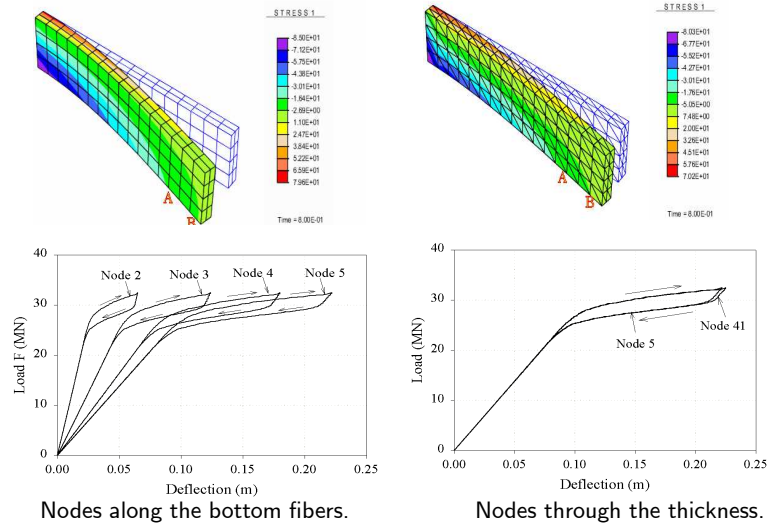


$\sigma - \epsilon$ in Tension & Compression

CEE - UIUC

22

Biaxial Bending of SMA beam



CEE - UIUC

23

Multiscale Structural Response to a Multiscale Force

The Model Problem

$$\mathcal{L}u = f \quad \text{in } \Omega$$

The standard Galerkin form

$$(w, \mathcal{L}u) = (w, f)$$

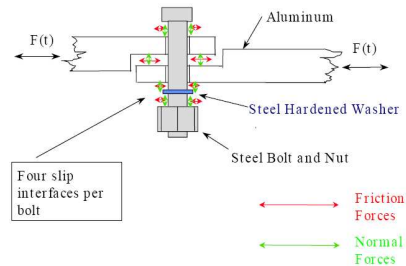
Two-Level Scale Separation

1. **Level one:** Additive decomposition of the solution

$$u(x) = \underbrace{\bar{u}(x)}_{\text{coarse scale}} + \underbrace{u'(x)}_{\text{fine scale}}; \quad w(x) = \underbrace{\bar{w}(x)}_{\text{coarse scale}} + \underbrace{w'(x)}_{\text{fine scale}}$$

2. The modified Galerkin form

$$(\bar{w} + w', \mathcal{L}(\bar{u} + u')) = (\bar{w} + w', f)$$



CEE - UIUC

24

3. **Level two:** Additive decomposition of the forcing function

$$\mathbf{f}(\mathbf{x}) = \underbrace{\bar{\mathbf{f}}(\mathbf{x})}_{\text{coarse scale}} + \underbrace{\mathbf{f}'(\mathbf{x})}_{\text{fine scale}}$$

- $\bar{\mathbf{f}} :=$ coarse scales (or low frequency) force component
- $\mathbf{f}' :=$ fine scales (or high frequency) force component

4. The decomposition of \mathbf{f} yields a further decomposition of $\bar{\mathbf{u}}$ and \mathbf{u}'

$$\begin{aligned}\bar{\mathbf{u}} &= \underbrace{\bar{\mathbf{u}}_{\bar{\mathbf{f}}}}_{\text{coarse-coarse}} + \underbrace{\bar{\mathbf{u}}_{\mathbf{f}'}}_{\text{coarse-fine}} \\ \mathbf{u}' &= \underbrace{\mathbf{u}'_{\bar{\mathbf{f}}}}_{\text{fine-coarse}} + \underbrace{\mathbf{u}'_{\mathbf{f}'}}_{\text{fine-fine}}\end{aligned}$$

- $\bar{\mathbf{u}}_{\bar{\mathbf{f}}}$ and $\mathbf{u}'_{\bar{\mathbf{f}}}$: coarse and fine scale components that arise because of $\bar{\mathbf{f}}$
- $\bar{\mathbf{u}}_{\mathbf{f}'}$ and $\mathbf{u}'_{\mathbf{f}'}$: coarse and fine scale components that arise because of \mathbf{f}'

Two-level scale separation

$$\left(\bar{\mathbf{w}} + \mathbf{w}', \mathcal{L} \left((\bar{\mathbf{u}}_{\bar{\mathbf{f}}} + \bar{\mathbf{u}}_{\mathbf{f}'}) + (\mathbf{u}'_{\bar{\mathbf{f}}} + \mathbf{u}'_{\mathbf{f}'}) \right) \right) = (\bar{\mathbf{w}} + \mathbf{w}', \bar{\mathbf{f}} + \mathbf{f}')$$

Employing bi-linearity and additive decomposition of the forcing function

- Sub-Problem 1: $(\bar{\mathbf{w}} + \mathbf{w}', \mathcal{L}(\bar{\mathbf{u}}_{\bar{\mathbf{f}}} + \mathbf{u}'_{\bar{\mathbf{f}}})) = (\bar{\mathbf{w}} + \mathbf{w}', \bar{\mathbf{f}})$
- Sub-Problem 2: $(\bar{\mathbf{w}} + \mathbf{w}', \mathcal{L}(\bar{\mathbf{u}}_{\mathbf{f}'} + \mathbf{u}'_{\mathbf{f}'})) = (\bar{\mathbf{w}} + \mathbf{w}', \mathbf{f}')$

$$\begin{aligned}\text{Coarse scale system} \quad (\bar{\mathbf{w}}, \mathcal{L}(\bar{\mathbf{u}}_{\bar{\mathbf{f}}} + \mathbf{u}'_{\bar{\mathbf{f}}})) &= (\bar{\mathbf{w}}, \bar{\mathbf{f}}) \\ (\bar{\mathbf{w}}, \mathcal{L}(\bar{\mathbf{u}}_{\mathbf{f}'} + \mathbf{u}'_{\mathbf{f}'})) &= (\bar{\mathbf{w}}, \mathbf{f}')$$

$$\begin{aligned}\text{Fine scale system} \quad (\mathbf{w}', \mathcal{L}(\bar{\mathbf{u}}_{\bar{\mathbf{f}}} + \mathbf{u}'_{\bar{\mathbf{f}}})) &= (\mathbf{w}', \bar{\mathbf{f}}) \\ (\mathbf{w}', \mathcal{L}(\bar{\mathbf{u}}_{\mathbf{f}'} + \mathbf{u}'_{\mathbf{f}'})) &= (\mathbf{w}', \mathbf{f}')$$

Key idea: extract the components $\mathbf{u}'_{\bar{\mathbf{f}}}$ and $\mathbf{u}'_{\mathbf{f}'}$.

Important Features of the Formulation:

1. Multiscale decomposition of \mathbf{f} provides two sub-systems
2. **System driven by $\bar{\mathbf{f}}$** : Solve the fine scale problem to obtain $\mathbf{u}'_{\bar{\mathbf{f}}}$.
 - Substitute $\mathbf{u}'_{\bar{\mathbf{f}}}$ in the corresponding coarse scale subproblem \Rightarrow multiscale formulation for coarse scale $\bar{\mathbf{u}}_{\bar{\mathbf{f}}}$
3. **System driven by \mathbf{f}'** : Solve the fine scale problem to obtain $\mathbf{u}'_{\mathbf{f}'}$.
 - Substitute $\mathbf{u}'_{\mathbf{f}'}$ in its corresponding coarse scale subproblem \Rightarrow yields multiscale formulation for the bridging scales $\bar{\mathbf{u}}_{\mathbf{f}'}$.
4. Problem driven by \mathbf{f}' can be solved over a smaller subdomain $\Omega_{\text{sub}} \subset \Omega$
5. Total solution obtained via principle of superposition: $\bar{\mathbf{u}} = \bar{\mathbf{u}}_{\bar{\mathbf{f}}} + \bar{\mathbf{u}}_{\mathbf{f}'}$
6. For the geometrically nonlinear case employ the Lagrange multiplier method for overlapping solutions (Belytschko et al 2003).

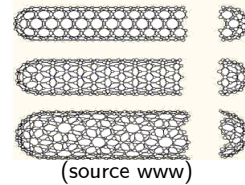
CEE - UIUC

27

Example: Application of Two-level Scale Separation to the Modeling of Carbon Nanotubes

Mechanical Properties of Nanotubes

- Diameter: SWNT 1-2 nm, MWNT up to 25 nm
- Length: 100 μm (and larger)
- Young's modulus $\approx 1 \text{ TPa}$
- Properties depend on chirality of nanotubes



Technical Issues

- Atomistic simulations have limitations concerning time scales (10^{-12} – 10^{-9} second) and length scales (10^{-9} – 10^{-6} meter)
- Atomistic simulations have difficulty for systems with multiple nanotubes

CEE - UIUC

28

Key Idea: Two-level scale separation

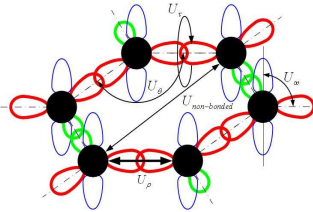
- Yields evolution equations for the bridging-scales
 - Accommodates two concurrent domains
1. Quasi-continuum domain \Rightarrow defect-free nano-material
 - Material moduli based on nanoscale internal variables
 2. Atomic-scale domain \Rightarrow modeling of point defect
 - Incorporates interatomic potentials
 3. Shear-stabilized Geometrically Exact Shell Model employed as the underlying quasi-continuum model for the nanotubes

CEE - UIUC

29

Molecular Mechanics

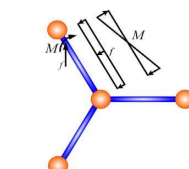
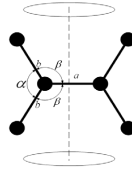
$$U = U_\rho + U_\theta + U_\varphi + U_\omega + U_{vdw} + U_{es}$$



Stick-Spiral Model

(Gao *et al.* 2003)

$$U = U_\rho + U_\theta$$



Armchair nanotube

- Force-equilibrium: $f \sin(\frac{\alpha}{2}) = F(\Delta r)$
- Moment-equilibrium: $f \frac{r}{2} \cos(\frac{\alpha}{2}) = M(\Delta \alpha) + M(\Delta \beta) \cos \Phi$
- Expressions for ε and ε' are derived in terms of $\Delta r, \Delta \alpha, \Delta \beta$

CEE - UIUC

30

Non-Linear Spring Analogy: Modified Morse Potential

$$U = U_\rho + U_\theta$$

$$U_\rho = D_e \{ [1 - e^{-\beta(\Delta r)}]^2 - 1 \}$$

$$U_\theta = \frac{1}{2} K_\theta (\Delta\theta)^2 [1 + K_{sextic}(\Delta\theta)^4]$$

1. Force-stretch relation

$$F(\Delta r) = 2\beta D_e (1 - e^{-\beta(\Delta r)}) e^{-\beta(\Delta r)}$$

2. Moment-angle variation relation

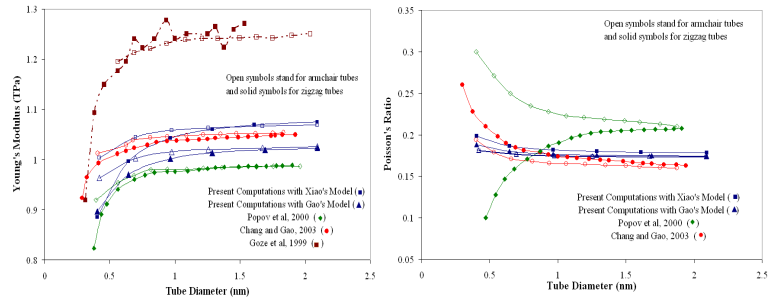
$$M(\Delta\theta) = K_\theta(\Delta\theta)[1 + 3K_{sextic}(\Delta\theta)^4]$$

- Substituting 1 & 2 in the force and moment equilibrium relations yields a nonlinear relation between Δr and $\Delta\theta$
- Stick-spiral model yields a relation between ε , Δr and $\Delta\theta$

CEE - UIUC

31

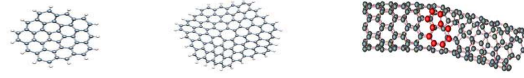
Nanotube: Mechanical Properties



CEE - UIUC

32

Modeling of Point Defects in Carbon Nanotubes



5-sided pentagons and 7-sided heptagons. (source www)

1. The local defects in the nanotube and graphene sheet induce an atomic-scale (fine scale) force field which is indicated by \mathbf{f}' .
2. \mathbf{f}' is obtained as the difference of the energy minima for the defective and the non-defective nano-material.

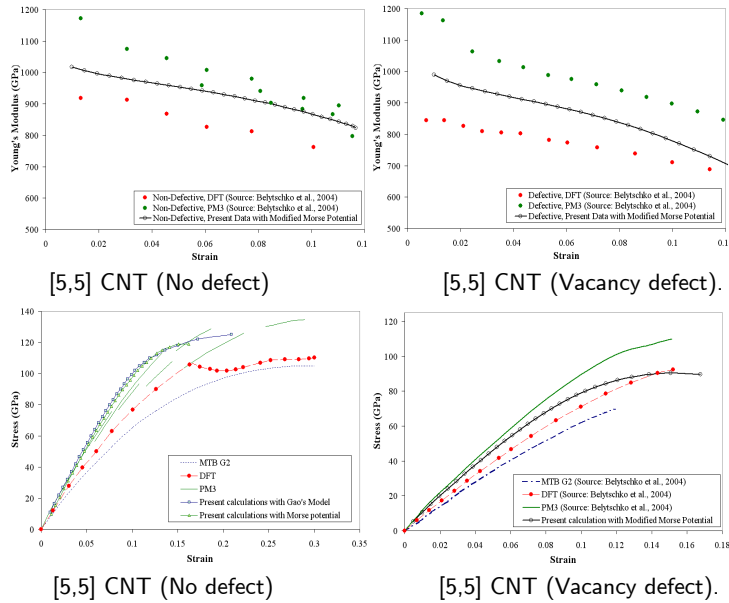
$$\mathbf{f}' = \left\{ \left(\frac{\partial V(\mathbf{r})}{\partial \mathbf{r}} \right)_{relative} \right\} = \left\{ \left(\frac{\partial V(\mathbf{r})}{\partial \mathbf{r}} \right)_{defect} - \left(\frac{\partial V(\mathbf{r})}{\partial \mathbf{r}} \right)_{non-defect} \right\}$$

3. If during deformation bond angles/lengths change and defect disappears, i.e., $\mathbf{f}' = \{(\partial V(\mathbf{r})/\partial \mathbf{r})_{relative}\} = \mathbf{0} \Rightarrow$ localized effect also disappears.

$$(\bar{\mathbf{w}}, \mathcal{L}\bar{\mathbf{u}}_{f'}) + (\mathcal{L}^*\bar{\mathbf{w}}, \mathbf{u}'_{f'}) = (\bar{\mathbf{w}}, \mathbf{f}')$$

CEE - UIUC

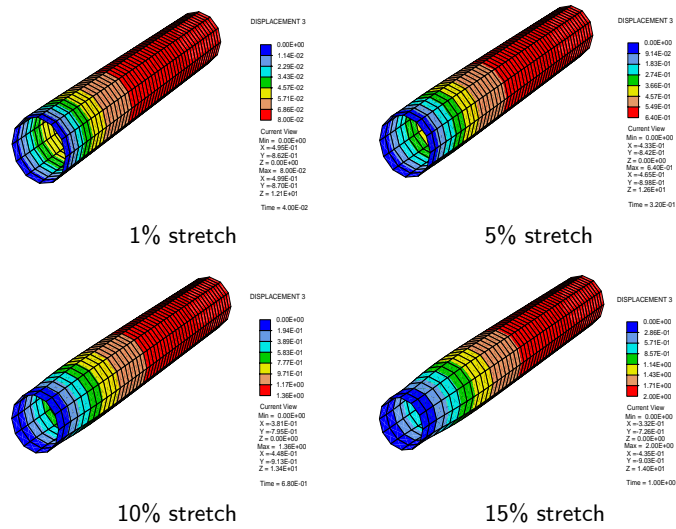
33



CEE - UIUC

34

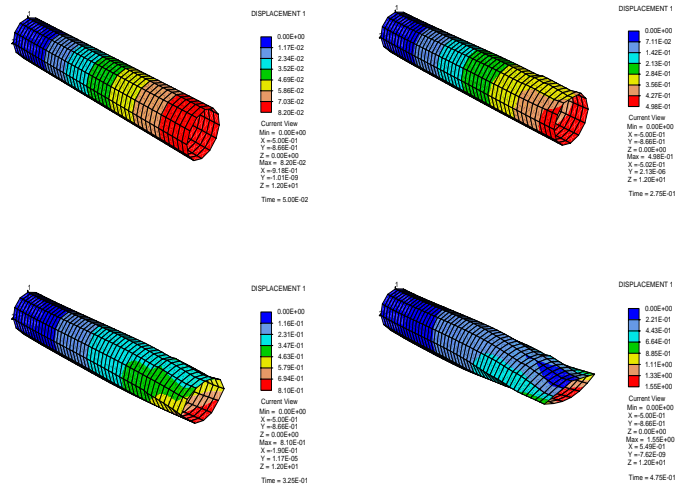
Quasi-continuum Modeling: Stretching of a single wall nanotube



CEE - UIUC

35

Quasi-continuum Modeling: Bending of a single wall nanotube



CEE - UIUC

36

A Hierarchical Framework for the Modeling of Scales

Model Problem: $\mathcal{L}u = f \quad \text{in } \Omega$

Standard Weak Form: $(w, \mathcal{L}u) = (w, f)$

Three-Level Scale Separation

1. Additive decomposition of the solution

$$\begin{aligned} u(x) &= \underbrace{\bar{u}(x)}_{\text{coarse}} + \underbrace{u'(x)}_{\text{fine}} + \underbrace{\hat{u}(x)}_{\text{very fine}} \\ w(x) &= \underbrace{\bar{w}(x)}_{\text{coarse}} + \underbrace{w'(x)}_{\text{fine}} + \underbrace{\hat{w}(x)}_{\text{very fine}} \end{aligned}$$

2. Substitute u and w in the standard Galerkin form

$$(\bar{w} + w' + \hat{w}, \mathcal{L}(\bar{u} + u' + \hat{u})) = (\bar{w} + w' + \hat{w}, f)$$

CEE - UIUC

37

3. Linearity of the weighting function slot leads to three coupled problems

$$\begin{aligned} (\bar{w}, \mathcal{L}(\bar{u} + u' + \hat{u})) &= (\bar{w}, f) \\ (w', \mathcal{L}(\bar{u} + u' + \hat{u})) &= (w', f) \\ (\hat{w}, \mathcal{L}(\bar{u} + u' + \hat{u})) &= (\hat{w}, f) \end{aligned}$$

4. **Assumption:** The projection of the very-fine scales onto the coarse scale space is approximately zero.

$$(\bar{w}, \mathcal{L}\hat{u}) \approx 0$$

5. This assumption is reasonable if a clear scale separation between the coarse and the very-fine scales can be established.

6. Coarse scales are influenced by the very-fine scales, however through the "intermediate" or the fine scales.

7. Same argument leads to restriction on the opposite projection

$$(\hat{w}, \mathcal{L}\bar{u}) \approx 0$$

CEE - UIUC

38

Concluding Remarks

Presented a hierarchical multiscale framework for embedding fine scales of the problem directly into the mathematical formulation

Present method can also be viewed as a method for consistent embedding of the part of physics that is otherwise lost in the classical Galerkin approach.

Presented an application of the multiscale computational framework for bridging molecular mechanics and quasi-continuum mechanics

Material moduli are based on nanoscale internal variables and interatomic potentials are employed for the modeling of point defects

Unlike the classical Galerkin approach where the fine scales can only be resolved via successive mesh refinements, in the proposed method **fine scales are consistently represented in the coarse scales.**

A.8 Slide Presentation of Mark Robbins, Johns Hopkins University, Baltimore, MD: *Contact and Friction: Connecting Atomic Interactions to Macroscopic Behavior*

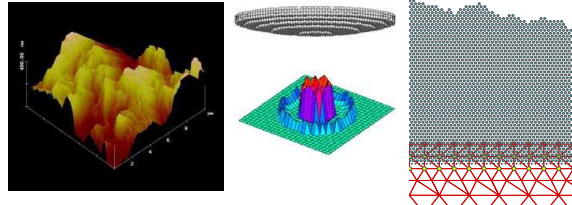
Contact and Friction: Connecting Atomic Interactions to Macroscopic Behavior

NSF-Sandia Joints Modelling Workshop, Oct. 16, 2006

Collaborators: B. Luan, L. Pei, S. Hyun, J. F. Molinari,
N. Bernstein, J. A. Harrison, B. Luan

Supported by NSF DMR-0454947, CMS-0103408

Rough Surface Contact **Atomic Effects** **Multiscale Model**



Why are contacts interesting?

Regions where two surfaces contact control friction, adhesion, stiffness, plastic deformation, thermal and electrical conduction, ...

of bearings, granular media, gecko feet, ...

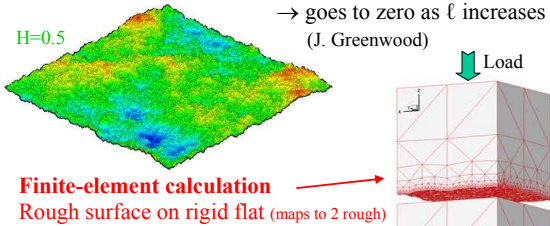
Calculating contact is a hard multiscale problem because most surfaces are rough on a wide range of length scales, different physical processes are important at different scales

Atomic scale interactions at interface produce friction and adhesion forces, but contact area, geometry and properties determined by elastic and plastic deformation on all larger scales

Surfaces Often Rough on Many Scales \Rightarrow Self-Affine

Height variation Δh over length $\ell \rightarrow \Delta h \propto \ell^H \quad H < 1$
 Average slope $\Delta h / \ell \propto \ell^{-(1-H)} \rightarrow$ diverges as scale ℓ decreases
 \rightarrow goes to zero as ℓ increases
 (J. Greenwood)

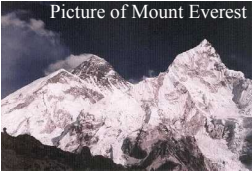
$H=0.5$



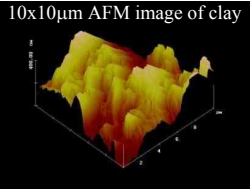
Finite-element calculation
 Rough surface on rigid flat (maps to 2 rough)
 Elastic or J2 isotropic plastic constitutive law
 Periodic boundary conditions, $L=512$ nodes per edge
 Full range of H and roughness amplitudes

Hyun, Pei, Molinari, & Robbins, Phys. Rev. E **70**, 026117, '04; J. Mech. Phys. Sol. **53**, 2385, '05

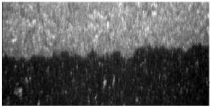
Examples, with $H=0.8$ (www.phys.ntnu.no)



Picture of Mount Everest



10x10 μ m AFM image of clay



Crack in a plexiglass block

Fractured and polished surfaces self-affine over large range of scales

Polished wood, granite, lucite $H \sim 0.6$

Simple way of parameterizing large range of roughness scales
Find similar results for non-fractal experimental surfaces

Contact Mechanics Results for Area A vs. Load N

- Single spherical contact $A \propto N^{2/3}$ (Hertz)
- Multi-asperity elastic models $A = \kappa N/E' \Delta$ for small N
 where $E' = E/(1-\nu^2)$, E =Young's modulus, ν =Poisson ratio,
 Δ =rms surface slope $\Delta \equiv \sqrt{\langle |\nabla h|^2 \rangle}$
 Same radius, different height - Greenwood and Williamson, 1966
 Random radii and ellipticity - Bush et al., 1975 $\kappa = (2\pi)^{1/2}$
 Self-affine surfaces - Persson, 2001 $\kappa = (8/\pi)^{1/2}$
- Multi-asperity plastic models $A = W/H$ with hardness $H \sim 3\sigma_y$
 and yield stress σ_y
- Previous simulations elastic and only for Poisson ratio $\nu=0$
 Batrouni et al. $A \propto N^{1.1}$
 Borri-Brunetto, Chiaia, Ciavarella $A \propto N$, but don't focus on κ
 S. Hyun, L. Pei, J.F. Molinari, and M.O. Robbins, "Finite-element
 analysis of contact between elastic self-affine surfaces", *Phys.
 Rev. E*, **70** (2), 026117 (2004).
 Paper on plasticity *J. Mech. Physics of Solids* **53**, 2385 (2005).

Area \propto load N for nonadhesive contact

Constant mean pressure in contact $\langle p \rangle = N/A$ at low N
 Controlled by rms local slope, Δ , not total roughness

Elastic: $\langle p \rangle / E' = \Delta / \kappa$

$E' = E/(1-\nu^2)$

=effective modulus

$$\Delta \equiv \sqrt{\langle |\nabla h|^2 \rangle}$$

=rms surface slope

$\kappa(H, \nu)$ from 1.8 to 2.2

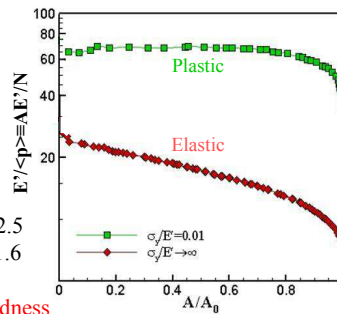
Analytic predictions:

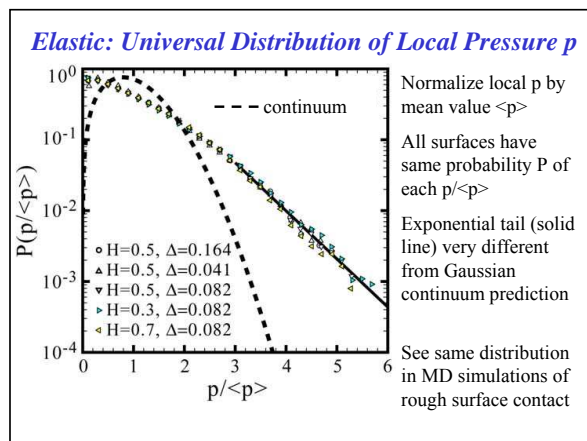
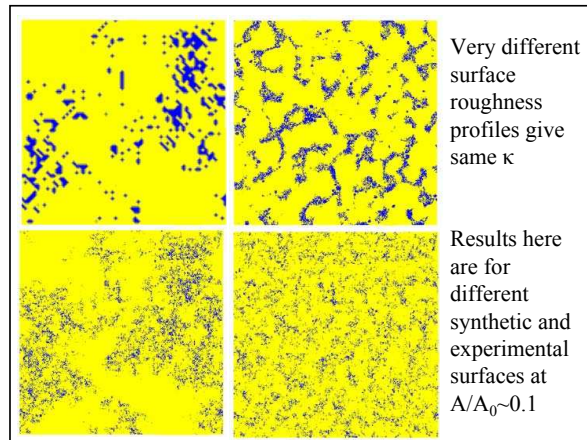
Bush et al., $\kappa = (2\pi)^{1/2} \approx 2.5$

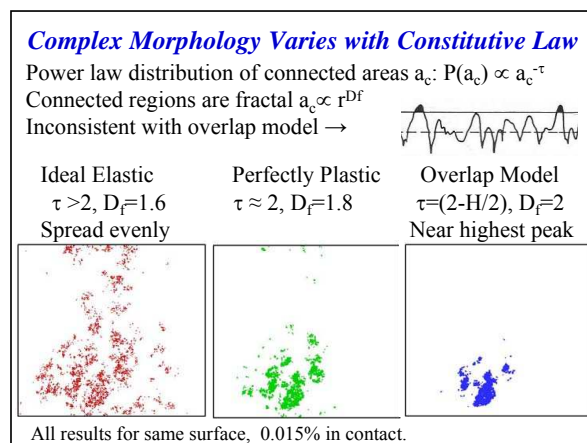
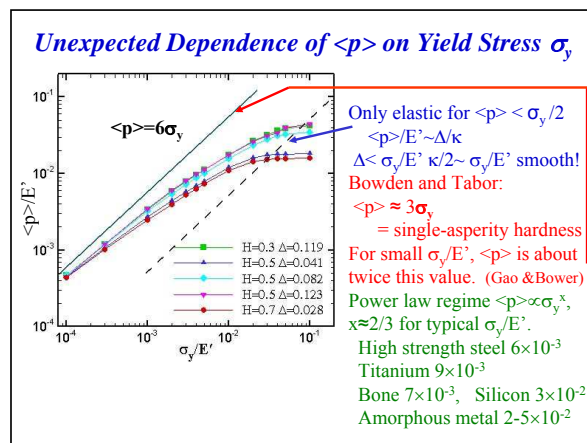
Persson $\kappa = (8/\pi)^{1/2} \approx 1.6$

Plastic: $\langle p \rangle \neq 3\sigma_y$

$3\sigma_y$ =single-asperity hardness

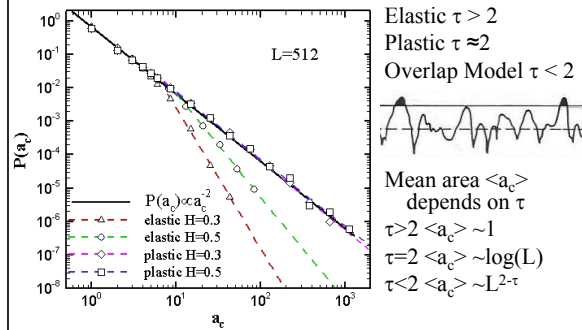






Probability Distribution of Cluster Areas a_c

Power law distribution $P(a_c) \sim a_c^{-\tau}$: τ depends on H if elastic, not if plastic. Cluster areas fractal.



Conclusions of Continuum Studies of Non-Adhesive Contact

- Area proportional to load $\rightarrow \langle p \rangle = \text{constant}$
Elastic: $\langle p \rangle / E^* = \Delta / \kappa$ Plastic: $\langle p \rangle \propto \sigma_y^{2/3}$
- Constitutive law changes:
Power law distribution of contact sizes
Fractal dimension of contact areas
- Ignoring interactions between asperities gives qualitatively wrong spatial distribution of contacts
- Most contacts at smallest scale
 \rightarrow results dominated by small scale cutoff Δ, a_c
 \rightarrow continuum mechanics may fail even though total area is very large
 \rightarrow reason why T important in macroscopic scale friction?

What are limits of Continuum Theory?

Continuum theories: Hertz, Johnson-Kendall-Roberts (JKR),

Derjaguin-Muller-Toporov (DMT), Maugis-Dugdale

Assume: 1) continuous displacements, bulk elastic const.

2) smooth surface (often spherical) at small scales

Only tested for atomically flat mica bent into cylinders
and elastomers with liquid behavior on small scales

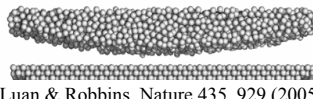
Find (1) valid down to a few atomic diameters, but atomic
scale roughness causes failure of continuum theories.

Important for small contacts between rough surfaces
and ideal single asperities: scanning probe or nanoindenter

Macro View



Molecular View



Luan & Robbins, Nature 435, 929 (2005)

Basics of Molecular Dynamics Simulations

- Choose initial positions & velocities of atoms or molecules
- Integrate Newton's equations numerically in time steps of dt
 - ⇒ Calculate forces from interaction potentials between atoms
 - ⇒ Calculate new positions & velocities after time step dt
 - ⇒ Calculate new forces and repeat
- As system evolves, follow → detailed motion of atoms
 - average quantities (pressure, temperature, volume, force, energy, heat flow, work, scattering cross-section, ...)
 - that would measure in an experiment or calculate in equilibrium using thermodynamics
- Can work in microcanonical ensemble (fix energy, volume, N)
or add extra degrees of freedom to work at fixed T , p , μ
(i.e. allow bounding walls to move in and out under fixed p)
Should choose limit closest to experiment

Continuum vs. MD for Sphere or Cylinder on Flat

Rigid cylinder or sphere, elastic flat
(dimensions $W, t \gg a$ so \sim irrelevant)

Purely repulsive (Hertz) or adhesive

Substrate ideal elasticity E'
or Lennard-Jones

$R = 100-1000\sigma \sim 30-300\text{nm}$

$\sigma = \text{mol. diameter}$

Units: length $\sigma \sim 0.3\text{nm}$

binding energy ϵ ,

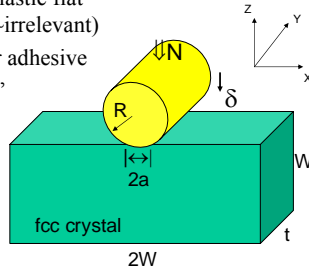
force $\epsilon/\sigma \sim 5\text{pN}$

Vary atomic scale roughness

amount of adhesion $V_{\text{int}} = 4\epsilon'[(\sigma/r)^{12} - (\sigma/r)^6]$ $r < r_{\text{cut}}$

Examine normal displacement δ , radius a , friction F ,

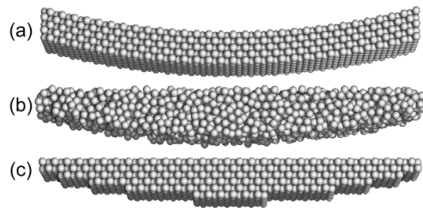
lateral stiffness k & pressure distribution $P(x)$ vs. load N

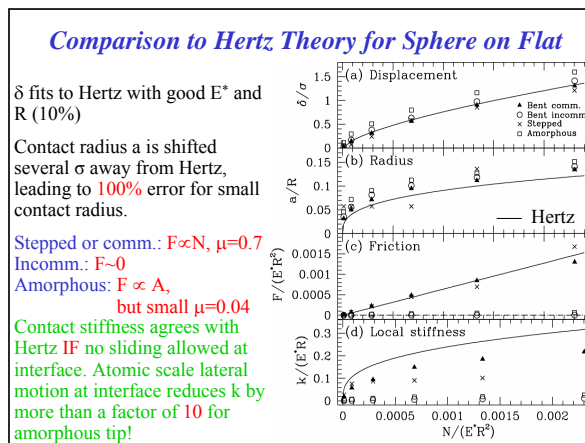
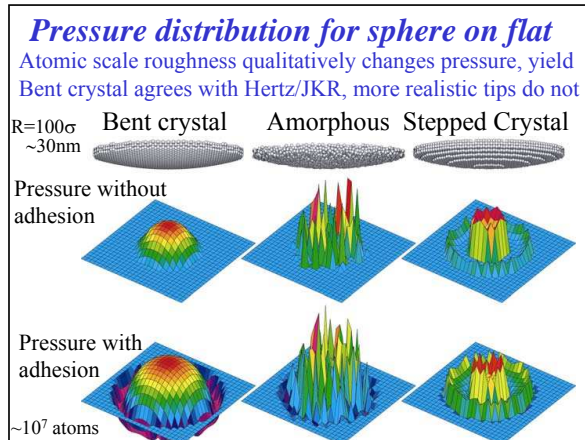


Atomic tip structure \rightarrow Close as possible to curve

- Substrate- atomically flat 100 or 111 fcc surface
- Cylindrical or spherical tip constructed by:
 - a) Bending crystalline solid
 - b) Cutting amorphous solid
 - c) Cutting crystalline solid

commensurate or
incommensurate
with substrate





Effect of Adding Adhesion

Maugis-Dugdale (M-D) Model:

Constant adhesion force σ_0 for separations $< h_0$

Interpolates between DMT (long, rigid, $\lambda < 0.1$) and JKR (short, pliant, $\lambda > 5$) limits by varying $\lambda \equiv \sigma_0(9R/2\pi w E^*)^{1/3}$,

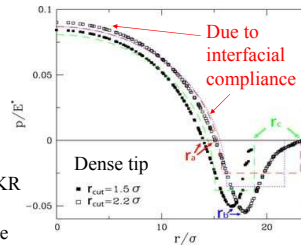
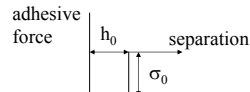
with $w = \sigma_0 h_0$ = surface energy.

Typically $0.1 < \lambda < 1$ for AFM

Dimensionless pulloff force N_c
always between DMT and JKR
 $|N_c|/\pi w R$ between 1.5 and 2

Compare to inner repulsion r_a ,
radius at minimum r_b -close to JKR
and outer radius r_c .

Deviations similar to nonadhesive



An adhesion Map for the contact of Elastic Spheres, K.L. Johnson and J.A. Greenwood, J. Colloid Interface Sci. 192, 326 (1997)

Atomic Scale Roughness Changes Adhesion



Pulloff force N_c may be **outside** JKR/DMT bounds

$|N_c|/(\pi w R) = 1.5$ for JKR, 2.0 for DMT

Maugis-Dugdale $|N_c|/(\pi w R) = 1.74$ for $w = 0.46 \epsilon \sigma^2$

Tune interactions so all tips have $w = 0.46 \epsilon \sigma^2$, find:

Commensurate: $|N_c|/(\pi w R) = 1.77$

Incommensurate: $|N_c|/(\pi w R) = 1.79$

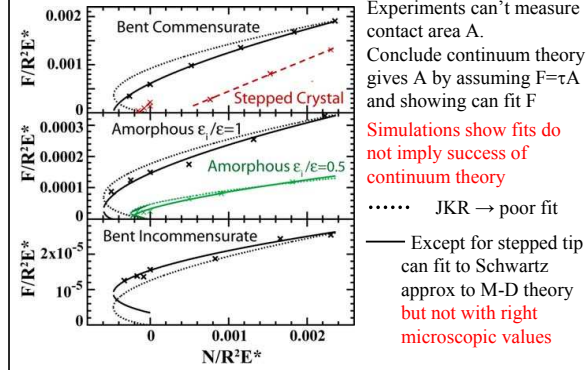
Amorphous: $|N_c|/(\pi w R) = 2.26$

Stepped: $|N_c|/(\pi w R) = 0.72$ -less than half JKR

Reduces adhesion energy up to factor of five for same interactions as go from bent commensurate to amorphous

Luan & Robbins, Phys. Rev. E74, 026111 (2006)

Fits of Friction to Continuum With $F = \tau A_{M-D}$

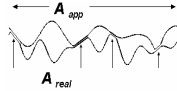


Single Asperity Conclusions

- Bulk elastic modulus describes stress/strain to $\sim 3\sigma$
 Atomic roughness \Rightarrow deviations from continuum theory
- Molecular scale geometry has little effect on normal displacement vs. force curves
 \rightarrow Moduli from continuum fits are accurate
- Contact areas, morphologies and pressures are changed
 \rightarrow Yield stress, areas, pulloff force off by factor ~ 2
 \rightarrow Adhesive energy off by factor ~ 5
- Lateral stiffness and friction vary by more than order of magnitude with atomic geometry
 \rightarrow Contact stiffness dominated by interface
 \rightarrow Friction scales with real contact area for bent or amorphous tips, but not stepped tips
 \rightarrow Shear stresses from continuum fits too high

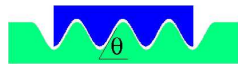
Why is friction often proportional to load?

- Not just $A_{\text{real}} \propto \text{Load}$ and $F \propto A_{\text{real}}$ since A_{real} varies with parameters like Δ that have weaker effect on μ
 - Friction between clean surfaces very sensitive to local structure, surface orientation, ... but measured μ is not
 - ➔ Assume friction from yield stress τ_s of molecular contacts
- Glassy systems: τ_s rises linearly with pressure p
- If: $F_s = A_{\text{real}} \tau_s(p)$ with $\tau_s = \tau_0 + \alpha p$
- Then: $F_s = A_{\text{real}} \tau_0 + \alpha \text{Load}$
- $\mu_s = F_s / \text{Load} = \alpha + \tau_0 / \langle p \rangle$

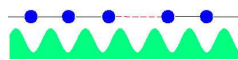


- ➔ Constant μ if $\langle p \rangle = \text{Load} / A_{\text{real}} = \text{const.}$
 - or $\tau_0 \ll \langle p \rangle$ (Independent of distribution of pressure)
 - ➔ Friction at zero or negative load with adhesion, as observed
- How do surfaces lock together to give $\tau_s(p)$?

Friction Mechanisms in Contacts



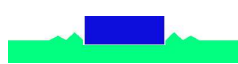
Geometrical Interlocking: $F = N \tan \theta$
 Unlikely to mesh, F goes up as smooth
 Kinetic friction vanishes



Elastic Metastability:
 Intersurface interaction too weak



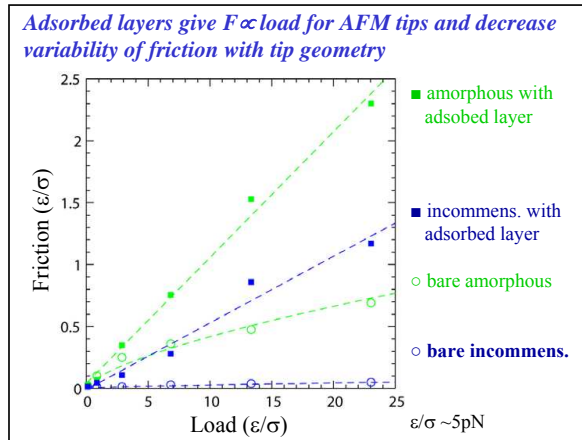
Mixing or Cold-Welding
 Hard to observe in sims. even with clean, unpassivated surfaces in vacuum



Plastic Deformation (plowing)
 Load and roughness dependent
 ⇒ High loads, sharp tips



Mobile third bodies → "glassy state"
 hydrocarbons, wear debris, gouge, ...
 ⇒ Give $\tau_s = \tau_0 + \alpha P$ with small τ_0 , nearly indep. of factors not controlled in exp.



Adsorbed layers explain many experiments

→ Explain Amontons's Law and Adhesive Terms

⇒ $F_s = \tau_0 A_{\text{real}} + \alpha \text{ Load}$

⇒ $F_s \approx$ independent of uncontrolled experimental parameters

→ Kinetic friction also linear: $F_k = \tau_{0k} A_{\text{real}} + \alpha_k \text{ load}$

→ At low v , α_k is 10 to 20% smaller than for static case

→ α_k shows $k_B T \log v$ dependence seen in experiment

→ Most molecules stable at any time, resist sliding just as for static friction, each pops and dissipates separately

⇒ As v decreases, more thermal excitation, $F \propto \log v$

He, Müser & Robbins, Science 284, 1650 (1999)

He & Robbins, Phys. Rev. B64, 035413 (2001), Tribol Lett. 10, 7 (2001)

Müser, Wenning & Robbins, Phys. Rev. Lett. 86, 1295 (2001)

J. Ringlein and M. O. Robbins, Am. J. Phys. 72, 884-891 (2004)

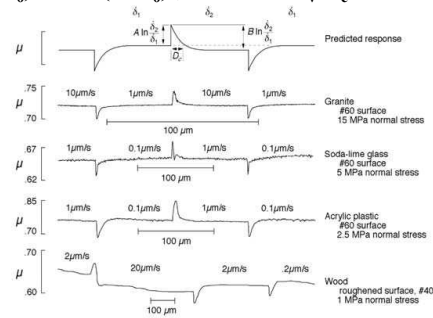
Complex Dynamics of Kinetic Friction

Rate-state models (Dieterich, Ruina, Rice,...)

$$\mu = \mu_0 + A \ln(v/v_0) + B \ln(\Theta/\Theta_0) ; \quad d\Theta/dt = 1 - \Theta v/D_c$$

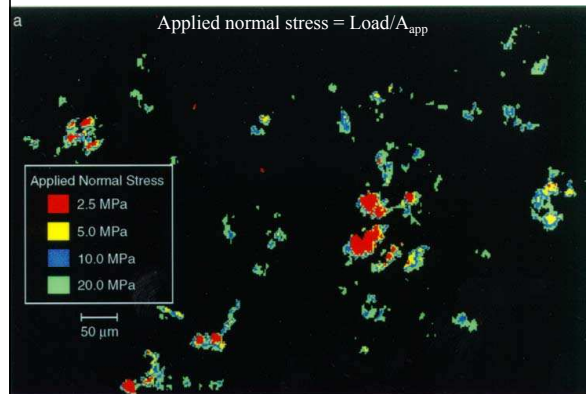
A → change
in shear
stress
with v

B → change
in area of
contact
with time



Dieterich & Kilgore

Dynamic Images of Contact Area (Dieterich & Kilgore)



Connection to “Rate-State” Models

For rocks, wood, metals,... (Dieterich, Ruina, Rice,...)

$$\mu = \mu_0 + A \ln(v/v_0) + B \ln(\Theta/\Theta_0); \quad d\Theta/dt = 1 - \Theta v/D_c$$

→ A represents change in shear stress with v

→ B change in area of contact with time

Our model has fixed area → only see A

Find: $A \approx 0.001$ vs. 0.005 to 0.015 for rocks,

$A/\mu_0 \approx 0.05$ vs. 0.008 to 0.025 for rocks

$A \propto T$ as in experiments

$\mu \propto T \ln v$ follows from simple activation model

→ most molecules stable at any time

→ resist sliding just as for static friction

→ thermal activation over barrier reduces F

⇒ lower v, more thermal excitation → $F \propto \log v$

Single Scale Simulation Conclusions

Continuum

AFM tips

Third Bodies

- Area proportional to load → $\langle p \rangle = \text{constant}$
Elastic: $\langle p \rangle/E' = \Delta/\kappa$ Plastic: $\langle p \rangle \propto \sigma_y^{2/3}$
Expect plastic for $\Delta > \sigma_y/E'$ – usual for bulk σ_y
- Most contacts at smallest scale, Δ dominated by small scale cutoff → *continuum mechanics may fail*
- Surface roughness → big changes from continuum
- Pulloff force not bounded by DMT, JKR
- Interfacial compliance, shear stress dominate k, F
- Lock any surface pair together
- $\tau_s = \tau_0 + \alpha p$ up to GPa → $F = \tau_0 A + \alpha \text{ Load}$
- Independent of parameters not controlled in experiment
- $\tau_k \sim \tau_s$ because atoms pop rapidly between equivalent local minima, dissipating most of energy

Building Atomic Scale Physics Into Meso- and Macro-scale Calculations

- Boundary conditions (BC) + Constitutive Relations
 - velocity or stress stress vs. strain (rate)
 - slip, friction, adhesion viscous, elastic, plastic
 - Counterintuitive flows requiring new BC's
 - Fracture energy of glassy polymers
- Coarse-Grained Models: Potentials, Phase-Field Models, ...
 - Test common assumptions in Phase-Field Models
 - Provide complete parametrization with some surprises
- Coupled Molecular and Continuum Calculations
 - Treat each region with optimal description:
 - ⇒ atomic at interface, continuum in bulk
 - New multiscale method for fluids and solids
 - Results for singular corner flow, contact, stick-slip friction

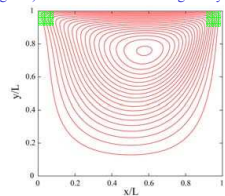
Linking Atomistic and Continuum Regions

Three overlap regions where solve both continuum and MD
 Outermost → Continuum solution gives MD boundary condition
 Innermost → MD gives continuum boundary condition
 Middle → Two solutions equilibrate independently

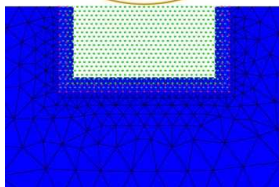
Fluids: Apply boundary conditions to velocities

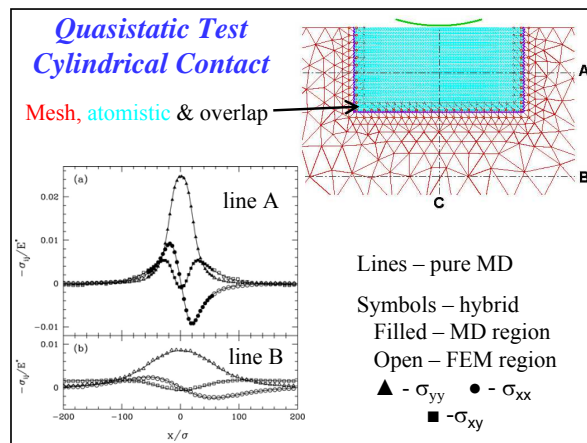
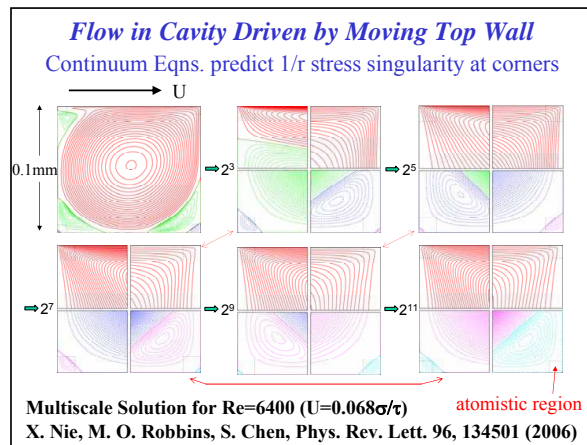
Solids: Apply boundary conditions to displacements

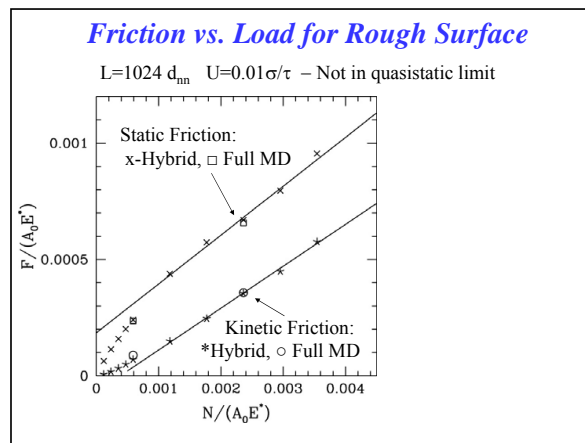
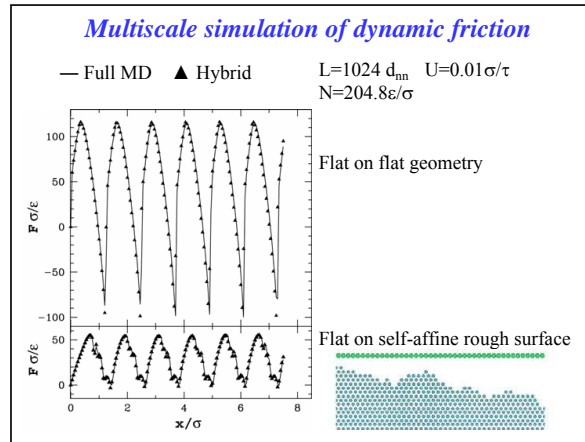
Streamlines in $L \sim 300\text{nm}$ channel with moving top wall. Atomistic solution in $<1\%$ of area (green) removes continuum singularity



Model contact region atomistically, elastic deformations with finite-elements, constrain deformations in overlap region

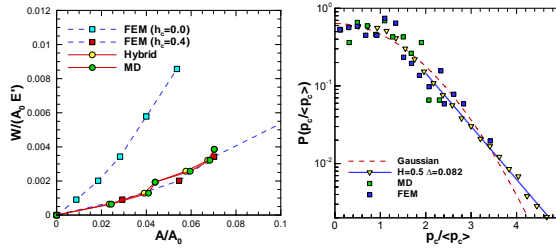






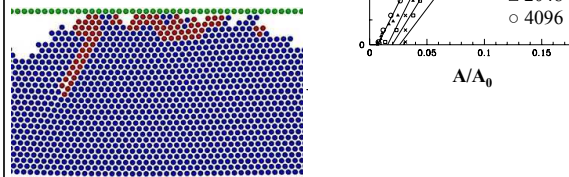
2D Results from MD, FEM, and Hybrid model

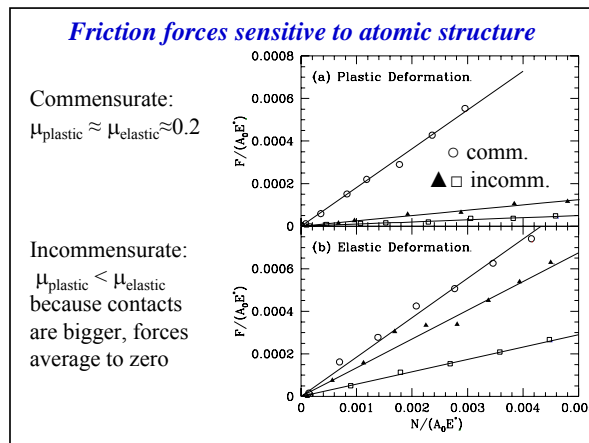
- Hybrid model reproduces MD curves for load W vs. area A .
- FEM area too small unless include regions with finite separation $h_c = 0.4\sigma$ in contact area (σ =atomic diameter)
- Universal distribution of local pressures for all methods.



Plastic results for $\Delta=0.78$ show size effects

- Still have $A \propto W$, but L dependent
- Surface flattening before dislocations important





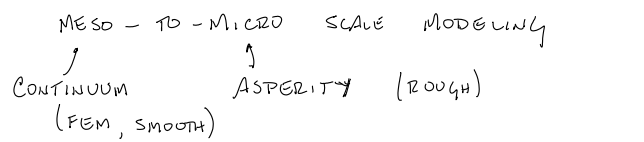
Conclusions for Hybrid Method

- Have robust multiscale method for both fluids and solids
- Implemented for quasi-2D flows near solids
 → lengths to $\sim 1\mu\text{m}$ for dynamic cases, $\sim 1\text{mm}$ for quasistatic
- Implemented for quasi-2D contact between self-affine surfaces
- Incorporated heat flux for sheared fluids
- Comparisons to MD and continuum results show limitations of continuum approximation at interfaces
 → Position and rate dependent slip near solids
 → Sensitivity of contact area and stress to atomic scale structure, unexpected mode of plastic deformation at interface
- First calculation of drag force in singular corner flow
 → integrate stress over 5 orders of magnitude in length
- First calculation of atomistic effects in self-affine contact
 → rough over 4 orders of magnitude in length scale

Appendix B

Notes From Break-Out Sessions

There were multiple break-out sessions, some time of which was spent in developing common nomenclature. Following are notes taken from three of the sessions where common outlooks were beginning to develop.



HOW TO CHARACTERIZE THE SURFACE

HOW MUCH TO CHAR. / PARAMETERS? LENGTH SCALE?

- THINGS YOU MIGHT NEED @ THE BOTTOM
- ROUGHNESS MICRO / MACRO SLIP
 - LUBRICATION

LENGTH SCALES?

ATOMISTIC



ROUGHNESS



WAVINGNESS



ELEMENT

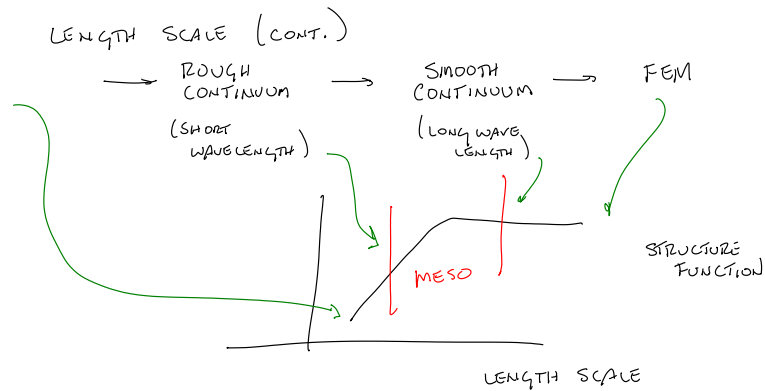
MICROSTRUCTURE

DEVELOP CONTINUUM DESCR.
& CONSTITUTIVE EQNS.
FOR INTERFACE

UPPER SCALE ORDER
LARGER THAN ASPERITY
SCALE SIZE OF CONTACT
PATH

WHERE TO DEFINE / HOW TO
IDENTIFY THE IMPORTANT SCALES

Figure B.1. Notes from break-out session 1



FUNCTIONAL RELATIONSHIP BETWEEN FUNCTIONAL LOADS (FEM INPUTS) & SMALL LENGTH SCALE EFFECTS (INPUTS)

HOW DO LARGER SCALES INFLUENCE INTERFACE?

WHAT SIZE CONTROL VOLUME DO WE NEED TO FOCUS TO PROVIDE INFO. TO NEXT LEVEL?

CAN WE IDENTIFY EXPERIMENTS THAT WILL IDENTIFY THE SCALES?

- DEPENDS ON SCALE OF MEASUREMENTS
- MINIMUM NO. OF EXPERIMENTS NECESSARY TO ID SCALES & PARAMETERS

CONVERGENCE OF NUMERICAL & PHYSICAL EXPERIMENTS

DYNAMIC EFFECTS ON JOINT RESPONSE

MONOLITHIC VS. INTERFACE EXPERIMENTS

INVERSE FORMULATION TO IDENTIFY THE INTERFACE LAWS

Figure B.2. Notes from break-out session 1

WHAT STATE VARIABLES WILL APPEAR IN
CONSTITUTIVE LAWS?

NEEDED \rightarrow A STATE VARIABLE DESCRIPTOR
OF THE INTERFACE \leftarrow SMOOTH IDEAL
INTERFACE
• MAT. STRUCTURE

SMALL SCALE \rightarrow LARGE SCALE

\hookrightarrow (MATERIAL, GEOMETRY, TRACTION, TEMPERATURE,
HUMIDITY, ENVIRONMENT, HISTORY) = 0

HOW MUCH DO WE NEED TO KNOW?

DEVELOP A MODEL THAT CAN BE INCORPORATED
INTO A LARGER MODEL.

WHAT EXISTS BETWEEN SURFACE PROFILE & TRACTIONS?
NOTHING ... BUT WE NEED TO INTRODUCE
SOMETHING ...

INTERFACE CHARACTERISTICS

SPECTRUM OF ROUGHNESS

CONTACT SIZE

CHARACTERISTIC DISPLACEMENTS

GRAINS

LOADING

TEMPERATURE

DYNAMICS | HISTORY

Figure B.3. Notes from break-out session 1

GOAL 3:

PROVIDE CONSTITUTIVE RELATIONSHIP THAT
WILL RELATE TRACTIONS, ETC. FOR FEM

GOAL 2:

HOW CAN WE BUILD IN DEPENDENCE ON
SURFACE PROPERTIES, BULK MATERIAL PROPERTIES,
ETC. TO THE CONSTITUTIVE RELATIONS

EXPERIMENTS TO DEVELOP CONSTITUTIVE
EQNS. USING INVERSE METHODS

GOAL 1:

ON WHAT DO THE CONSTITUTIVE LAWS DEPEND
† WHAT ARE THE STATES

SURFACE TOPOGRAPHY (ROUGHNESS + WAVINESS)

MATERIAL PROPERTIES (BULK + SURFACE)

• GRAIN STRUCTURE, FAULTS, DEFECTS

SURFACE ENERGY (HUMIDITY, LUBRICATION, DEBRIS)

TEMPERATURE

EVOLUTION OF THE INPUTS w/ HISTORY
(WEAR, SHAKEDOWN)

ANISOTROPY

WHAT GROUP A CAN PROVIDE TO US REGARDING
LOADING

SOME ARE INPUTS † SOME ARE INTERNAL
STATE VARIABLES

Figure B.4. Notes from break-out session 1

STATE OF CURRENT KNOWLEDGE / OPEN QUESTIONS

MUCH WORK HAS BEEN DONE FOR STEADY SLIDING
BUT LIMITED WORK IS AVAILABLE FOR MICROSLIP
(ROCKING MOTION, VARYING TRAJECTORIES, ETC.)

MANY APPLICATIONS ALSO INVOLVE SEPARATION

NORMAL DAMPING VS. SHEAR DAMPING

← DUE TO MICRO-ASPERITY IMPACTS (VERY LITTLE KNOWN)
↑ SEPARATION

TRANSFER OF ENERGY TO HIGHER MODES
WHICH CAN THEN BE DISSIPATED

WHAT LENGTH SCALES COME IN TO THIS LEVEL?

HOW SMALL SHOULD WE CONSIDER?

INFLUENCE OF LENGTH SCALES ON THE CONSTITUTIVE
FORMULATIONS...

HOW DO WE INTEGRATE THE SMALLER SCALES
INTO THIS LEVEL?

TIME SCALES? AT THE ASPERITY SCALE IS THE
INERTIA IMPORTANT FOR THE PROBLEMS OF
INTEREST?

OTHER TIME SCALES SUCH AS THERMAL DIFFUSION?
↑ ON WHAT SCALES?

CRITICAL ISSUES

- PARTIAL SLIP & DYNAMIC EFFECTS IN
EXPERIMENTAL SYSTEMS

Figure B.5. Notes from break-out session 1

HIGHEST LEVEL

CONSTITUTIVE LAW FOR INTERFACE

- BOUNDARY CONDITION DEPENDS ON
 - DISPLACEMENT RATE
 - TRACTION
 - INTERNAL STATES

AS COMP. TOOLS ARE DEVELOPED, EXP. & EXISTING INFORMATION SHOULD BE USED TO VALIDATE TOOLS

CURRENTLY, FRICTION LAWS LOOK LIKE PLASTICITY & ARE 'PHENOMENOLOGICAL ...

CAN WE RELATE PARAMETERS TO SMALLER SCALES?
MESH DEPENDENT? WITH FINE SCALE MODELS & SIMULATIONS

GOAL: DEVELOPMENT OF TOOLS TO MOVE FROM SMALL SCALE EXP. & SIMULATIONS TO LARGER SCALE PARAMETERS

TOP-DOWN APPROACH MAY LIMIT COMPLEXITY BUT LIMIT UNDERSTANDING
(GOOD) (BAD)

BUILD A PHENOMENOLOGICAL MODEL FROM EXPERIMENTS

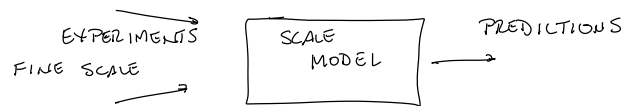


Figure B.6. Notes from break-out session 3

IMPORTANT COMPONENT:

- STEADY SLIDING vs. TRANSIENT FRICTION (MACRO - vs. MICRO-SLIP)
- DIRECTIONALITY OF MOTION
- ISOTROPY OF INTERFACES

MACRO MODELS CAN INCORPORATE BUT EXISTING MODELS MAY NOT BE ABLE TO ADDRESS

SYSTEMATIC METHOD TO MOVE BETWEEN SCALES

- OVERLAPPING SCALES
 - NONLINEARITY
 - ASSUMPTIONS BETWEEN SCALES
- SCALE SEPARATION?

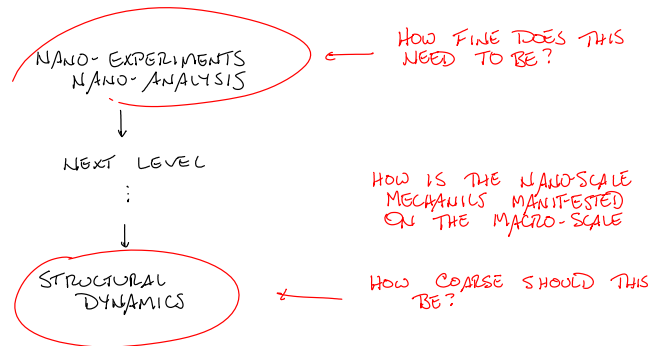
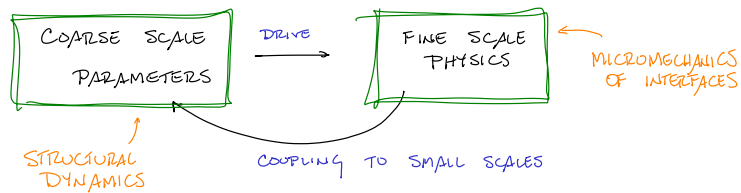


Figure B.7. Notes from break-out session 3

LENGTH SCALES

- GLOBAL ELEMENT SIZE
- INTERFACE ELEMENT SIZE

WHAT IS THE LEVEL OF ACCURACY?

- FRICTION MODEL
- DEPENDENCE ON TRACTIONS
- CONSTRAINED BY FEM ELEMENT SIZE

CONVENTIONAL FEM w/ VERY FINE INTERFACE
MESH DO OK... BUT REQUIRE UNACCEPTABLY
LONG TIMES ^{↑ SOMETIMES}

GOAL: MAKE PREDICTIONS BASED ON
PHYSICS INSTEAD OF TUNED PARAMETERS

WITH A GOOD FRICTION MODEL WE CAN UNDERSTAND
THE EFFECT OF THE INTERFACE ON THE
STRUCTURAL DYNAMICS

DIFFERENT FRICTION MODELS WORK WELL IN
DIFFERENT OPERATING CONDITIONS

Figure B.8. Notes from break-out session 3

HOW PREDICTIVE & VARIABILITY IS EXPECTED?
EXPERIMENTS VARY SUBSTANTIALLY...

NANO-SCALE PHYSICS REDUCES TO A SINGLE
OR SMALL NUMBER OF PARAMETERS
AT THE MACRO-LEVEL

LIMIT THE UNDERLYING PHYSICS TO LIMIT
THE COMPLEXITY

DEVISE EXPERIMENTS TO IDENTIFY SPECIFIC
DETAILS OF THE FRICTION INTERFACE

- SURFACE FORCE APPARATUS
- NEED GOOD SPATIAL RESOLUTIONS IN
EXPERIMENTS & SIMULATIONS

- CAN WE DESIGN AN EXPERIMENT TO DESCRIBE
HOW MUCH ERROR IS INTRODUCED
BY COULOMB FRICTION

WHEN IS COULOMB FRICTION A GOOD
APPROXIMATION TO AN ASPERITY-BASED MODEL

WILL BE STRONGLY DEPENDENT ON
MATERIAL & GEOMETRY

- WHEN IS A LENGTH SCALE IMPORTANT
- RATE DEPENDENCE
- ILL-POSEDNESS OF COULOMB FRICTION
- THERE ARE MANY LENGTH SCALES FOR WHICH
COULOMB FRICTION IS INSUFFICIENT

Figure B.9. Notes from break-out session 3

Summary of discussion from Groups A, B (Polycarpou)

- “State of the art” in Joints:
- Currently use phenomenological models fitted to experimental data (simple damping coefficient etc)
- One can do extremely fine meshing of jointed interfaces using simple
 - (1) Coulomb friction and
 - (2) A “slope” from zero to finite friction coefficient value (somewhat arbitrarily chosen)
- Using such fine meshing and lots-lots of computer time, one can get “reasonable” predictions, especially if vibro-impacts are not considered

Figure B.10. *Notes from combined break-out session A+B*

Summary of discussion from Groups A, B—"The Need"

- Make interface/friction predictions based on physics (important parameters need to enter: material properties, surface topography, surface energy, grain size effects, third body)
- Friction models may not need to be too general else the complexity will be too large (too many parameters need to be known, which may not easily be found)
- Moreover, computationally this may not be feasible
- Ultimately the need is for a better (than Coulomb) friction model, but still simple to be used at the structural level

Figure B.11. *Notes from combined break-out session A+B*

Summary of discussion from Groups A, B --Goals

- The tribology (micro/nanotribology) community has certainly looked and proposed models (atomistic, MD, continuum-based) for SLIDING conditions (especially static and steady-state sliding)
- Develop friction models that are “appropriate,” or account for
 - (1) partial slip
 - (2) dynamic effects

Figure B.12. *Notes from combined break-out session A+B*

Summary of discussion from Groups A, B --Goals

- Development of tools (experimental and simulation) to move from small scale effects to large scale effects/parameters
- Better investigate/understand the coupling between normal (vibro impacts) and shear (friction) modes

Figure B.13. *Notes from combined break-out session A+B*

Appendix C

Participant List

Participants

| Participant | Institution | email |
|---------------------|------------------------------|--|
| Akay, Adnan | NSF | aakay@nsf.gov |
| Barber, James R. | University of Michigan | jbarber@umich.edu |
| Berger, Edward | University of Virginia | berger@virginia.edu |
| Bergman, Larry | UIUC | lbergman@uiuc.edu |
| Chu, Tze-Yao | Sandia National Laboratories | TYCHU@sandia.gov |
| Ciavarella, Michele | Polytecnico di Bari | mciava@poliba.it |
| Coghlan, Richard | Rolls-Royce, UK | richard.coghlan@rolls-royce.com |
| Conner, Steven | Pratt & Whitney | steve.conner@pw.utc.com |
| Cooper, Clark | NSF | ccooper@nsf.gov |
| Couchman, Louise | ONR | couchml@onr.navy.mil |
| Ewins, David | Imperial College | d.ewins@imperial.ac.uk |
| Garay, Greg | GE Aviation | gregory.garay@ge.com |

Figure C.1. *Workshop Participants*

Participants

| | | |
|-----------------------------|------------------------------|--|
| Garraway, Kevin | AWE | kevin.garraway@awe.co.uk |
| Giurgiutiu, Victor | AFOSR | victor.giurgiutiu@afosr.af.mil |
| Greenaugh, Dr. Kevin | NNSA | Kevin.Greenaugh@nnsa.doe.gov |
| Gregory, Danny | Sandia National Laboratories | dlgrego@sandia.gov |
| Gresham, Jennifer | AFOSR | jennifer.gresham@afosr.af.mil |
| Hills, David | Oxford University | david.hills@eng.ox.ac.uk |
| Ind, Phil | AWE | phil@xcra.com |
| Katz, Reuven | Michigan, University of | reuven@umich.edu |
| Kim, Kyung-Suk | Brown University | Kyung-Suk_Kim@Brown.EDU |
| Laursen, Tod A. | Duke University | laursen@duke.edu |
| Lawrence 'Robbie' Robertson | AFRL/VS | Lawrence.Robertson@Kirtland.af.mil |

Figure C.2. *Workshop Participants*

Participants

| | | |
|---------------------|--------------------------|----------------------------|
| Leen, Sean | University of Nottingham | sean.leen@nottingham.ac.uk |
| Leo, Donald | DARPA | donald.leo@darpa.mil |
| Mark O. Robbins | Johns Hopkins University | mr@pha.jhu.edu |
| Masud , Arif | UIUC | amasud@uiuc.edu |
| Misawa, Eduardo | NSF | emisawa@nsf.gov |
| Nowell, David | Oxford University | david.nowell@eng.ox.ac.uk |
| Petrov, Evgeny | Imperial College | y.petrov@imperial.ac.uk |
| Polycarpou, Andreas | UIUC | polycarp@uiuc.edu |
| Popova , Marina | University of New Mexico | mpopova@me.unm.edu |
| Quinn, Donald D. | University of Akron | quinn@uakron.edu |

Page 3

Figure C.3. *Workshop Participants*

Participants

| | | |
|--------------------------|---|-----------------------------|
| Segalman, Dan | Sandia National Laboratories | djsegal@sandia.gov |
| Vakakis, Alexander | National Technical University of Athens | vakakis@central.ntua.gr |
| Willner, Kai | University of Erlangen | willner@itm.uni-erlangen.de |
| Wilson, Peter | Sandia National Laboratories | PJWILSO@sandia.gov |
| Bold for speakers | Academia | |
| | Government (pattern for funding agency) | |
| | Industry | |

Figure C.4. *Workshop Participants*

DISTRIBUTION:

- 10 Professor David Ewins
Mechanical Engineering Department
South Kensington Campus
Imperial College London
London
England
- 10 Professor Lawrence Bergman
306 Talbot Lab
104 S. Wright St.
University of Illinois
Urbana, IL 61801
- 10 Dr. Adnan Akay
Division of Civil and mechanical Systems
National Science Foundation
4201 Wilson Boulevard
Arlington, VA 22230
- 10 Dr. Ken P. Chong
Mechanics & Materials Program, Engineering Directorate,
National Science Foundation,
4210 Wilson Blvd., Suite 545,
Arlington, VA 22230
- 1 Professor James R. Barber,
Department of Mechanical Engineering
The University of Michigan
2350 Hayward Street
Ann Arbor, Michigan 48109-2125
- 1 Professor Edward Berger,
Department of Civil Engineering
The University of Virginia
Thornton Hall, Office: D203
351 McCormick Road
PO Box 400742
Charlottesville, VA 22904-4742
- 1 Dr. Michele Ciavarella,
CEMEC-PoliBA - V.le Japigia 182,
Politecnico di Bari, 70125 Bari
Italy

- 1 Richard Coghlan,
Rolls-Royce plc,
PO Box 31,
Derby DE24 8BJ,
UK
- 1 Clark Cooper,
National Science Foundation
4201 Wilson Boulevard
Arlington, VA 22230
- 1 Dr. Louise Couchman,
ONR
CODE ONR-02
800 N Quincy St
Rm 704
Arlington, VA 22217
- 1 Greg Garay,
Leader, Damping Technology
GE Aircraft Engines
One Neumann Way MD-A413
Cincinnati, OH 45215
- 1 Garraway, Kevin
Engineering Analysis Group
AWE Aldermaston
Reading
RG7 4PR
England, UK
- 1 Dr. Victor Giurgiutiu,
Air Force Office of Scientific Research
875 North Randolph Street, Suite 325
Arlington, VA 22203
- 1 Dr. Kevin Greenaugh
Dir., Systems Sim & Val. Div.
NNSA
Dept. of Energy
1000 Independence Ave.
Forrestal Bldg., 1FO06
Washington, DC 20585
- 1 Dr. Jennifer Gresham,
Air Force Office of Scientific Research
875 North Randolph Street, Suite 325
Arlington, VA 22203

- 1 Professor David Hills,
Department of Engineering Science
University of Oxford
Oxford, OX1 3PJ
England, UK
- 1 Professor Reuven Katz,
100-b Dow Building
Department of Mechanical Engineering
2350 Hayward Street
College of Engineering, University of Michigan
Ann Arbor, Michigan 48109-2125
- 1 Professor Kyung-Suk Kim,
Division of Engineering,
Brown University,
182 Hope Street,
Providence, RI 02912
- 1 Professor Tod A. Laursen,
127 Hudson Hall
Box 90287
Duke University
Durham, NC 27708
- 1 Dr. Lawrence Robertson
U.S. Air Force Research Laboratory
AFRL/VSSV
3550 Aberdeen Avenue SE
Kirtland AFB, NM 87117
- 1 Professor Sean Leen, School of Mechanical Materials & Manuf Eng,
Faculty of Engineering
The University of Nottingham
Room B104 Coates
University Park
NG7 2RD
UK
- 1 Dr. Donald Leo,
DARPA
3701 North Fairfax Drive
Arlington, VA 22203-1714
- 1 Professor Mark O. Robbins
Dept. of Physics & Astronomy
The Johns Hopkins University
3400 North Charles Street
Baltimore, MD 21218-2686

- 1 Professor Arif Masud
Department of Civil & Environmental Engineering,
University of Illinois at Urbana-Champaign
Urbana, IL 61801
- 1 Dr. Eduardo Misawa,
The National Science Foundation,
4201 Wilson Boulevard,
Arlington, Virginia 22230
- 1 Professor David Nowell,
Department of Engineering Science
University of Oxford
Parks Road
Oxford OX1 3PJ
UK
- 1 Dr. Evgeny Petrov,
Mechanical Engineering Department
Imperial College London
South Kensington Campus
London, SW7 2AZ,
UK
- 1 Professor Andreas Polycarpou,
Department of Mechanical and Industrial Engineering
342 MEB,
1206 West Green Street
University of Illinois at Urbana-Champaign
Urbana, Illinois 61801
- 1 Dr. Marina Popova
Department of Mechanical Engineering
University of New Mexico
Albuquerque, NM 87131
- 1 Professor Dane Quinn
Dept. of Mechanical Engineering
The University of Akron
Akron, OH 44325-3903
- 1 Professor Alexander Vakakis,
National Technical University of Athens
P.O. Box 64042,
GR-157 10 Zografos, Greece

1 Professor Kai Willner,
Institute of Applied Mechanics
University of Erlangen-Nuremberg
Egerlandstrasse 5, D-91058 Erlangen
Germany

| | | |
|----|---------|---|
| 1 | MS 0346 | Michael J. Starr, 01526 |
| 1 | MS 0346 | Thomas Baca, 01523 |
| 1 | MS 0372 | James M. Redmond, 01525 |
| 1 | MS 0372 | John Pott, 01524 |
| 1 | MS 0380 | Harold S. Morgan, 01540 |
| 1 | MS 0380 | Joseph Jung, 01542 |
| 1 | MS 0380 | Garth M. Reese, 01542 |
| 1 | MS 0384 | Arthur Ratzel, 01500 |
| 1 | MS 0557 | Brian R. Resor, 01521 |
| 10 | MS 0557 | Daniel Segalman, 01525 |
| 1 | MS 0557 | Danny L. Gregory, 01521 |
| 1 | MS 0557 | David B. Clauss, 01521 |
| 1 | MS 0557 | Fernando Bitsie, 01521 |
| 1 | MS 0824 | Tze-Yao Chu, 01500 |
| 1 | MS 0847 | Peter Wilson, 01520 |
| 1 | MS 9042 | James P. Lauffer, 08776 |
| 1 | MS 9042 | Michael D. Jew, 08774 |
| 1 | MS 9042 | Mike Chiesa, 08774 |
| 1 | MS 0899 | Technical Library, 9536 (electronic copy) |

